SADAF ALMAS

BIOLOGICAL PROPERTIES OF POLYOXOMETALATES AGAINST BACTERIAL ANTIBIOTIC RESISTANCE

Faculdade de Ciências e Tecnologia

2023

SADAF ALMAS

BIOLOGICAL PROPERTIES OF POLYOXOMETALATES AGAINST BACTERIAL ANTIBIOTIC RESISTANCE

Erasmus Mundus Mestrado em Qualidade em Laboratórios Analíticos

Trabalho efetuado sob a orientação de:

Maria Leonor Faleiro

Manuel Aureliano Pereira Martins Alves

Faculdade de Ciências e Tecnologia

2023

BIOLOGICAL PROPERTIES OF POLYOXOMETALATES AGAINST BACTERIAL ANTIBIOTIC RESISTANCE

Declaration of Authorship

I declare I am the author of this work, which is original and unpublished. The sources consulted have been duly cited in the text and included in the list of references.

_____

(Sadaf Almas)

Contents

Acknowledgement:

I am grateful to Allah Almighty for providing me with the knowledge, fortitude, ability, and opportunity to excel in my academic career. I would like to extend my sincere appreciation to my thesis advisor, **Professor Leonore Faleiro**, and co-supervisor, **Professor Manuel Aureliano** for their unwavering support, invaluable expertise, and constant encouragement throughout the research process. I am blessed to get a chance to work under the supervision of professional scientists. Your mentorship, insightful feedback, and dedication to my academic growth have been instrumental in shaping this thesis. I am also thankful to **Professor Fraqueza Gil** for providing me immense guidance during my biochemistry practical work.

I extend my thanks to the **University of Algarve** for providing the resources and facilities necessary for conducting this research. I would like to acknowledge my family for their unwavering support, encouragement, and understanding during the challenging moments of this academic journey. Your belief in my abilities and your unconditional love have been a constant source of motivation. I am also grateful to the members of my thesis committee, for their valuable insights, constructive critiques, and the time they invested in reviewing and evaluating this work. Your diverse perspectives enriched the quality of this research.

To my friends specially, **Sarah Iqbal**, **Saman Chaudhary** and **Aqsa Zainab** and to my colleagues **Ze Matos**, **Isabel Matos** and in particular, **Amponsah Preko Appiah**. Your encouragement and willingness to lend a helping hand during this endeavour are deeply appreciated. Finally, I want to express my gratitude to all the participants and individuals who contributed their time, knowledge, and insights to this study specially, **Professor Maria Clara Costa** for providing me unstoppable facilitation and **Marta Valente** who supported my internship and thesis completion. Without their cooperation, this thesis would not have been possible. In conclusion, the knowledge and skills acquired during this journey will serve as a solid foundation for future academic and professional endeavors therefore, I am truly grateful to European Union for this incredible Scholarship as an opportunity to contribute to the field of Quality in analytical laboratories.

Sincerely,

Sadaf Almas

Dedication:

I dedicate this thesis to my father **Muhammad Zaman**, and mother **Shameen Akhtar** for having faith in me and my abilities and always motivating to be the best version of me.

List of Figures:

List of Tables:

Abbreviations:

Polyoxometalates	POMs	$K_9(C_2H_8N)_5[H_{10}Se_2W_{29}O_{103}]$	Se_2W_{29}
Escherichia coli	*E. coli*	Tryptic soy broth	TSB
$(Hnic)_2\{[Co(H_2O)_3(nic)_2]_2[\mu V_{10}O_{28}]\}.6H_2O$	$Co(nic)V_{10}$	$\{[Co(H_2O)_4]_2[Co(H_2O)_2(\mu\text{-}pyz)_2][\mu\text{-}V_{10}O_{28}]\}\cdot 4H_2O$	$Co(pyz)V_{10}$
$(NH_4)_{14}[NaP^{V}_5W^{VI}_{30}O_{110}]\cdot 31H_2O$	P_5W_{30}	Phosphate-buffered saline	PBS
$[Cu(phen)(H_2O)(Mo_3O_{10})]$	$Cu(phen)\ Mo_3$	$[H_4W_{12}O_{40}]$	W_{12}
$[Mo_{72}Fe_{30}O_{252}(CH_3COO)_{12}\{Mo_2O_7(H_2O)\}_2\{H_2Mo_2O_8(H_2O)\}(H_2O)_{91}]$	$Mo_{72}Fe_{30}$	$(TEAH)_6[H_2VMo_{17}O_{54}(VO_4)_2]$ $(C_{36}H_{96}N_6Mo_{17}V_3O_{80})$	
Antibiotic-resistant genes	ARGs	Plasma membrane Ca^{2+} ATPase	PMCA
Antimicrobial resistance	AMR	Gold nanoparticles	AuNPs
ATP-binding cassette	ABC	Federal Drug Administration	FDA
Bacille Calmette-Guerin	BCG	Alanine aminotransferase	ALT
Bacillus cereus	*B. cereus*	Muller Hinton agar	MHA
Bacillus subtilis	*B. subtilis*	Muller Hinton broth	MHB
Bis(N-hydroxylamidoiminodiacetato)vanadium(IV)	HAIDA- V(IV)	Nuclear magnetic resonance spectroscopy	NMR
Circulating tumor DNA	ctDNA	Maximum velocity	Vmax
Clostridium difficile infections	CDI	Potassium Chloride	KCl
Colony forming units	CFU	Pyruvate kinase	PK
Community-associated- Methicillin-Resistant Staphylococcus aureus	CA-MRSA	Polyoxometalates- Ionic liquids	POM-ILs
Deoxyribonucleic acid	DNA	International unit	IU
Differentially expressed genes	DEGs	Flavin mononucleotide	FMN
Double- Minimum inhibitory concentration	2x MIC	Lactate dehydrogenase	LD
Enterobacter faecalis	*E. faecalis*	Methyl methacrylate	PMMA
Enterobacter faecium	*E. faecium*	Lauria-Bertani agar	LBA
Extensively drug-resistant	XDR	Silver phosphotungstic acid	AgPW
Fifty percent effective time	ET_{50}	Phosphoglycerate mutase	dPGM
Fifty percent growth inhibition	IG_{50}	Phosphatase	PhoE

Fifty percent inhibitory concentration	IC_{50}	Glutathione	GSH
Galleria mellonella	*G.mellonella*	Adenosine triphosphatase	ATP
$H_2CoTiW_{11}O_{40}$	$CoW_{11}Ti$		V_4O_{12}
$H_3PW_{12}O_{40}$	PW_{12}	$H_3PMo_{12}O_{40}$	PMo_{12}
$H_4SiMo_{12}O_{40}$	$SiMo_{12}$	$K_7[PTi_2W_{10}O_{40}]$	PTi_2W_{10}
$H_4SiW_{12}O_{40}$	SiW_{12}	Tetrabutylammonium salt - TBA4$H_5[PMo_6V_6O_{40}]$	PV_6Mo_6
$H_5PMo_{10}V_2O_{40}.32H_2O$	$Mo_{10}V_2$	$K_5H(PV_4W_8O_{40}).8H_2O$	PV_4W_8
$H_6[P_2Mo_{18}O_{62}]$	P_2Mo_{18}	$H_3[PMo_{12}O_{40}]$	PMo_{12}
Half -Minimum inhibitory concentration	½ MIC	Nicotine amide dinucleotide hydrogenase	NADH
Helicobacter pylori	*H. Pylori*	Metronidazole	MTN
Horizontal gene transfer	HGT	Sodium/Potssium -ATPase	Na^+/K^+ ATPase
Human immunodeficiency virus	HIV	Aspartate aminotransferase	AST
Human umbilical vein endothelial cells	HUVEC	Mouse memory carcinoma	MM46
Immortalized human embryonic kidney cells	HEK293	Human malignant glioma cell	U251
$K_{10}(P_2W_{17}O_{61})$	P_2W_{17}	$Na_{12}[Cu_3(H_2O)_3(BiW_9O_{33})_2]$	Cu_3BiW_9
$K_{12}[(VO)_3(BiW_9O_{33})_2]$	BiW_9	$Na_{12}[Ni_3(H_2O)_3(BiW_9O_{33})_2]$	Ni_3BiW_9
$K_{13}[La(SiW_{11}O_{39})_2]$	$LaSiW_{11}$	$K_{13}[Ce(SiW_{11}O_{39})_2]$	$CeSiW_{11}$
$K_{14}[As_2W_{19}O_{67}(H_2O)]$	As_2W_{19}	Bis(maltolato)oxovanadium (IV)	BMOV
$K_{27}[KAs_4W_{40}O_{140}]$	As_4W_{40}	$K_{18}[KSb_9W_{21}O_{86}]$	Sb_9W_{21}
$K_5MnV_{11}O_{33}.10H_2O$	MnV_{11}	$K_7MnV_{13}O_{38}.18H_2O$	MnV_{13}
$K_5PW_{11}TiO_{40}\cdot 14H2O$	$W_{11}Ti$	$Na_7CeW_{10}O_{35}$	CeW_{10}
$K_6(P_2W_{18}O_{62})$	P_2W_{18}	$Cs_{5.6}H_{3.4}PV_{14}O_{42}$	PV_{14}
$K_6[Mo_{18}O_{62}P_2]$	Mo_{18}	$K_{12}(P_2W_{15}O_{56})$	P_2W_{15}
$K_9H_5[\alpha\text{-}Ge_2Ti_6W_{18}O_{77}]$	$Ge_2Ti_6W_{18}$		
Lipopolysaccharide	LPS	United States dollar	USD
Listeria monocytogenes	*L. monocytogenes*	*N*, *N*, *N′*, *N′*-tetramethyl-*N″*, *N″*-dioctyl guanidinium	DOTMG-1
Methicillin-Resistant *Staphylococcus aureus*	MRSA	Polyoxovanadates	POVs

Methicillin-susceptible *Staphylococcus aureus*	MSSA	Polyoxomolybdates	POMos
Minimum inhibitory concentration	MIC	Phosphoenol pyruvate	PEP
$Mo_{154}O_{462}H_{14}(H_2O)_{70}$	Mo_{154}		
Mobile genetic elements	MGEs	Sarcoplasmic/endoplasmic reticulum Ca^{2+}-ATPase	SERCA
Molecular weight	MW	Centre of Disease Control	CDC
Moraxella catarrhalis	*M. catarrhalis*	Calcium Chloride	$CaCl_2$
Multidrug-resistant	MDR	Poly-dopamine	PDA
Mycobacterium bovis	*M. bovis*		
Mycobacterium smegmatis	*M. smegmatis*	Mycobacterium smegmatis	*M. tuberculosis*
Na_{12} $[Co_3(H_2O)_3(BiW_9O_{33})_2]$	Co_3BiW_9	Na_{12} $[Mn_3(H_2O)_3(BiW_9O_{33})_2]$	Mn_3BiW_9
$Na_{12}[H_4W_{22}O_{74}]$	W22	$H_2P_2W_{12}O_{48}$	P_2W_{12}
$Na_6[TeW_6O_{24}]$	TeW_6	Decaniobdate	Nb_{10}
Na_9 $[Fe_3^{III}(H_2O)_3(BiW_9O_{33})_2]$	Fe_3BiW_9	$H_3P_2W_{15}V_3O_{62}$	$P_2W_{15}V_3$
$Na_9[B\text{-}\alpha\text{-}AsW_9O_{33}]$	AsW_9	$Na_{10}[\alpha\text{-}SiW_9O_{34}]$	SiW_9
Optical density	OD	Rat pheochromocytoma cell	PC12
Penicillin-binding protein	PBP	American-type culture collection	ATCC
Polymerase chain reaction	PCR	Decavanadate	V_{10}
Polysaccharide intercellular adhesin	PIA	human breast cancer cell line	MDAMB-231
Pseudomonas aeruginosa	*P. aeruginosa*	Sodium Chloride	NaCl
Quorum sensing	QS	World health organization	WHO
Reactive oxygen and nitrogen species	RNS	Eudesmic acid	EU
Reactive oxygen species	ROS	Virus like particles	VLPs
Ribonucleic acid	RNA	Michaelis constant	Km
Save our souls	SOS	Carnitine palmitoyl transferase	CpTi
Staphylococcal Chromosome Cassette mec	SCC*mec*	Antibiotic resistance	ABR
Staphylococcal epidermidis	*S. epidermidis*	Magnesium Chloride	$MgCl_2$
Staphylococcus aureus	*S. aureus*	Amino-methyl benzoxyl- N-acylureido	AMB-acy

Staphylococcus aureus	*S. aureus*	Polyoxotungstates	POTs
Streptococcus albicans	*S. albicans*	Brain and Heart infusion	BHI
Streptococcus pneumoniae	*S. pneumoniae*	Lauria-Bertani medium	LBM
Tunsgtophosphoric acid	WPA	Poly-4-vinyl pyridine	P4VP
$V_{10}O_{28}$	V_1	$[V_{15}O_{36}(CO_3)]$	V_{15}
Vancomycin resistant-Staphylococcus aureus	VRSA	Metal-organic cages	MOCs
Verocytotoxin-producing Escherichia coli	VETC	4-(2-hydroxyethyl)-1-piperazineethanesulfonic acid	HEPES
Vertical gene transfer	VGT	Secretory pathway Ca^{2+}-ATPase	SPCA

Abstract

The current study addresses the urgent problem of antibiotic resistance and investigates the potential of metal-based compounds as antibacterial agents to combat important bacterial pathogens. Five Polyoxometalates (POMs), $Mo_{17}V_3$, PV_2Mo_{12}, $Mo_{10}V_2$, Co(pyz)V_{10}, Co(nic)V_{10} and one metal complex $V_5P_4O_{35}C_{14}N_6H_{52}$**,** were examined for antibacterial activity, yet none exhibited any antibacterial effects against *Staphylococcus aureus* ATCC6538 and *Escherichia coli* DSM1077. The research also explored the osmotolerance of the methicillin susceptible *S. aureus* ATCC 6538 and the methicillin resistant *S. aureus* (MRSA16) in response to different NaCl concentrations. Both *S. aureus* strains demonstrated dose-dependent responses to salt, with increased susceptibility at 1.5%, 3%, and 4% salt concentrations, elevated susceptibility at 7%. These findings shed light on how *S. aureus* strains adapt to salt stress and its potential implications for antibiotic resistance and growth kinetics. The antimicrobial properties of P_5W_{30} Preyssler-type polyoxometalates in combination with varying NaCl concentrations revealed that P_5W_{30} effectively inhibits *S. aureus* ATCC 6538, with a MIC of 32 μM, and MRSA16, with a MIC of 600 μM. These findings provide insights into P_5W_{30} potential for inhibiting bacterial growth and its interactions with salinity. The study also assessed the impact of salt and P_5W_{30} on virulence using *Galleria mellonella* larvae as an infection model against *S. aureus* ATCC 6538. The results showed that while larvae injected with control bacterial culture alone experienced a significant decrease in survival over five days (6.7% survival), in contrast the exposure of bacterials cells to the MIC value of P_5W_{30} (32 μM) enhanced the survival of larvae, reaching 26.7% by day-5. Furthermore, the research explored the inhibitory properties of $Mo_{17}V_3$, a molybdenum-based polyoxometalate (POMo), on $Ca2^+$-ATPase enzymes, with a specific focus on sarcoplasmic reticulum calcium ATPase (SERCA). It successfully determined an IC_{50} value of approximately 1.84 μM, demonstrating its superior inhibitory efficiency. The stability of $Mo_{17}V_3$ in experimental conditions, revealing its instability during a 2 hrs incubation at room temperature, potentially due to speciation or decomposition. A key point is $Mo_{17}V_3$ acts as a mixed-type inhibitor of SERCA, indicating direct binding and an impact on enzyme activity and indicating $Mo_{17}V_3$ as a promising mixed-type inhibitor of SERCA and highlights its potential in diverse biomedical applications.

1. Introduction

1.1. Emergence of Antibiotic Resistance

Bacterial infections continue to pose significant public health concerns globally due to their substantial morbidity and death rates.[1] Therefore, antibiotics have emerged as a vital resource in contemporary medicine, effectively preserving innumerable lives and assuming a pivotal function in medical interventions, such as cesarean deliveries and organ transplants.[2,3] Microbial contamination on surfaces is a prevalent issue encountered in the medical and food processing sectors.[3,4] Bacterial organisms include genetic processes that facilitate their ability to adapt and develop resistance against antibiotics. These mechanisms primarily involve genetic mutations occurring inside genes, as well as the acquisition of exogenous DNA through horizontal gene transfer. Mutations related with antibiotic resistance arise when bacterial cells undergo genetic modifications that impact the efficacy of the treatment, hence enabling their survival in the presence of the antibiotic. Conjugation, plasmids, transposons, and integrons play significant roles in facilitating the transmission and accumulation of genes associated with antimicrobial resistance, hence contributing to the process of bacterial evolution.[5]

Bacteria have developed intricate mechanisms of drug resistance in order to prevent the lethal effects of antimicrobial compounds, a phenomenon that is believed to have occurred through extensive periods of evolution spanning millions of years. In **Figure 1**, the main mechanisms involved in antibiotic resistance in bacterial cells are illustrated. Firstly, bacteria develop resistance to antibiotics by producing enzymes that modify or destroy the antibiotic molecule, rendering it ineffective. Enzymatic modifications of antibiotics commonly involve acetylation, phosphorylation, and adenylation reactions, leading to steric hindrance and reduced drug efficacy. Aminoglycoside-modifying enzymes are a prominent example of drug modification resistance.[5,6] The main mechanism of β-lactam resistance is the destruction of the antibiotic molecule by β-lactamases, which break the amide bond of the β-lactam ring. Newer generations of β-lactams are constantly being developed, but bacteria quickly evolve enzymes to destroy these compounds, leading to antibiotic resistance.[5,6]

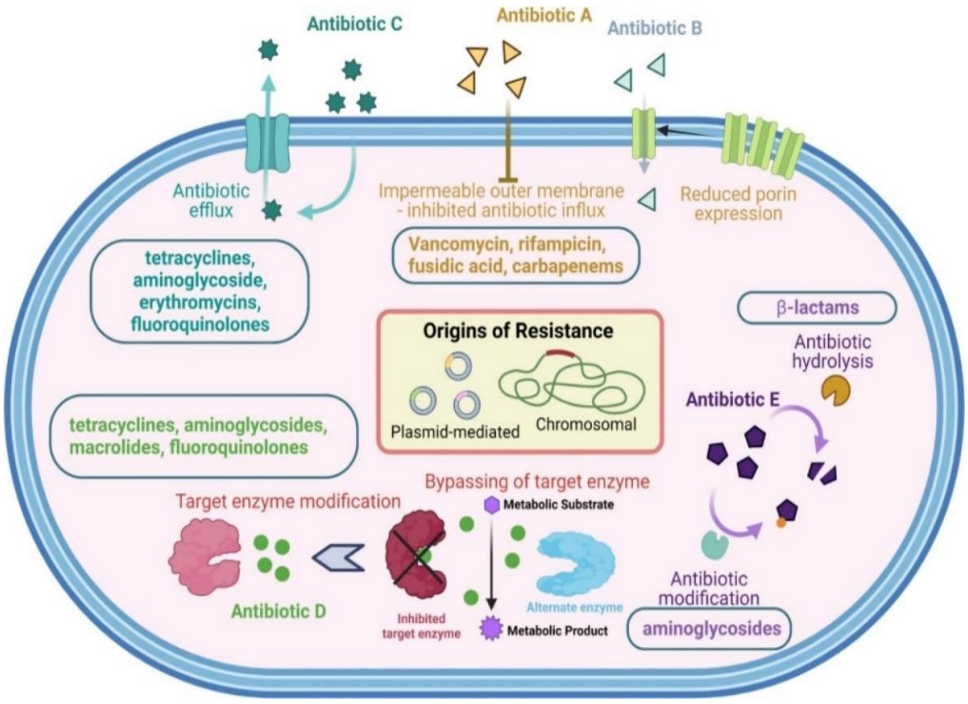

Figure 1- *Antibiotic resistance mechanism: Antibiotic A shows bacterial intrinsic resistance to hydrophilic medicines due to their inability to permeate the channel-like outer membrane porin proteins, which facilitate the passage of smaller hydrophilic antibiotics across the membrane. Antibiotic B shows the lowering porin downregulation or replacing porin with more selective channels might lessen the amount of antibiotics that permeate the outer membrane of membranes that contain lipopolysaccharides. Antibiotic C shows the efflux pumps, which actively transport different medications out of the cell. Antibiotic D shows the bacteria alter the structure of target proteins, preventing effective antibiotic binding, allowing the bacteria to continue functioning normally and potentially spreading quickly. Antibiotic E shows the enzyme-catalyzed modification of antibiotics.*[6]

Secondly, antibiotics must penetrate the outer and/or cytoplasmic membrane to exert their antimicrobial effect. Gram-negative bacteria have developed mechanisms to decrease the uptake of antibiotics, limiting their effectiveness.[5,6] Changes in permeability of the outer membrane can affect the efficacy of certain antibiotics, such as β-lactams and tetracyclines. Alterations in porins, which are proteins that facilitate the entry of antibiotics into bacteria, can lead to low-level resistance and are often associated with other resistance mechanisms.[5,6] Thirdly, efflux pumps are bacterial machinery that can extrude toxic compounds out of the cell, leading to antimicrobial resistance.[5–8] There are many classes of efflux pumps found in both Gram-negative and Gram-positive pathogens, with some being substrate-specific and others having broad substrate specificity.[5–8] Efflux pumps can be encoded in mobile genetic elements (MGEs) or in

the chromosome, and chromosomally encoded pumps can explain inherent resistance in certain bacterial species.[5–8] Fourthly, bacteria develop antimicrobial resistance by interfering with the action of antibiotics on their target sites. They achieve this through tactics, such as protecting the target site and modifying the target site to decrease affinity for the antibiotic. [5–8] Tetracycline resistance determinants Tet(M) and Tet(O) dislodge tetracycline from its binding site on the ribosome, preventing rebinding of the antibiotic. [5–8] Fifthly, modification of the target site is a common mechanism of antibiotic resistance in bacterial pathogens, involving point mutations, enzymatic alterations, or replacement of the original target. [5–8] Rifampin resistance is an example of mutational resistance, where single-step point mutations in the *rpoB* gene decrease the drug's affinity for its target but spare the catalytic activity of the polymerase. [5–8] Finally, enzymatic alteration of the target site can lead to resistance, such as methylation of the ribosome catalyzed by *erm* genes, resulting in macrolide resistance.[5–8]

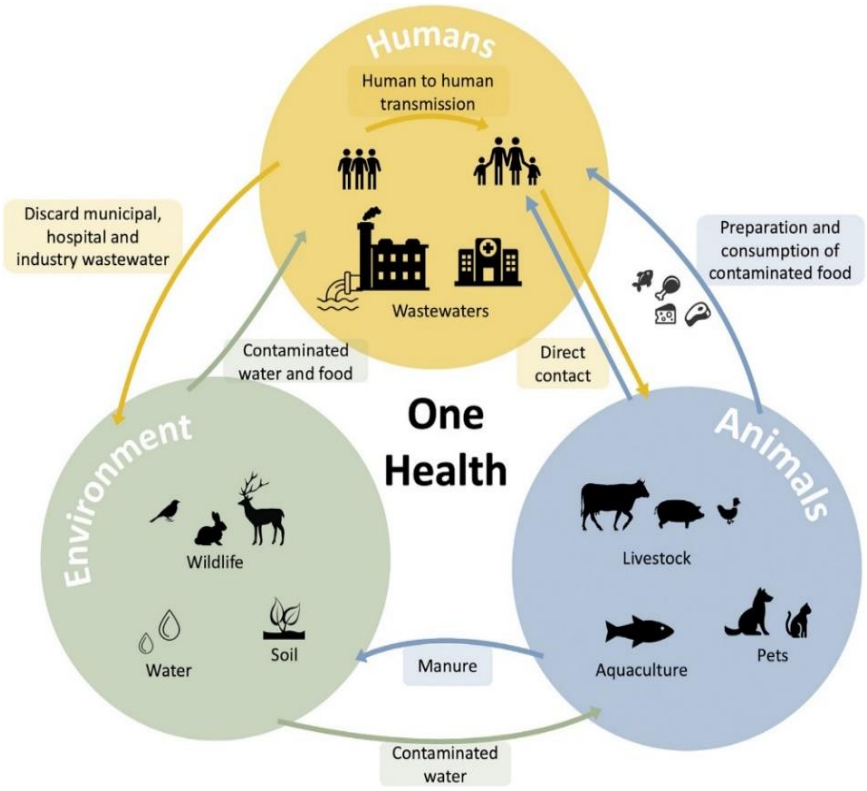

Figure 2- *Antibiotic resistance dynamics under one health concept shows that the transmission of antibiotic resistance from inherently resistant to susceptible bacterial populations is a critically significant factor in the preservation of human, animal*

The development of antibiotic resistance in bacteria can also occur in the process of attachment to surfaces with the formation of an aggregate (biofilm) in which the microbial members display a different phenotype, including becoming resistant to antibiotics and other antimicrobial

agents.[2,3] Antibiotic resistance arising in both human and veterinary medicine is a significant concern in the healthcare field. The improper utilization of antibiotics renders the treatment of bacterial diseases challenging.[2,8] As shown in **Figure 2**, the discharge of antibiotics into agricultural soils through irrigation with treated wastewater and land application of biosolids and animal manures can promote antibiotic resistance in soil bacterial communities and turn the treatment of human infections with make antibiotics ineffective.[9–11] Specific antibiotic kinds in saline soils are more important in showing antibiotic resistance responses to salinity. However, antibiotic bioavailability at various salinity levels in soils is poorly understood. Soil salinity can potentially reduce the bioavailability of dissolved antibiotics to microorganisms.[9] The primary incongruity of chronic infections lies in their enigmatic nature, predominantly attributed to the production of biofilms. Biofilms have been identified as the causative agents in around 60% of human infections.[2]

Similarly, food-borne illnesses are a global concern, with several drug-tolerant bacteria are also being a global concern.[12] Biofilms formed by food-pathogenic bacteria, such as *Staphylococcus aureus*, and *Pseudomonas aeruginosa* on food processing equipment offer up to 1000 times greater antibiotic resistance and tolerance than planktonic forms.[7,12,13] The food industry faces a significant issue with biofilm formation, a leading cause of secondary contamination. Research indicates that biofilms are an evident factor of bacterial resistance, which account for about 80% of microbial contamination in food processing equipment and raw materials.[12]

The economic impact of bacterial resistance is significant. According to a publication in the journal Health Affairs, it has been anticipated that if not adequately addressed, bacterial resistance might lead to an annual mortality rate of 10 million individuals and incur a financial burden of up to $100 trillion USD on the global economy by the year 2050.[14] In the report titled "Global Priority List of Antibiotic-resistant Bacteria for research, discovery, and development of new antibiotics," the World Health Organization (WHO) designates methicillin-resistant *S. aureus* (MRSA) and *Escherichia coli* as pathogens of high and critical risk.[15] Therefore, in this study, the focus will be given to Gram-positive *S. aureus and* Gram-negative *E. coli*. Hence, there is a heightened emphasis on the significance of the challenges being encountered by *S. aureus and E. coli*.

1.2. Critical Antibiotic Resistant Pathogens

1.2.1. *Staphylococcus aureus*

Staphylococcus aureus exhibits a positive reaction to the Gram stain, possesses catalase activity, and can display resistance to different antibiotics. *S. aureus* is a nonmotile, tiny, spherical

bacterium (cocci) that, when observed under a microscope, is grouped in pairs, short chains, or clusters that resemble grapes.[16–19]

1.2.1.1 Taxonomy

According to comparative oligonucleotide analysis of the *16S rRNA* gene and DNA-ribosomal RNA (rRNA) hybridization, *Staphylococcus* constitute a cohesive genus-level group. This genus is part of the larger Bacillus-Lactobacillus-Streptococcus cluster, which is used to describe Gram-positive bacteria with low DNA G + C percentage. A minimum of 30 *Staphylococcus* species have been identified using biochemical profiles. Eleven of these can be kept apart from people and function commensally however, the most pathogenic potential is shared by the common commensals *S. aureus* and *S. epidermidis.*[138]

1.2.1.2 Growth Characteristics

The growth and survival of *S. aureus* are influenced by a variety of environmental parameters, including temperature, water activity (a_w), pH, oxygen levels, and food content. However, for many *S. aureus* strains, these physical growth characteristics change. *S. aureus* may grow in a temperature range of 7 to 48 °C, with an ideal temperature of 37 °C. *S. aureus* can withstand freezing temperatures and thrive in food kept below -20°C, however, viability is diminished at temperatures between -10 and 0°C. In the course of pasteurization or cooking, *S. aureus* is easily eradicated. In the pH range of 4.0 to 10.0, with an optimum of 6-7, S. *aureus* grows.[20] *S. aureus* has a special tolerance for challenging circumstances, such as low a_w, high salt content, and osmotic stress. Numerous substances build up in the bacterial cell in reaction to low a_w, lowering the intracellular a_w to match the exterior a_w.[21] Therefore, *S. aureus* strains are generally quite tolerant of salts and sugars.[19] The strains can endure temperatures of 50 °C for 30 minutes and are comparatively resistant to drying. It thrives in culture media with 9% sodium chloride, and some strains may even grow in media with higher sodium chloride levels.[22] As a result, the majority of *S. aureus* strains are capable of growing over an a_w range of 0.83 to >0.99.[19] Despite being a weak competitor, *S. aureus* may thrive in a variety of foods.[21] This includes meals that are high in osmotic and pH stress. Being a facultative anaerobe, *S. aureus* may flourish in both aerobic and anaerobic environments. However, growth moves forward much more slowly in anaerobic environments.[20] The organism is obtained through the process of streaking material derived from the clinical specimen or blood culture onto solid media, like blood agar, tryptic soy agar, or heart infusion agar.[137] In order to facilitate the growth of halo-tolerant *staphylococci*, specimens that are prone to contamination with other bacteria can be cultured on mannitol salt agar supplemented with 7.5% sodium chloride.[137]

1.2.1.3 Ecology

Bacteria of the genus Staphylococcus are widely distributed and pose a significant challenge in terms of complete eradication from the environment.[19] It is frequently seen as a colonizer of the human body. These bacteria are commonly present on mucosal surfaces, such as the nares, throat, and rectum, as well as in moist areas of the skin, such as the axilla, groin, and perineum.[16–18] It is typically harmless as a commensal organism, but when it penetrates the bloodstream or tissues, it can become pathogenic and cause a variety of infections, from minor skin infections to life-threatening diseases.[23–25] *S. aureus* is a prevalent bacterium frequently acquired in hospital settings. *S. aureus* is capable of causing infection in both animals and humans, and its survival is limited to dry skin. The transmission of the disease can occur via contaminated surfaces, airborne particles, and human-to-human contact. *S. aureus* is known to asymptomatically colonize the skin of human hosts, affecting approximately 30% of the normal healthy population. While many instances of host colonization may have a benign nature, the introduction of this bacterium into a wound through a puncture or break in the skin can lead to the development of infections.[138]

1.2.1.4 Infections by *S. aureus*

S. aureus is well-known for its propensity to induce various superficial skin diseases in humans, such as boils, furuncles, styes, and impetigo.[26] Additionally, it has the potential to result in more severe infections, particularly in individuals who are weakened by chronic diseases, traumatic injuries, burns, or immunosuppression.[26] The aforementioned illnesses encompass pneumonia, deep abscesses, osteomyelitis, endocarditis, phlebitis, mastitis, and meningitis.[26] These conditions are frequently linked to patients receiving hospital care, as opposed to persons in the general population who are in good health. *S. aureus* and *S. epidermidis* are frequently implicated in infections that are linked to the presence of indwelling medical equipment, including joint prostheses, cardiovascular devices, and artificial heart valves.[26]

1.2.1.5 Adherence of *S. aureus*:

The cells of *S. aureus* exhibit the expression of surface proteins that facilitate the adherence to host proteins, including laminin and fibronectin, which are integral components of the extracellular matrix.[137] Fibronectin is found on the surfaces of epithelial and endothelial cells, and it is also a constituent of blood clots. Furthermore, the majority of strains exhibit the presence of a fibrinogen/fibrin binding protein, commonly referred to as the clumping factor, which facilitates adherence to both blood clots and damaged tissue.[137] The majority of *S. aureus* strains exhibit the expression of proteins that bind to fibronectin and fibrinogen.[137]

1.2.1.6 Virulence of *S. aureus*

The α-toxin of *S. aureus* is widely recognized as a significant virulence factor in the context of skin infections. The secretion of water-soluble monomeric pore forming toxin, predominantly composed of beta sheet, is a characteristic feature of most strains of *S. aureus* and this toxin specially targets red blood cells.[27] Panton-Valentine leukocidin is a potent cytotoxin consisting of two protein components that can cause lysis of neutrophils, leading to dermonecrosis, chronic skin and soft tissue infections, recurrent mucocutaneous infections, and necrotizing pneumonia. *S. aureus* produces various exoproteins, including *staphylococcal* enterotoxins, exfoliative toxins, leukocidin, toxic shock syndrome toxin, and pyrogenic toxin superantigens.[27] A sphingomyelinase called β-toxin harms membranes that contain an excessive amount of this lipid.[27] Most strains of *S. aureus* produce the little peptide toxin known as "δ-toxin¨.[27] Two-component protein toxins that harm the membranes of sensitive cells include the leukocidins and the γ-toxin.[27] Although the proteins are expressed independently, they work together to harm membranes.[137] The quorum-sensing system of *S. aureus* includes an accessory regulatory factor (Agr) system and LuxS/AI-2 system that allow it the regulation of these virulence factors.[28,29]

1.2.2 Methicillin-resistant *Staphylococcus aureus* (MRSA)

MRSA can refer to any strain of *S. aureus* that has developed resistance to penicillin, methicillin, or cephalosporin antibiotics over time.[30] The virulence and transmission of *S. aureus* and MRSA strains are impacted by a variety of genetic and molecular variations. MRSA genotypes have grown increasingly virulent because MRSA contains numerous pathogenicity islands, a family of genetic mobile elements.[30,31] In addition to encoding genes, such as enterotoxin C, MRSA encodes superantigen genes. A key difference between strains of *S. aureus* and MRSA is the acquisition of the *mecA* gene, which is located on a large mobile genetic element called *Staphylococcal Chromosome Cassette mec* (SCC*mec*), of which there are at least 12 distinct varieties.[30–32]

1.2.2.1 Multi-drug Resistance

MDR is defined as resistance to at least three classes of antimicrobials.[25] MRSA is resistant to all β-lactam antibiotics except to the fifth generation, limiting treatment options.[16,33] Additionally, these strains often have resistance to other antibiotic groups, earning the name “superbug” fifth generation. Methicillin resistance is caused by changes in penicillin-binding proteins caused by *mecA* or *mecC* genes. MRSA was initially connected with nosocomial infections, but 20–30 years later, community-associated MRSA (CA-MRSA) infections started

emerging.[16,33] One public health threat is MRSA is developing resistance to various drug classes. Therefore, *S. aureus* treatment must be sought.[34]

1.2.2.2 Severity of MRSA

The WHO listed MRSA among the 12 deadliest and most drug-resistant bacteria.[34–36] Among these, *Staphylococcus* spp, notably vancomycin, and methicillin-resistant staph infections, pose a significant threat because of their multi-resistant patterns and ability to attach to surfaces.[23,37] MRSA is a highly resistant strain of bacteria leading to increased mortality, morbidity, and healthcare costs.[23–25] The bacterium is known to induce a variety of ailments, spanning from minor dermatological conditions like pimples, impetigo, boils, cellulitis, scalded skin syndrome, folliculitis, furuncles, carbuncles, and abscesses, to severe and potentially fatal diseases, such as pneumonia, osteomyelitis, meningitis, Toxic Shock Syndrome, endocarditis, and septicemia.[25] Recent evidence indicates that 60% of the population is transiently colonized, whereas 30% is persistently colonized.[34,38] *S. aureus*, including Methicillin-Susceptible *S. aureus* (MSSA) and MRSA, is a highly effective and adaptable organism that causes community-associated and nosocomial infections.[33,39]

Neopane et al. 2018 [40] evaluated S. *aureus* from sputum samples with increased antibiotic resistance as 86.7% of *S. aureus* isolates were multidrug-resistant.[40] Dash et al. 2023 [41] assessed that 11.7% of blood samples were positive for bacterial growth, and *S. aureus* was discovered in the majority of the samples of febrile patients. *S. aureus* was resistant to penicillin, ampicillin, erythromycin, and azithromycin in a large percentage of isolates.[41] In a recent study by Mastoor et al. 2022 [36], clinical isolates of *S. aureus* were collected from diagnostic centers and most of the isolates were multidrug-resistant, with 53.1% and 34.3% of isolates resistant to ciprofloxacin and ampicillin, respectively. Gentamicin and chloramphenicol-sensitive *S. aureus* isolates were 93.7% and 90.6%, respectively.[36] Moreover, in a recent study, there were notable variations seen among isolates of MSSA and MRSA in terms of their susceptibility to routinely employed antibiotics. In the CV tube adherence assay was performed to evaluate the adherence of bacterial cells aggregates with the help of 0.1% crystal violet, it was observed that 37% of isolates were of MSSA and 39% were of MRSA. Similarly, when Congo red agar plates were employed, 41% of isolates were MSSA and 44% of MRSA. The prevalence of *S. aureus* isolates was highest among cases with catheter-associated infections.[42]

Nevertheless, there are significant geographical variations in the prevalence of MRSA infections. In Northern Europe, the prevalence ranges from approximately 1% to 10%. In the United States, it ranges from 15% to 30%. In Southern and Eastern Europe, the prevalence is higher, ranging from 40% to 50%.[16,17] In certain regions of Asia, the prevalence may surpass 80%. There are

several risk factors that are related to the acquisition of an MRSA infection.[16,17] These include being of advanced age (≥60 years), having a lengthy hospital stay, receiving prior antimicrobial therapy, and using nasogastric tubes or endovascular catheters. MRSA infections have been found to be linked with a decline in quality of life, increased death rates, and significant financial burdens.[16,17]

1.2.3 *Escherichia coli*

Escherichia coli is a Gram-negative bacterium that resides as a commensal organism within the intestinal tracts of both humans and animals. It is a member of the *Enterobacteriaceae* family that resides primarily in the lower gastrointestinal tract of mammals.[43,44] *E. coli* has the potential to result in several ailments, including intestinal and extra-intestinal infections, urinary tract infections, stomach infections, meningitis, peritonitis, and septicemia.[43]

1.2.3.1 Multidrug Resistance in *Escherichia coli*

In *E. coli*, certain genes play a crucial role in enhancing the bacteria's survival. For instance, *Rec A* is responsible for detecting DNA damage and then initiating its activation.[45] The use of quinolone antibiotics leads to the inactivation and hydrolysis of *Lex A* protein involved in DNA repair mechanism resulting in the inhibition of cellular division.[2] Furthermore, to provide resistance to the external environment microbes develop physio-mechanical linkages by self-aggregating.[45] Curli fibers dominate *E. coli* biofilms where *csgBAC* encodes *CsgB* and *CsgA* for these fibers. The operon csgDEFD yields CsgE, F, D, and G, however CsgD controls cellulose and curli fibers, while CsgG translocates CsgA. β-sheet curli fibers abound the protein network for protection. BcsABZC controls cellulose synthase hence, cellulose imparts rigidity and provides protection against damaging environmental conditions.[45]

E. coli's dynamic ability to exchange genetic-resistant genes among themselves, as well as other factors, such as mutations, antibiotic use, and negligence has raised the ABR challenge. Recent research findings illustrated a direct association between the existence of MDR or extensively drug-resistant (XDR) phenotypes and the ability to produce bacterial clusters in isolates of *E. coli*. Additionally, an association is shown between the creation of biofilms and the development of resistance to certain antibiotics, including cefoxitin, ceftriaxone, cefazolin, and gentamicin.[43] Pathogenic and antibiotic-resistant *E. coli* cause diseases, such as the notoriously fatal hemorrhagic uremic syndrome, hemorrhagic colitis, and diarrhea, and in some cases are responsible for medical treatment failures.[44]

In a study by Kichana et al. 2022 [44] , a high incidence of MDR- *E. coli* was noticed in 48.7% of the isolates. The fact that the isolates displayed absolute resistance to certain antibiotics and a

high level of multidrug resistance suggests that antibiotics may have been misused or overused in the study area.[44] In the study by Abalkhail et al. 2022 [46], an extended spectrum beta lactamse-*E. coli* was found in 33.49 percent of *E. coli* isolates, with a higher prevalence among women (67.27%), in contrast with men (33.79%). However, the strains were sensitive to carbapenems, aminoglycosides, and nitrofurantoin.[46] Moreover, another study by Jain el at. 2021[47], an investigation was done with 100 clinical *E. coli* isolates, and it was found that 98% of them were MDR. PCR analysis revealed the presence of metallo-β-lactamase gene *bla* NDM (80%), ESBL genes *bla* OXA (48%) and *bla* CTX-M-15 (32%), *ampC* gene (68%), and *tetC* gene (32%) among the isolates. High resistance rates, inadequate antimicrobial resistance (AMR) surveillance, and irrational use of antibiotics indicate an alarming situation.[47]

1.3. Antibiotic Resistance as an Emanate Challenge

Antimicrobial resistance is driven by various factors including environmental, drug-related, patient-related, and physician-related factors.[10,11] Misuse and overuse of antibiotics in both humans and animals, misconceptions about antibiotics, lack of adequate diagnostic facilities, unnecessary prescription of antibiotics by physicians, and significant rise in antibiotic consumption to improve the quality of life have accelerated the development of antibiotic resistance.[10,48] The emergence and spread of new resistant mechanisms pose a significant threat to the effectiveness of treatment for common illnesses, such as urinary tract infections, upper respiratory tract infections, typhoid, and influenza, leading to treatment failure, permanent disability, or even death.[49] The success of cancer chemotherapy, transplantation surgery, and even minor dental procedures is at serious risk due to antimicrobial resistance unless new drugs are developed.[10,11] Infections caused by antimicrobial-resistant organisms necessitate prolonged treatment, resulting in higher healthcare costs and potentially requiring the use of expensive alternative drugs.[49] As per the ABR criticality the term "superbugs" is used to describe microorganisms that have demonstrated the ability to resist the effects of antimicrobial medications often employed in their treatment.[10,11] In actuality, there is a limited or negligible availability of therapeutic options for infections caused by antibiotic-resistant bacteria.[10,11]

Antimicrobial resistance genes are frequently associated with toxin-antitoxin systems, hence enabling their persistence even in the absence of therapeutic interventions. [2] In the era of DNA sequence data, the presence of antibiotic resistance gene (ARG) significantly impacts the ability of clinical bacteriology to deliver optimal treatment. [2] Anticipating the occurrence of resistance by horizontal gene transfer (HGT) during the first stages of antibiotic development poses an additional obstacle.[2] The comprehension of genotypes in order to exploit gaps in resistance to

phenotype is of utmost importance.[2] Hypoxia-induced antibacterial resistance in *P. aeruginosa* is a result of the modification of multidrug efflux transporters.[39,45,50] Due to a change in the expression of the multidrug efflux pump link protein, energy metabolism, and gene expression are downregulated.[16,45,50] The stress response of bacteria renders them resistant to oxidative stress, DNA damage, nutritional deficiency, temperature fluctuations, and low levels of water [2,7,16,39,45,50]. Due to alterations in DNA repair genes and oxidative stress, which can also promote antibiotic resistance with a higher mutation rate and increased likelihood of HGT.[2,36,45] In *P. aeruginosa* virulence genes are regulated by quorum sensing, and also biofilm formation, synthesis of protective molecules, response to antibiotic therapy and the innate immune system [2,36,45] Furthermore, the lack of worldwide statistical data on antibiotic use and the status of AMR hinders the implementation of intervention strategies.[10] Addressing the existing knowledge gap is crucial for successful intervention approaches involving various stakeholders to combat AMR.[10] Immediate actions are imperative in addressing AMR, encompassing the implementation of surveillance and monitoring systems, reduction of antibiotic utilization in healthcare and agriculture, provision of accessible and cost-effective medications, and strict enforcement of legislative measures.[10]

1.4. Strategies to Combat the Antibiotic Resistance

The issue of antimicrobial resistance poses a significant challenge for both the industrial and biomedical sectors. In order to address this pressing concern, alternative medicines that have been approved by the FDA for their anti-inflammatory, anticancer, and antidepressant properties, as well as non-antibiotic medicines, have shown potential in inhibiting bacterial and fungal infections.[7] Antivirulence drugs are a new type of medication that targets bacterial virulence factors instead of killing bacteria, preventing the establishment of infection, and reducing the likelihood of antibiotic resistance.[10] These drugs have been approved by the FDA for toxin-mediated diseases and have shown effectiveness against MRSA infections in mice, but they may be more suitable as a combination therapy with antibiotics due to development and clinical challenges.[10] Antibacterial strategies include chemical methods like antibiotics, peptides, and quaternary ammonium compounds, as well as non-chemical methods like nanotechnology-based nanostructures and external stimuli, such as light, electricity, magnetism, and heat-activated therapies. [45] Inducing transformation involves lowering bacterial adherence and viability and managing the unique bacterial-infected microenvironment.[45]

Bacteriocins are natural antimicrobial peptides produced by certain bacteria that can kill or inhibit the growth of similar or related bacterial strains.[10] Bacteriocins, such as nisin, have

potential as antibacterial therapy and are used in food production to prevent the growth of dangerous bacteria, extending the shelf life of food.[10] Nisin also shows antibacterial activity against drug-resistant pathogens.[10] Furthermore, QS system inhibitors, monoclonal antibodies, and natural items are being widely explored to disrupt and eradicate biofilms, which are one of the dominating reasons for ABR.[45] Interruption of microbial communication and adhesion with biomaterial-based medication delivery methods is advancing.[45,51] Due to their varied microbial biological processes, complexes are being used more to fight bacterial infections.[45,51] Similarly, metal complexes improve efficacy and minimize antibacterial resistance. Complexes can inhibit QS or microbial adherence as the positively charged chemicals can electrostatically interact with negatively charged biofilm components, such as polysaccharides, proteins, and DNA, boosting their anti-biofilm effectiveness. For example, metal ions interact with QS components, adhesins, or the exopolysaccharide matrix to remove biofilm. ROS and RNS from redox-active metal ions help combat bacterial infections therefore, incorporating such a molecule into organic or inorganic carriers is being explored.[51] Due to their multi-target, intricate mechanism, metal complexes are intriguing bacterial aggregates disrupting agents. The exploration of metal oxides as antibacterial agents has been undertaken in order to identify substances capable of impeding the progression of antibiotic resistance.[51]

Polyoxometalates (POMs) have been intensively investigated for their antibacterial activity against Gram-positive and Gram-negative reference strains, as well as bacterial strains resistant to a variety of antibiotics, including those in the β -lactam class (such as penicillins and cephalosporins), for over two decades.[52] The antibacterial effects of reduced POMs were seen on both *S. aureus* and *E. coli* bacteria. Treatment with reduced POMs, laser irradiation, and H_2O_2 resulted in a decrease in bacterial clusters.[13] Moreover, high concentrations of NaCl in culture broths osmotically stress microbial cells, causing a reduction in the turgor pressure of the cell membrane, the release of cytoplasmic water, and cell contraction.[53] Hence, there exists a necessity to explore alternate options to antibiotics, including chemicals derived from plants or metals that have the ability to combat antibiotic resistance.[10] As the challenging situation of antibiotic resistance is stated, there is an evident factor of the antibiotic targeting sites, which includes the ionic pumps of the cell membranes or subcellular organelles, in particular P-type ATPases.[54] Among these ionic pumps, the Ca^{2+} ATPases are of significant notice.

1.5. Antibiotic Targeting Site

1.5.1 Ca^{2+} ATPase Pumps:

Ca^{2+} ions are pivotal for the intracellular functions of the cells as they are the regulators of several metabolic and biochemical processes e.g., muscular contraction, photosynthesis, the plasticity of the synaptic, and apoptosis. At the cellular level, Ca^{2+} ions play an essential role in homeostasis, signaling, response to stress, motility, division, transpiration, host interaction, and secretion.[54] Homeostasis is maintained by several channels, ionic pumps, and exchangers, present in the cell membranes or sub-cellular organelles e.g., mitochondria, Golgi apparatus, sarcoplasmic reticulum, or endoplasmic reticulum. The P-ATPases play a specific role as the ion carriers and detoxifying function in the case of metal ions.[54] These ATPases are putative targets of some drugs to inhibit the ionic pumps, such as Na^{+}/K^{+} ATPases and Ca^{2+} ATPases. Several neurological disorders are linked with the malfunctioning of Sarcoplasmic/endoplasmic reticulum Ca^{2+}-ATPase (SERCA) and plasma membrane Ca^{2+} ATPase (PMCA), preventing the calcium ions homeostasis in particular diseases.[54,55] This is why finding P-type ATPase modulators is promising. In certain disorders, Na+/K+-ATPases and Ca^{2+}-ATPases inhibitors can avoid calcium homeostasis abnormalities.[54]

1.5.1.1. Types of Ca^{2+} ATPases

As the target of the drug, the P-type ATPases are well recognized as a good model to check the effect of the pump inhibitors.[56] PMCA, which pump the excessive Ca^{2+} ions out of the cell. SERCA, is the intracellular pump that accumulates the Ca^{2+} ion. It is important for maintaining the Ca^{2+} homeostasis and it is involved in the muscle relaxation process, cell death through apoptosis, necrosis, and diabetes. Secretory pathway Ca^{2+} ATPases (SPCA), is the intracellular pump that accumulates the Ca^{2+} ion.[55–57] **Figure 3**, depicts the SERCA function of healthy cardiac myocytes. Nevertheless, the primary emphasis of our investigation was directed towards Sarcoendoplasmic reticulum Ca2+ ATPases.

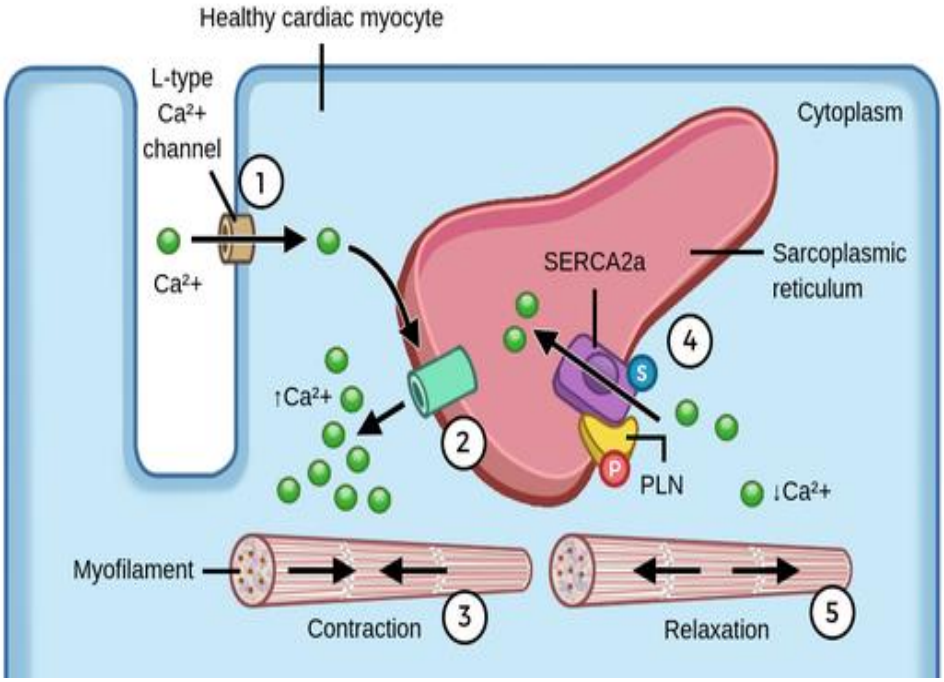

Figure 3- *Schematic depiction of SERCA2a's function in healthy cardiac myocytes. Ca^{2+} enters the cell during diastole and triggers the release of significant quantities of Ca^{2+} from the sarcoplasmic reticulum (SR) (2). This results in the contraction of the myofilaments (3). Simultaneously, SERCA2a is liberated from its inhibitor PLN and shuttles $CaCa^{2+}$ back into the SR (4), which relaxes the myofilaments (5).*[58]

An in-depth review has been conducted to examine the biological applications of POMs as an alternative drug target in the context of increasing antibacterial resistance, bacterial biofilm phenomena, and the understanding of common problematic bacteria, such as *E. coli* and *S. aureus*. The study further highlighted the significance of Ca^{2+} ATPAses as a proposed target for POMs. Acquiring a thorough comprehension of the intricate chemical and biological characteristics of POMs are of utmost importance. This knowledge is essential in order to effectively utilize POMs in mitigating the escalating issues associated with bacterial biofilm development and antibiotic resistance as these obstacles are prevalent in various domains, including industrial and medicinal industries.

1.6. Polyoxometalates

POMs are said to have magical qualities, and among those features, the most cutting-edge characteristics of POMs are highlighted in this study to focus on the necessity of using POMs as metallic medications to treat serious medical health and industrial problems.[57,59–68] POMs are a distinguished and chemically variable collection of anionic polynuclear metal oxide compounds containing transition metals, which can be molybdenum, vanadium, tantalum, tungsten, and nobelium, in the maximum oxidation state and covalently linked with oxygen atom.[57,59–68] The

POM structures can also be a combination of phosphorous, arsenic, or silicon, in addition to deletion or substation of metals e.g., manganese, or cobalt.[65] Iso-polyanions with the formula $[M_mO_y]^{n-}$ and hetero-polyanions with the formula $[X_xM_mO_y]^{n-}$ are the two main categories of the POMs.[60,61,66,67,69,70]

M = Addenda atom (W, Mo, V),

Whereas X= Central heteroatom (any other element).

As shown in **Figure 4**, Isopolyanions are commonly represented by the Lindqvist structure $[M_6O_{19}]^{n-}$ whereas Dawson $[X_2M_{18}O_{64}]^{n-}$, Anderson $[XM_6O_{24}]^{n-}$, and Keggin $[XM_{12}O_{40}]^{n-}$ are heteropolyanions are the common archetypes.[60,61,66,71]

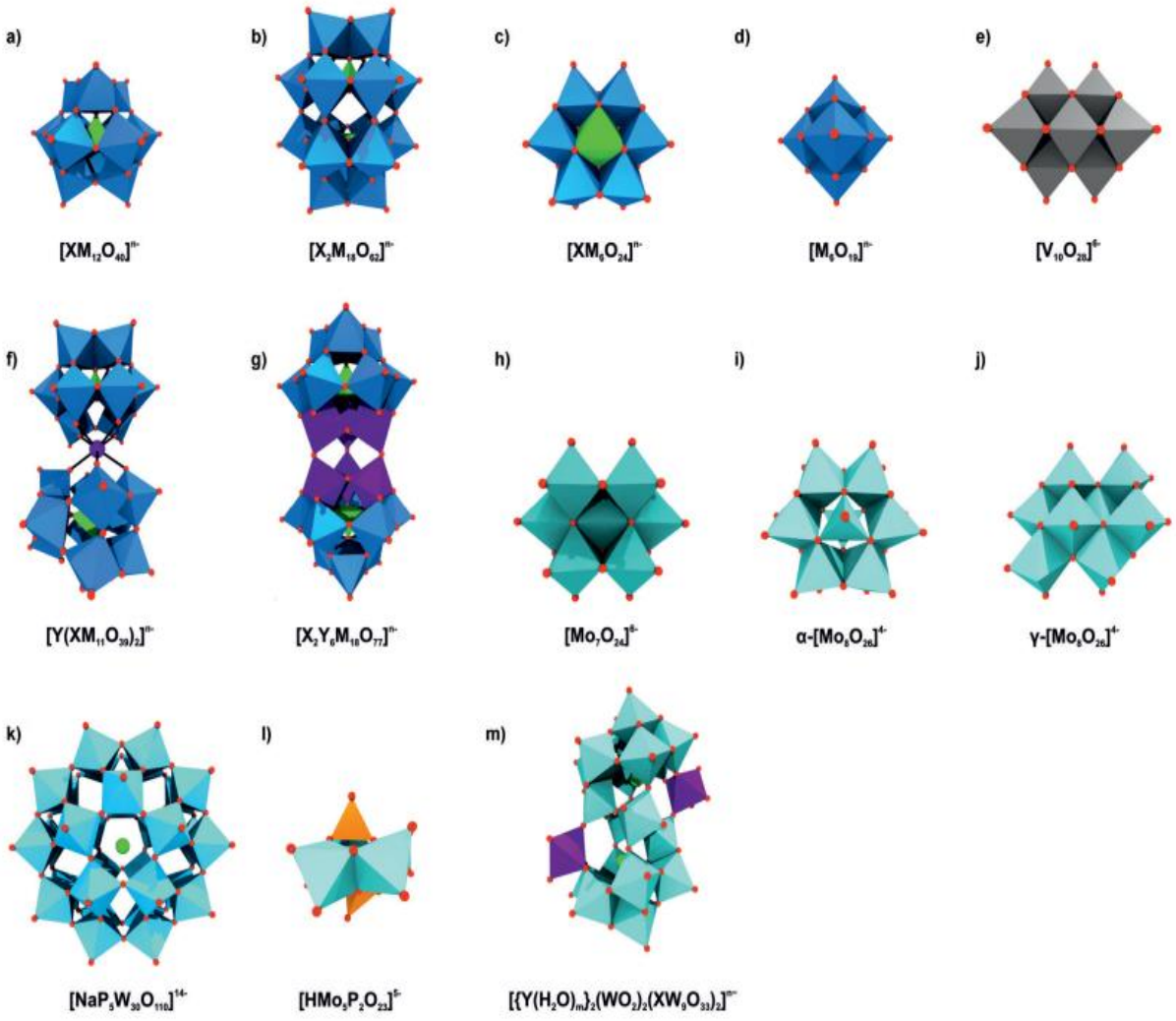

Figure 4- *A summary of typical POM archetypes. a) Keggin, b) Wells–Dawson, c) Anderson, d) Lindqvist, e) decavanadate, f) sandwich Keggin, g) double Keggin, h) heptamolybdate, i) a- and j) g-octamolybdate, k) Preyssler, l) Strandberg, and m) Krebs-type*[72]

1.6.1. Chemical Properties of POMs

The negative charge of the POMs, in combination with mixed cations e.g., amino acids, proteins, peptides, or surfactants, gives robust ionic interaction with the driving force of electrostatic interaction hence the new complexes are made.[60–62] The overwhelming characteristics of the POMs are their redox potential, shape, size, distribution of charge, Bronsted acidity, polarity, and solubility in water. Therefore, their acceptance of incorporating the transition metals in the structure has made them applicable in catalysis with, less toxicity for Human beings.[60–63,66,67,71,73–76] The POMs modification can increase reduction-oxidation properties, catalytic functions, conductive functions, enhancement of sensing chromophores signals, and alteration of certain chemical and geometric functional groups.[60–62,67,77] Over the last decade, the physiochemical properties of POMs have been applied in several research fields e.g., electrochemistry, photochemistry, catalysis, material science, metal-organic framework, and crystallography of proteins.[57,60,61,67–70,75,77,78] POMs have a chaotropic property with low charge density making them weak in hydration and retaining the potential to merge with organic moieties and biomolecules.[62,63] Nanostructured POMs in polymeric matrixes improve cell adhesion and bone tissue regeneration in healthy cell lines.[64,79]

1.6.2. Biological Properties of POMs

The biological activity of POMs was first studied in 1970, with the evaluation of silicotungstic acid enzymatic inhibition on sarcoma viruses and murine leukemia.[62,80] POMs can suppress the transcription and inhibit the binding of the virus to the host cell for penetration.[73] POMs inhibit aquaporins as hormone receptors (cell signaling), capsaes, glucosidases, polyphenol oxidases, phosphatases, kinases, ectonucleotidases, and histone deacetylases.[56,57,62,70,71,78] POMs can interact covalently with biological molecules with an alteration impact to enhance their benefits dramatically, such as synthetic nanocomposites and organic-inorganic hybrids which have important roles in developing therapeutic drugs.[61,63,66,69,71,76,77] There are several drugs targeting the pumping activity of Na^+/K^+-ATPase and in-vitro and in-vivo the activity of Ca^{2+}- ATPases (P- Type) which is of prime importance, biologically.[57,59] The big size of the POMs can induce its extracellular function in the cells impacting P-type ATPases and other associated enzymes including sialyl and sulfotransferases.[57,59,71] The isopolyoxovandate decavanadate (V_{10}) is significantly studied for biochemical processes and cellular functions. G-actin's structure is an essential protein in the biological system for muscle contraction, cell division, adhesion, and migration. Gumerova and Rompel 2020[81] showed that V_{10} binds to G-actin protein and inhibits the polymerization to F-actin which prevents the decomposition of V_{10}.

POMs' artificial metalloenzyme properties were checked for the hydrolysis of peptide bonds.[63,66,71] It is speculated that the POM activities in biological systems are due to electrostatic interaction with proteins or enzymes, which was witnessed by the crystallographic studies in terms of the negative charge of POM metal in junction with positive charges of proteins. However, enzyme inhibition can initiate the malfunctioning of the core cellular function.[69,76,77] They have the potential to cease respiration and there by disclosing antibacterial, antiviral, antiprotozoal, and antitumor attributes.[57,61,63–66,70,71,73,76–78,82]

1.6.3. Applications of the POMs

Metallic compounds have undeniably magical characteristics and have been pioneering in pharmacology since the 20th century. Due to the successful treatment of the first FDA-approved cisplatin, metallic drugs have captured attention, especially in the field of inorganic medicine chemistry.[62,73] The cost of POM synthesis is relatively less as compared to organic pharmaceuticals which is advantageous for POM's efficiency.[61,66,76] Hence, they have widespread environmental, biomedical, chemical, and industrial applications.[65,71] POMs have been studied to check the activity with diseases, such as Alzheimer's, inflammatory bowel disease, HIV, Covid, and diabetes.[56,61,62,65,75,78,83] POMs have solutions for environmental problems, such as water pollution, plastics, pesticides, and antibiotic degradation. Tungsten-based POMs degrade pesticides and medicines. Emerging contaminants are a potent reason for antibiotic resistance and cancer.[65]

As mentioned earlier, POMs have a wide range of applications. However, this discussion will mostly focus on the notable uses of POMs in molecular assemblies, drug delivery methods, and their effectiveness in combating tumors, viruses, and bacteria.

1.6.3.1 Molecular Assemblies of POMs

Organic or carbon-based materials often have a range of chemical tunability to allow for selected POM entities to attach in a controlled manner. POM anions' accumulation on inorganic substrates may profit from the higher hydrophilicity. Because of their comparable chemistry, metal oxides, for instance, might directly covalently link with POM clusters to join them to the M-O-M formation of bonds without linking organic groups.[66,67] Complex nanoparticles and antigens are being used as adjuvants in vaccines. It increases B-cell proliferation and antigen exposure to antigen presenting cells. Inorganic nanoparticles have adamant structures, longer shelf lives, adjuvant properties, and immunological roles.[84] Metal oxides exhibit synergism with antibacterial properties whereas synthetic metal organic cages (MOCs) with several organic-

inorganic hybrids and nanocomposites have improved biocompatibility and targeted activity in drug-delivery systems.[62,67,68,84] Encapsulating POMs in biomaterials and conjugating POMs with organic ligands, both of which increase the biocompatibility of the POMs, are two new directions in research that are expected to reduce POMs' toxicity. However, in-vitro studies have shown that POM is toxic therefore, selecting appropriate ligands is critical for maximizing synergistic effects.[61,62,68,75,85] Croce et al. 2019 [86], used P_2W_{18}, Sb_9W_{21} and Mo_7O_{24} POMs encapsulations were done into chitosan nanoscale composites which enhanced the specificity to the cancerous cells and IC_{50} value ensured the lower dose in the therapy. Similarly, chitosan imidazolium modification was used to entrap the $MnMo_6$ anion as an organic nanocomposite.[79,85] Enrique González-Vergara et al. 2019 [87] has studied the antidiabetic properties of V_{10} compounds, specifically metformin decavanadate hybrid did not show any toxicological effects in the liver and kidney, these in vivo results which reflect a potential good treatment in comparison with metformin alone. The POM, such as 12- tungsto-phosphoric acid is a potential catalyst in biomass fuel generation and inhibits the ATPase.[74]

1.6.3.2 POMs Potential in Drug Delivery

Nanoscale pores in the 3D structure of POMs can optimize drug delivery by increasing drug surface area and controlling drug dissolution.[64] Counter ions can transport drugs by molybdenum and tungsten-based nanosized species such artificial Kelperates like the twenty $\{Mo_9O_9\}$- type and Mo_{132}.[64] Metronidazole and its derivatives may also reach anti-cancer medication delivery targets. The compound Mo_{132} and metronidazole-loaded poly methyl methacrylate scaffolds can improve POM bioactivity and reduce toxic side effects, making POM therapy safer and more effective.[64] Nanoparticles containing POM can target tumours without spreading whereas chitosan could be an anionic drug carrier.[79] In direct drug and nanocontainer careers, nanoparticles can improve penetration and retention. It was reported that the organic modification in the POMs is an effective approach to increase the fine-tuning of the bioactivity of the POM.[66]

1.6.3.3 Anti-tumour Activity of the POMs

Antibiotic resistance can lead to longer hospital stays, higher admission rates, and more difficult post-discharge care, which may indirectly impact cancer patients who are already immunocompromised, so drugs alternatives are required to face the challenging situation.[62] Eudesmic acid, which is an anti-tumour drug colchicine has a significant moiety to inhibit the tubulin.[88] Hybridization of covalent bonding increases POM conjugate stability and selectivity. The synergistic effect of Eudesmic acid (EU) was evaluated on Anderson-type POMo by

synthesizing EU_2POMo conjugate with amide binding and the cytotoxic effects were studied on HUVEC normal cell lines.[88] Decavanadate complexes proved to be effective for having specific toxicity against the tumour cells without any toxic effect on the normal Human cells despite high concentrations.[65] It can be hypothesized that decavanadate POV`s anticancer activity could be due to interaction with small non-coding RNA molecules.[71] POV (V_{18}) studies have shown the effect on the cellular cycle arrest, damaging the DNA, and causing apoptosis to several cell lines under the experimental conditions.[65,82] Furthermore, an organic moiety-POM aggregate, such as Mo_6O_{18} has been reported to suppress the Human malignant glioma cell (U251) without crossing the blood-brain barrier and making the core cleavable and metastable in the cell.[65,82] Similarly, POT (Iron heptatungsten phosphate-based complex) has shown anti-cancer activity against several cell lines and mice.[65] Moreover, an organic-inorganic hybrid compound (POT) was tested for the cancer cell lines and the reason for higher anticancer activity was suggested due to the higher cell penetration capacity. Another POT (PW_{11}) was reported as encapsulated to nanoparticles against the cancer cells and found effective against the cancer cell.[65]

According to the article by Zhao et al. 2020 [89], an investigation prompted with a multi-enzyme imitating CeO_2 NPs with montmorillonite and rhodium nanodots, tungsten based nanocluster POM was produced to test photothermal cancer treatment, which has been discovered with photothermal conversion ROS scavenging capabilities and tungsten-based nanocluster POM.[89] PM-8**,** $[NH_3Pri]Mo_7O_{24}]$ inhibited several cancer cell lines, including MX-1 murine mammary cancer, Meth A sarcoma, and MM46 adenocarcinoma, and showed better activity than approved drug (5-fluorouracil). which involves the biologically initiated reduction of PM-8 into PM-17 (more toxic than PM-8) with the formation of 12-electron-reduced PM-17. $[Mo_7O_{24}]^{6-}$ Flavin mononucleotide (FMN) complex inhibits tumors by inhibiting mitochondrial ATP production.[61,68,85] The biological reduction of PM-8 by FMN delivers electrons from NADH to coenzyme Q in a linked phase of cell respiration, inhibiting ATP formation.[68]

1.6.3.4 Antiviral Activity of POMs

Several Keggin-type and Wells Dawson-type POMs are studied for the inhibition activity against many viruses, such as Influenza, Dengue, immunodeficiency, and Distemper viruses. The POMs can inhibit hemagglutinin A and bind to the host cell receptor to initiate penetration. A few studies have also revealed that POMs can inhibit the proteases non-competitively in very low concentrations.[65] The POM, $(NH_4)_{17}Na$ $(NaSb_9W_{21}O_{86})$ can give protection against RNA and DNA viruses.[61] In order to establish a safe dosage for POM93 in humans, toxicological experiments were performed on rats. The compound exhibited antiviral properties against

hepatitis and HIV, as evidenced by previous studies.[75,8275,82] Furthermore, it was found to be non-toxic to cells cultured *in vitro*. No damage was observed in subjects exposed to acute doses of up to 5000 mg/kg and sub-chronic doses of 587 mg/kg for a duration of 90 days. After the cessation of the administered dosage, there was a notable elevation in the levels of aspartate aminotransferase (AST) and alanine aminotransferase (ALT).[75] However, histopathological examination revealed no evidence of organ damage. Furthermore, no mutagenicity or mortality was seen in Wistar rats, indicating a minimal degree of health hazards associated with drug development.[75] The study found that POM-AMB-acy exhibited degradability and minimal toxicity within a period of 22 hrs in U251 and PC12 cell lines.[82]

1.6.3.5 Antibacterial Activity of POMs

When comparing POMs and the antibacterial activity of the medications, the minimum inhibitory concentration (MIC) is an obvious factor to consider. Preyssler type POT $[NaP_5W_{30}O_{110}]^{14-}$ is reported with Gram-negative bacteria e.g*., S. aureus*, *M. catarrhalis,* and *E. faecalis*. Moreover, Kegging types, such as polyoxotungstates against *H. pylori*.[61,65] The synergistic effect is reported against several antibiotics in the presence of tungsten and molybdenum polyoxometalates. Polyoxovandates have been reported potent against *S. pneumoniae*, *M. smegmatis*, and *M. tuberculosis* and in combination with the other compounds described the enhancement in the toxicity against the *E. coli* and *S. aureus*.[65] P_2W_{18}, $SiMo_{12}$, PTi_2W_{10}, and $Ge_2Ti_6W_{18}$ were reported with the antibacterial activity of β- lactam, methicillin-resistant *S. aureus,* and vancomycin-resistant *S. aureus.* P_2W_{18}, $SiMo_{12}$, and PTi_2W_{10} have shown an inhibition effect on the *mecA* and *pbP* transcription process whereas, $Ge_2Ti_6W_{18}$ is linked with disturbance of the post-transcription process. Similarly, SiW_{11} has also improved the activity against β- lactam antibiotics against methicillin-resistant *S. aureus*.[61,65,66] Decavandate complex $[H_2V_{10}O_{28}]$ $[4\text{-picH}]^4$ has shown antibacterial activity against Gram-negative and Gram-positive bacteria without damaging the host DNA or causing cytotoxicity.[61]

The utilization of β-lactamase inhibitors in conjunction with POMs leads to the restoration of antibiotic efficacy and POMs possessing Keggin complete or lacunary structures, Wells-Dawson structures, or double sandwich Keggin structures exhibit increased antibacterial efficacy against MRSA and vancomycin-resistant *S. aureus* (VRSA).[52,90] The molecule $K_6[(VO)SiMo_2W_9O_{39}]$ as (POM7) exhibited antibacterial action specifically against *S. aureus*.[52] Several POMs in combination with oxacillin showed activity against MRSA and VRSA and the authors hypothesized that the observed suppression of bacterial cell growth was due to synergy between the POM and oxacillin.[35]

Structure and activity relation was evaluated for POMs against *H. pylori* and *S. pneumoniae.* Polyoxovanadates, such as V_{10} were the most effective against *S. pneumoniae*, however, most of the POMs were effective against *H. pylori*.[77] In the study of Balici et al. 2016 [91] the antibiotic characteristics of kegging type were checked, and the activity of seven tungsto-bismuthase compounds against Gram-positive multidrug-resistant and Gram-negative bacteria were tested. The antibacterial activity was promising against MRSA for Cu_3BiW_9 and BiW_9. For *S. aureus* and *S. pneumoniae* strains were checked for V_{10} activity and the MIC value was found 50 µg/mL against SR3605 and antibiotic drugs in the range from 0.001- 10 µg/mL.[66]

On the other side, in the case of *S. aureus*, some of the POMs have given poor antibacterial activity as compared to the range required for effective drugs. There are several POMs, which have poor antibacterial activity however, their redox activity is considerable, and their potential use as bacterial biosensors.[65] In another study, a supramolecular gel was synthesized with the surfactant and metronidazole, MTN-encapsulated Mo_{132} and converted to microfiber for controlled POM and MTN delivery to evaluate this application biocompatibility for guided bone regeneration membrane. Incorporation of the POM (Mo_{132}) into metronidazole-loaded PMMA (methyl methacylate) increased cell proliferation with increased concentration and controlled antibacterial drug release prevented anaerobic microorganism colonization.[64,85] Supra particle assemblies adjusted non-covalently with adjuvant, enriched in hydrogen bonding donor sites in MOCs and antigen assembly in conjunction with hydrogen bonding accepting polymers (P4VP) enhanced the immunogenicity as compared to BCG for *M. bovis*.[84]

In study by Enderle et al. 2022 [35] guanidinium-containing Polyoxometalates- Ionic liquids (POM-IL) and related compounds can improve broad-spectrum antibacterial activity, which can help design new antimicrobial drugs. *N*, *N*, *N*′, *N*′-tetramethyl-*N*″, *N*″-dioctyl guanidinium (DOTMG-1) in PMMA films can form hybrid polymeric materials with broad-spectrum antibacterial and antibiofilm capabilities, which can be used to develop new materials for medical devices and packaging applications. The DOTMG-1 POM-IL proved effective against *E. coli* DH5α, *B. subtilis, L. monocytogenes*, and verocytotoxigenic *E. coli*. The chemical was more effective against Gram-positive strains than Gram-negative strains of *E. coli*, suggesting that the cell wall structure is involved which contains lipopolysaccharides.[35]

1.6.3.5.1 Antibacterial Mechanism of POMs

Multiple potential mechanisms behind the antibacterial effects of POMs have been elucidated in the literature. For example, these chemicals have the ability to traverse the peptidoglycan layer

or enter the bacterial membrane through WtpABC and TupABC transporters. As a result, this process leads to the breakdown of the peptidoglycan layer and the dissolution of the bacterial membranes. It has been proposed that low-molecular-weight chemicals, which have the ability to rupture the cell membrane and enter bacterial cells through electrostatic interactions, can inhibit the transcription of DNA into RNA by directly interacting with DNA molecules.[52] It was suggested that hybrid POM as $[(CpTi)_3SiW_9O_{37}]^{7-}$, has the capacity to interact with the DNA probably due to the moiety of CpTi. Furthermore, $[PV_2Mo_{10}O_{40}]^{5-}$ and $[V_{18}O_{42}(H_2O)]^{12-}$ were also expected to be interactive with ctDNA. Another study revealed that $[Mo_7O24]^{6-}$ with the DNA model bis(p-nitrophenyl) phosphate cleaved the phosphodiester bond however, the mechanism remained unknown.[85]

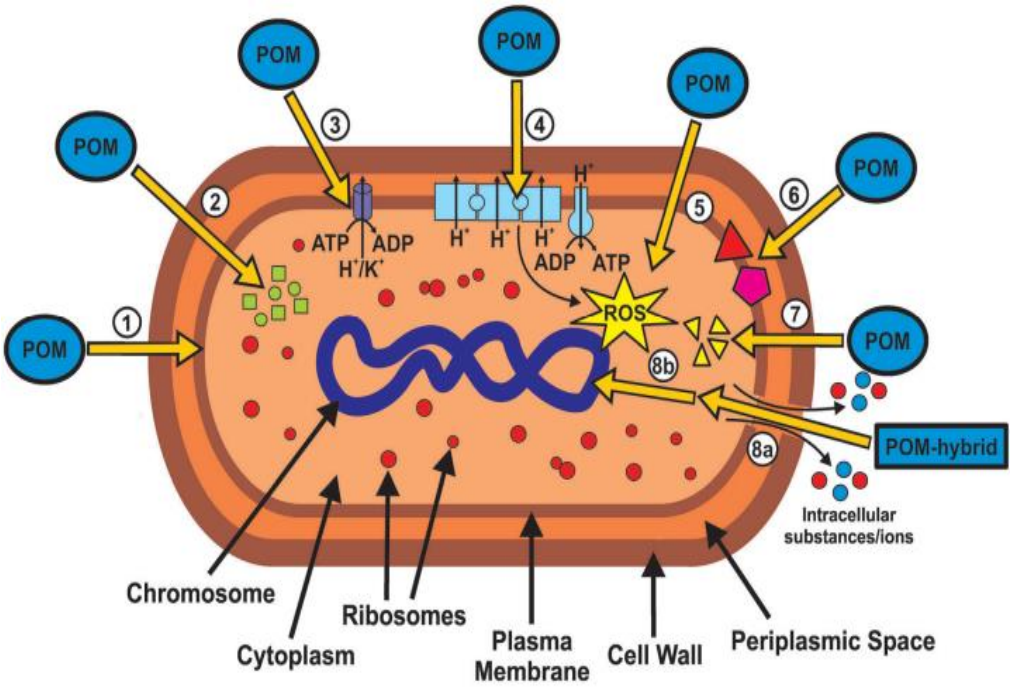

Figure 5- *Possible biological Mechanism of POMs.1- POMs are taken up through the inner bacterial cell membrane. 2- POMs inhibit the synthesis of both PBP2a and β-lactamases. 3- POMs targeting P-type ATPases. 4- POMs inhibit the electron transport chain of microorganisms. 5- Oxidation-based rise in ROS levels mediated by POM. 6- POMs reacting with membrane-anchored proteins and enzymes. 7 Interactions between POM and cytoskeletal elements that disrupt the bacterial cytoskeleton dynamics. (8a) POM-based nanocomposites disrupt the bacterial cell wall, causing intracellular substances to escape. (8b) Upon disruption of the cell wall, POMs may interact with cytoplasmic elements or anion-sensitive proteins, such as nucleic acid-binding proteins.*[69]

Based on the significant uses and underlying mechanisms of action, it can be postulated that POMs possess the potential to serve as pharmaceutical agents in the future. This potential can be

realized by their utilization either as standalone medications or in combination with other biomolecules, or even in conjunction with organic or inorganic elements. This study will focus on examining the antibacterial activity of the specific POMs listed in Table. 1 within the materials and methods section.

1.6.4 POMs used for the Screening of the Antibacterial Activity

1.6.4.1 Dawson-type POM:

In a work by Miras et al. 2011 [92], the synthesis and chemical characterization of Vanadate(V)-templated Dawson structured $\{V^{IV}M^{VI}{}_{17}(VO_4)_2\}$ was performed. The V^{IV} center in the Mo-based system is disorganized across 18 positions and shows no preference for a particular location (cap or belt).[92]

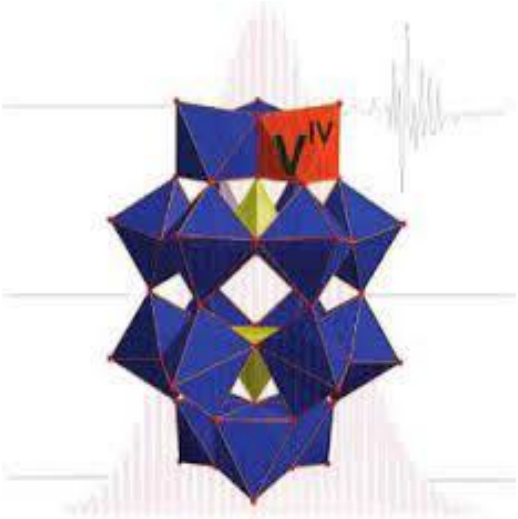

Figure 6- *Vanadate(V)-templated Dawson structured* $\{V^{IV}M^{VI}{}_{17}(VO_4)_2\}$.[92]

1.6.4.2 Bisphosphonate- Polyoxovanadate compound

Bisphosphonate molecules have been identified as therapeutic agents with significant potential in the field of medicine. These compounds primarily exhibit efficacy in the treatment of bone resorption disorders and possess notable anticancer properties.[93] In a study by Thakre et al. 2021[93] the compounds of bisphosphonate-polyoxovanadate ($V_5P_4O_{35}C_{14}N_6H_{52}$) were demonstrated for the paramagnetic characteristics and peroxidase-like functionality. These properties contribute to the augmentation of the antibacterial efficacy in the presence of H_2O_2 solution (0.5mM), particularly at lower concentrations (50 µg/mL).[93]

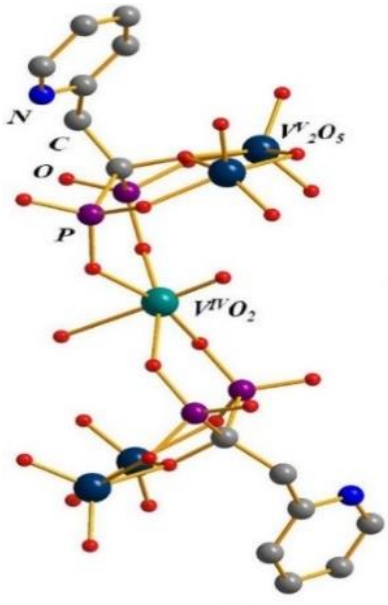

***Figure 7**-Ball-and-stick representation of $[(V^{IV}O_2)\ (V^{V}_2O_5)_2\{O_3P\text{-}C(O)(CH_2\text{-}2\text{-}C_5NH_4)\text{-}PO_3\}_2]^{10-}$* [93]

1.6.4.3 Phosphovanadomolybdic Acid

The crystal packing and secondary structure of $H_5PV_2Mo_{12}O_{40}$, revealing four unique structures and three solid phase transitions at temperatures between 25 and 55 °C, with loss of solvated water and contraction of volume and increase in packing density. Above 60 °C, $H_5PV_2Mo_{12}O_{40}$ becomes amorphous and anhydrous, but the polyoxometalate cluster remains stable up to 300 °C. At higher temperatures, the compound decomposes into crystalline MoO_3 and possibly amorphous vanadium oxide and vanadylphosphate. However, $H_5PV_2Mo_{12}O_{40}$ can be easily recovered by dissolution in water at 80 °C.[94]

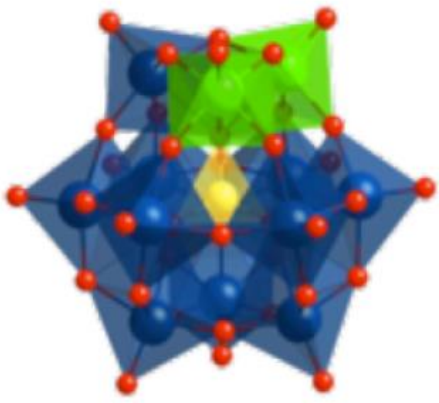

***Figure 8**- Structure of $H_5PV_2Mo_{12}O_{40}$.* [94]

1.6.4.4 Tungsto-vanadophosphate Anion

The anion $[PW_8V_4O_{40}]^{4-}$, known as the 8-tungsto-4-vanadophosphate anion, is a polyoxometalate cluster that exhibits distinctive characteristics. The compound is composed of

eight tungsten and four vanadium atoms, which are surrounded by oxygen atoms and has a charge of -4.[94] The aforementioned anion exhibits an intricate three-dimensional configuration and is renowned for its catalytic prowess, namely in the realm of redox reactions and acid-catalyzed mechanisms. The substance has super-acidic properties, enabling it to effectively protonate organic molecules.[94] The compound's versatility is seen in its wide range of applications, including catalysis, corrosion inhibition, and utilization in electrochemical devices. Furthermore, it exhibits remarkable stability across many environments, rendering it highly significant in the realms of chemical and materials science.[94]

1.6.4.5 Organic-inorganic Hybrid POM

Vanadate species frequently undergo intricate equilibration with both inorganic and organic ligands, resulting in a wide range of structurally varied vanadium complexes. The incorporation of decavanadate into cobalt (II) complexes enhances structural stability and inhibits breakdown, resulting in the compound's resilience in both aqueous environments and simulated buffer solutions. The findings of this study have significance for the prospective utilization of decavanadate as a ligand in diverse fields such as pharmacology, materials science, and energy research.[95]

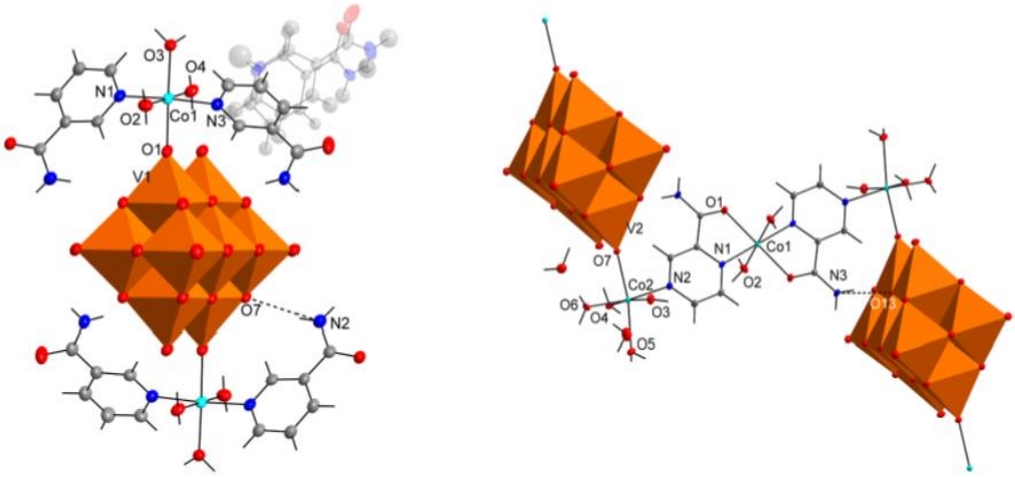

(a) (b)

Figure 9- *Transition metal ion – decavanadate – ligands. (a) (Hnicotinamide)$_2${[Co(H$_2$O)$_3$(nicotinamide)$_2$]$_2$[μ-V$_{10}$O$_{28}$]}.6H$_2$O. (b) {[Co (H$_2$O)$_4$]$_2$[Co(H$_2$O)$_2$(μ-pyrazinamiCo ((*$_2$*] [μ-V$_{10}$O$_{28}$]}·4H$_2$O.*[95]

1.6.4.6 Preyssler- type POM

Preyssler-type polyoxotungstate - [NaP$^{V}{}_5$W$^{VI}{}_{30}$O$_{110}$] $^{14-}$ refers as P$_5$W$_{30}$ has been extensively investigated due to its diverse range of biological properties. The substance demonstrates

antibacterial properties against strains of *S. aureus* and MRSA, with minimum inhibitory concentration (MIC) values ranging from 0.83 mg/mL to 3.31 mg/mL. P_5W_{30} exhibits anti-quorum sensing properties.[37] Moreover, it has antibiofilm properties, a crucial attribute in the fight against bacterial biofilm development. it is a versatile molecule with therapeutic potential in combating bacterial infections, addressing biofilm-related concerns, and managing viral infections. Additional investigation is required in order to comprehend the underlying mechanisms associated with these actions.[37]

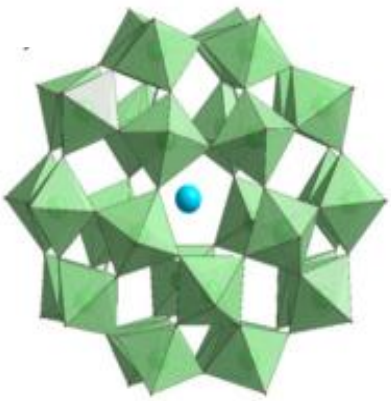

***Figure 10**- Structure of Preyssler type- POM.*[37]

1.6.5 ATPase Activity of the POMs

There are numerous studies that emphasize the significance of P-type, ATPAases as potential drug targets and the use of POMs as metallic pharmaceuticals. Several POMs and gold compounds were studied on PMCA and remarkable inhibition was found against the Ca^{2+} ATPase activity in the brain cell of the pig.[54,55,57] Aureliano et al. 2022 [57] , conducted several studies in which POMs showed the significant inhibition of SERCA Ca^{2+}ATPase, depending on the concentration of the compound.[57] The SERCA model was tested with gold, tungsten, and vanadate to evaluate the effect on P-type ATPases under identical conditions.[54,55,96] Gumerova et al. 2018 [70], investigated several POTs to check the effect on Ca^{2+}-ATPase from skeletal muscles and Na^{+}/K^{+}-ATPases from the skin epithelia of Kelli fish whereas, many POTs have seen very promising IC_{50} results from some of the POTs under the study.[70] Fraqueza et al. 2012[97] has reported SERCA Ca^{2+}-ATPase activity with tungsten-based POM in the presence of quercetin as a polyphenol and glutathione as an antioxidant and the ATPase enzyme inhibition values were remarkable as compared to Vanadium and Niobium based POMs.[98] Nevertheless, their possible suppression by the POMs employed in current therapeutics should be carefully examined to accurately set their dosage to avoid collateral and harmful effects on healthy neurological cells.

1.7 Objectives

The phenomenon of antibiotic resistance arises from the evolutionary adaptation of bacteria to withstand the effects of antibiotics. Consequently, there has been a notable rise in the occurrence of antibiotic-resistant illnesses, thereby exacerbating the challenges associated with their treatment and control. The bacterial resistance significantly impacts public health as several bacterial strains have developed resistance to many kinds of antibiotics, resulting in a phenomenon known as multidrug resistance. This phenomenon leads to a decrease in the available treatment alternatives and a corresponding increase in the ineffectiveness of treatment. There is dire need to investigate the alternatives ways to cope up with the increasing antibacterial resistance.

Therefore, this study is based on the perspectives of proposing the POMs as antibacterial agents with potential to be used as metallic drugs in this challenging global situation of MDR. In this study POMs based on molybdenum, tungsten, vanadate, and metal complex were screened for antibacterial activity against the Gram-positive *S. aureus* and Gram-negative *E. coli.* Furthermore, the previous investigation has demonstrated that Pressley ion – P_5W_{30} exhibits notable antibacterial efficacy against MRSA 16and *S. aureus* ATCC 6538, with MIC values of 600 μM and 32 μM, respectively. In this study the growth kinetics inhibition was assessed in the control and clinical *S. aureus* strains in the presence of NaCl and in synergism of NaCl and P_5W_{30}. In the end, the virulence of the P_5W_{30} was assessed in the larvae model *Galleria mellonella*, as P_5W_{30} is hypothesized to eliminate the *S. aureus* infection, eventually decreasing the antibiotic-resistant potentials of the threatening *S. aureus.* The second main aspect of this work focuses on investigating the inhibitory activity of the model SERCA (Ca^{2+}-ATPase), which is a target of antibiotics. With POMo ($Mo_{17}V_3$) as a potential metallic medication that can effectively impact the function of Ca^{2+} ion pumps which are highly essential to maintain the Ca^{2+} homeostasis in the muscle cells. In order to achieve this objective, the POMo ($Mo_{17}V_3$) was assessed for its inhibitory impact on the ATPase activity of the SERCA vesicles, marking the first instance of such evaluation. Hence, the determination of the compound's IC_{50} was conducted in conjunction with an incubation study conducted at ambient temperature. Additionally, an analysis of the inhibition type was performed to assess the inhibitor`s ($Mo_{17}V_3$) binding affinity towards the ATPase enzyme.

2.0 Materials and Methods

2.1 Screening of POMs for the Antibacterial Activity

To participate in suggesting the solution for the global issue of increasing bacterial resistance, a screening study was conducted to examine the efficacy of five POMs and one metal compound for the antibacterial activity. As indicated in Table.1, the compounds included in this study were never reported for any antibacterial activity except the POM P_5W_{30}. In the continuation of the previous study done by Faleiro et al. 2022 [37], the antibacterial activity of P_5W_{30} was further assessed under saline circumstances.

Table 1- The POMs were evaluated for antibacterial activity.

Formula	MW	Charge	Solubility	POM- Type	Ref.
$(TEAH)_6[H_2VMo_{17}O_{54}(VO_4)_2]$ $(C_{36}H_{96}N_6Mo_{17}V_3O_{80})$	3676 $gmol^{-1}$	-6	Water	Dawson-like	[92]
$(NH_4)_4[H_6(V^{IV}O_2)(V^{v}_2O_5)_2\{O_3P\text{-}C(O)(CH_2\text{-}2\text{-}C_5NH_4)\text{-}PO_3\}C_2].9H_2O$	1243.19 $gmol^{-1}$	-10	Water	Metal Complex	[93]
$H_5PMo_{10}V_2O_{40}.32H_2O$	2313 $gmol^{-1}$	-5	Water	Anderson	[94]
$K_5H(PV_4W_8O_{40}).8H_2O$	2686 $gmol^{-1}$	-6	Water	Anderson	[99]
$(Hnic)_2\{[Co\ (H_2O)_3(nic)_2]_2[\mu V_{10}O_{28}]\}.6H_2O.$	1998.21 $gmol^{-1}$	-6	Water	Hybrid-decavanadate	[95]
$\{[Co\ (H_2O)_4]_2[Co\ (H_2O)_2(\mu\text{-}pyz)_2]\ [\mu\text{-}V_{10}O_{28}]\}\cdot 4H_2O$	1632.65 $gmol^{-1}$	-6	Water	Hybrid-decavanadate	[95]
$*(NH_4)_{14}[NaP^{V}_5W^{VI}_{30}O_{110}]\cdot 31H_2O$	8264 $gmol^{-1}$	-14	Water	Preyssler	[37]

* P_5W_{30} was already screened and reported for the antibacterial activity.[37]

2.1.1 Agar Diffusion Plate Method

As mentioned in 2.1, five POMs and one metal complex in stock solution of 4 mM were screened for antibacterial activity against Gram-negative *E. coli* DSM1077 and Gram-positive *S. aureus* ATCC 6538. The solutions of compounds were prepared by dissolving the solid compound in water and thereafter storing the resulting solution at a temperature of 4° C. In order to assess the antibacterial efficacy of the compounds, 4 mM solutions of each compound were produced and subsequently diluted in Mueller-Hinton (MHB) culture medium to achieve the desired final concentrations for the assay. The agar slants were prepared for on the respective agars as Luria-Bertani agar (LBA) for *E. coli* and Brain and heart infusion agar (BHI) for *S. aureus*. Three

biological replicates of *E. coli* and *S. aureus* were streaked onto prepared Petri plates LB agar and brain heart infusion (BHI) agar. The agar plates incubated at a temperature of 37° C for a duration of 24 hrs. [37,100]

Following the incubation of the streaked plates, test tubes containing autoclaved phosphate-buffered saline (PBS) were prepared. A volume of 10 mL PBS was taken into each sterile test tube and two technical replicates were prepared for each biological replicate.[37,100,101] Five to six identical bacterial colonies were suspended in each test tube of PBS for the subsequent biological replicate as per the turbidity of 0.5 MacFarland solution. A volume of 8 mL of bacterial suspension was aliquoted into each of the sterile 50 mL centrifuge tubes. Thereafter, 40 mL of MHA was introduced into centrifuge tube and the mixture was quickly poured in the sterile Petri dish to avoid solidification of agar in the tubes. The pouring process in the Petri dishes was executed swiftly with a swirling motion, after which the plates were set aside to allow for the solidification of the media.[37,100,101] The identical procedure was conducted for all biological replicates of both *E. coli* and *S. aureus*, separately. Following a 15-minute solidification period, to create the 6 mm wells in the agar in the plates, the agar was punctured with the help of sterile Pasteur pipettes. Particular attention was given to ensuring that the wells were positioned roughly 15 mm away from the periphery of the plate and 30 mm apart from each other. The wells were punctured in the plates and 40 µL of each of the mentioned POM were added to the well. The tested concentrations of each POM were 100 µM, 200 µM, 400 µM, 600 µM, 800 µM, 1000 µM.[37,100,101] As negative control 40 µL of PBS was used. As positive control 40 µL of the antibiotic Chloramphenicol (30 µg/mL) was used. The compounds were allowed to diffuse through the agar for 15 minutes. This process was repeated for all the given compounds for both *E. coli* and *S. aureus.* The plates were incubated for 24 hrs at 37° C.[37,100,101]

As mentioned in 2.1 the antibacterial activity of POT- P_5W_{30} was screened previously by Faleiro et al. 2022 [37], therefore, in the continuation of their work the impact of NaCl on the susceptibility to P_5W_{30} was further evaluated.

2.2 Impact of NaCl on the susceptibility of *S. aureus* to P_5W_{30}

In order to assess the NaCl effect on the growth of *S. aureus* ATCC 6538 and MRSA 16, BHI agar slants were inoculated from maintenance stock at -80ºC and incubated for 24 hrs at 37° C.[37,102] To prepare the pre-inoculum the bacterial culture was recovered from the agar slant and a streak on MHA plate was performed. This inoculated plate was incubated at 37ºC for 24 h. From this culture a loop was transferred into 10 mL of MHB. The incubation was done in a water

bath at 37 °C with continuous agitation at a speed of 120 rpm. Three biological replicates were prepared. The optical density (OD) of the pre-inoculum cultures were verified by diluting the bacterial culture by a factor of 1:10.[37,101,102] In a sterile Eppendorf tube, 900 µL of MHB was added, followed by the addition of 100 µL of bacterial culture. Once the dilution was made, the bacterial suspension was transferred into the cuvette to check the absorbance with spectrophotometer ($OD_{660\ nm}$). The aforementioned procedure was repeated for the biological replicates. The results were recorded, and the viable cell count was done as CFU/mL by the Miles and Misra method.[37,101,102]

2.2.1 Preparation of NaCl Solutions

A stock solution containing 20% NaCl was prepared by dissolving 20 g of NaCl in 100 mL of distilled water. From the stock solution, solutions of NaCl (1.5%, 3%, 4%, 5%, 6%, and 7%, w/v) were prepared in MHB and autoclaving was performed at 120° C for 20 min to ensure sterilization of the solutions.

Note: The NaCl solutions were kept double strength in the concentration as per the equal dilution by the bacterial culture.

2.2.2 Bacterial growth under the Exposure to NaCl

To evaluate the bacterial growth pattern in the presence of saline conditions the microplate method was used with the periodic time and absorbance relation using the Spectra Max iD3 microplate reader. Polystyrene flat-bottom 96 wells microplates (Sarstedt Inc., Nümbrecht, Germany) were used. The bacterial pre-inoculum prepared as mentioned in 2.2 was used as a positive control, whereas the MHB devoid of any salt was used as a negative control. [101,102] Each well of the microplate was filled with 100 µL of MHB containing salt concentrations (1.5%, 3%, 4%, 5%, 6%, and 7%, w/v). Each well was inoculated with 100 µL of the bacterial pre-inoculum. The growth was followed by reading the $OD_{600\ nm}$ until 24 h.[101,102]

Note: The Control well and Blank well were 200 µL in total volume individually as the volume of the experimental wells.

2.3 Evaluation of the impact of P_5W_{30} and NaCl on Bacterial Growth

The MIC value of P_5W_{30} for *S. aureus* ATCC 6538 and MRSA 16was reported in the study of Faleiro et al. 2022 [37] and was used in this study to evaluate the effect of salt on the bacterial susceptibility to P_5W_{30}, namely 32 µM and 600 µM and ½ MIC, and 2x MIC. The tested concentrations of NaCl were 1.5%, 3%, and 6% (w/v), which were prepared in MH broth. Wells of a flat-bottom microplate (Sarstedt Inc., Nümbrecht, Germany) were filled with 100 µL of

MHB supplemented with the appropriate concentration of salt and P_5W_{30}. The Control and blank wells were prepared in total of 200 µL as the same volume of the experimental wells. The microplates were incubated at 37ºC. The growth was followed by reading the $OD_{600\ nm}$ using a Spectra Max iD3 microplate reader. Three biological and two technical replicates were used.[37,101]

As the compound P_5W_{30} shown the capacity of being antibacterial and antic-quorum sensing compound.[37] Consequently, it was crucial to investigate the antibacterial activity in an insect model to evaluate the impact of saline conditions and exposure to P_5W_{30} on the bacterial virulence. The insect model Greater Wax Moth *Galleria mellonella* L. (Lepidoptera: Pyralidae) was selected as a suitable and accessible model organism.[100,102,103]

2.4 Impact of P_5W_{30} on the Virulence using the Larvae *Galleria mellonella*

2.4.1 Bacterial Exposure to Salt and P_5W_{30}

The bacterial cultures were grown previously in MHB. For the assay the MHB medium was supplemented with 1.5%, 3%, and 6% (w/v) of NaCl and the MIC value of P_5W_{30} (32 µM). The culture was exposed to each NaCl concentration individually and the P_5W_3 were used as controls. The bacterial cultures were exposed to NaCl and P_5W_3 overnight at 37° C at 120 rpm.[100,102,103] Healthy larvae were selected with a weight range of 220-280 mg. Previously to injection the larvae surface was disinfected with 70% ethanol. A group of 10 larvae were injected with 10 µL of the bacterial suspension (10^6 CFU) of each condition on the second right proleg using a 50 µL microsyringe (Sigma-Aldrich, Madrid-Spain). [100,102,103] A group of 10 larvae injected with 10 µL of PBS was used as negative control. The larvae were maintained in sterile Petri dishes at 37ºC for 5 days and their survival was monitored each day by checking their reaction to touch (using a sterile brush).[100,102,103]

2.5 ATPase Assay

In section 1.6.5, the concern of antibiotic resistance is highlighted, prompting the investigation of drug-targeting sites, specifically the ionic pumps found in cell membranes and subcellular organelles. Among these pumps, the Ca^{2+}-ATPase pumps play a crucial part in maintaining cellular homeostasis. Therefore, the effect of POMo ($Mo_{17}V_3$) was evaluated as the Ca^{2+}-ATPase pumps inhibitor to evaluate the hypothesis of using $Mo_{17}V_3$ as a metallodrug.

2.5.1 Evaluation of Inhibitory Effect of POMo on Ca^{2+}-ATPase

In order to evaluate the inhibitory effect of POMo ($Mo_{17}V_3$) on the ATPase activity of the Ca^{2+}-ATPase pumps an enzyme-coupled assay as shown in **Figure 11** was performed in the presence of Phosphoenolpyruvate (PEP), pyruvate kinase (PK), Lactate dehydrogenase (LDH) and

Nicotine adenine dinucleotide dehydrogenase (NADH) and Adenosine triphosphate (ATP) to measure Sarcoendoplasmic reticulum calcium ATPase (SERCA) Ca^{2+}-ATPase activities at 22° C. The solutions and the enzymes required to perform the ATPase assay were prepared according to Table. 2 and 3.

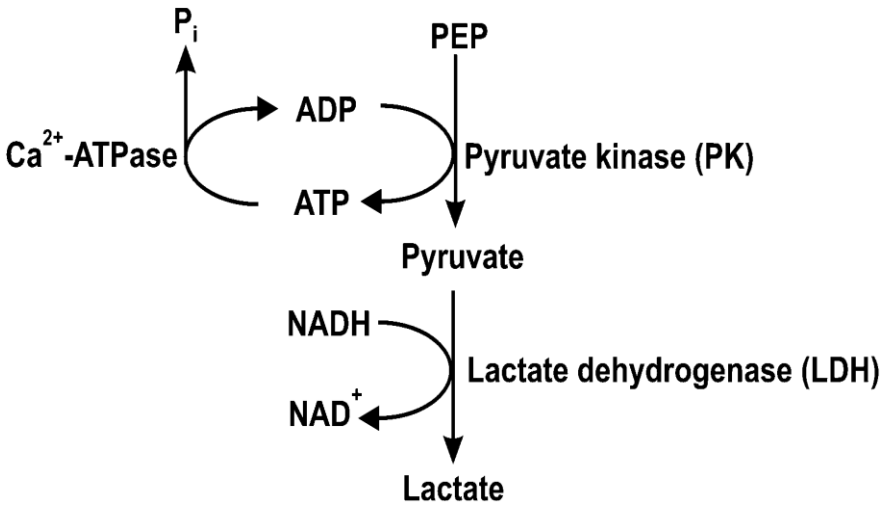

***Figure 11**- Coupled Enzyme Ca^{2+}- ATPase activity.*[70]

Table 2- The following solutions were prepared for the enzymatic reactions.

Ingredients	Concentrations
HEPES (pH 7.0)	25 mM
KCl,	100 mM
$MgCl_2$	5 mM
$CaCl_2$	50 µM
ATP	2.50 mM
Ionophore	4%

Table 3- The enzyme assay was performed with the addition of the following reagent to the medium.

Ingredients	Concentrations
phosphoenolpyruvate	0.42 mM
Nicotine adenine dinucleotide dehydrogenase	0.25 mM
lactate dehydrogenase	18 IU
pyruvate kinase	7.5 IU

2.5.1.1 Enzymatic Reaction

Three control samples were run at the beginning, mid, and end of the assay. Before the addition of the SERCA vesicles to the experimental mixture with medium, water, calcium, phosphoenolpyruvate, pyruvate kinase, and lactate dehydrogenase were added without the addition of POM in control samples and with the addition of POM in the experimental samples. The initiation of the experiment was started by adding SERCA vesicles in the concentration of 10 µg/mL. [54–57,78,96] Finally, NADH and ATPase enzymes were added in the cuvette mixture and the absorbance was noted through spectrophotometry (Shimadzau UV-2401PC) at 340 nm for 1 min which reflects the basal activity of the reaction. Calcium ionophore (Lasalo 123187) solution with 4% concentration was added to the same experimental cuvette and the decrease in absorbance was noted for 2 min because of the uncouple ATPase activity. [54–57,78,96] Four rounds of the experiments with POMo concentrations of 0.5 µM, 1 µM, 2 µM, 3 µM, 4 µM and 5µM, were performed under identical experimental conditions were conducted in order to estimate the IC_{50} while the controls (with 100% ATPase activity) were performed in the start, mid and end of the experimental activities and the resulting enzyme kinetics graphs were recorded**.**[54–57,78,96]

2.5.1.2 The Inhibitory Concentration (IC_{50}) of POMo ($Mo_{17}V_3$)

According to other enzyme kinetic reports recorded, ATPase uncoupled activity and inhibition were measured considering the decreases in absorbance per minute in the absence of the inhibitor (100% ATPase activity) and in the presence of the inhibitor (50% drop-in ATPase activity), respectively. The kinetics graphs were evaluated for the basal ATPase activity in the control samples and the presence of the $Mo_{17}V_3$. Based on the Michalis and Menten equation the inhibitory power of the $Mo_{17}V_3$ was calculated as IC_{50} value considering the POM concentration that inhibits the 50% activity of Ca^{2+}ATPase enzyme.[70]

2.5.2 Incubation of the POMo ($Mo_{17}V_3$)

To estimate the stability of the POMo in the experimental medium (HEPS) used for the experimental conditions, the POMo was kept for consecutive 2 hrs in the medium at room temperature 22° C in the dark condition and the effect of the POMo was evaluated on the ATPase activity.

2.5.3 Type of Inhibition with the POMo ($Mo_{17}V_3$)

To understand the type of inhibition of the POMo ($Mo_{17}V_3$) as an inhibitor of the ATPase enzyme the type of inhibition was performed spectrophotometrically as per IC_{50} concentration of the

POMo calculated in 3.5.1.2. As shown in Table 4, POMo ($Mo_{17}V_3$) was used with increasing concentrations of ATP substrate ranging from 0.1 mM, 0.25 mM, 0.50 mM, 1.0, and 2.5 mM. For each concentration of ATP substrate one reading was taken without the POMo and a second experiment was performed with the IC_{50} concentration of the POMo. The graphics with the ATPase activity in the absence (Control) and presence of POM were recorded for Lineweaver-Burk graph. The experiments were performed as per scheme mentioned in Table 4, in triplicates.[70]

Table 4- The scheme of experiments was performed to determine the type of inhibition of Ca^{2+} ATPase activity.

Reagents	**ATP (0.1mM)**		**ATP (0.25mM)**		**ATP (0.5mM)**		**ATP (1.0mM)**		**ATP (2.50mM)**		**ATP (3.75mM)**	
Medium	800uL	800uL	800uL	800uL	800uL	800uL	800uL	800uL	800uL	800uL	800uL	800uL
MiliQ-water	137uL	135uL	131uL	129uL	121	119	101	99	131	129	126	124
Ca	5uL	5uL	5uL	5uL	5uL	5uL	5uL	5uL	5uL	5uL	5uL	5uL
PEP	10uL	10uL	10uL	10uL	10uL	10uL	10uL	10uL	10uL	10uL	10uL	10uL
PK	10uL	10uL	10uL	10uL	10uL	10uL	10uL	10uL	10uL	10uL	10uL	10uL
LDH	10uL	10uL	10uL	10uL	10uL	10uL	10uL	10uL	10uL	10uL	10uL	10uL
$Mo_{17}V_3$	---	2uL	---	2uL	---	2uL	---	2uL	---	2uL	---	2uL
NADH	10uL	10uL	10uL	10uL	10uL	10uL	10uL	10uL	10uL	10uL	10uL	10uL
ATP	4uL	4uL	10uL	10uL	20uL	20uL	40uL	40uL	10uL	10uL	15uL	15uL
Vesicles	10uL	10uL	10uL	10uL	10uL	10uL	10uL	10uL	10uL	10uL	10uL	10uL
Ionophore	4uL	4uL	4uL	4uL	4uL	4uL	4uL	4uL	4uL	4uL	4uL	4uL

2.5.3.1 Lineweaver-Burk Plot

The type of inhibition of POMo was assessed by evaluating the results obtained from the kinetic reactions mentioned in 2.5.3 section. Based maximum velocity of the enzyme (Vmax) and utilised ATP concentration (Km) a Lineweaver-Burk plot of Ca^{2+} ATPase activity was drawn where, Vmax is the maximum velocity of the enzyme-substrate reaction, where further addition of the substrate doesn't affect the velocity of the reaction. Moreover, Km is described as the substrate concentration at a point where half of the Vmax (½ Vmax) is achieved. The inhibition type of the enzyme was assessed as per Table 5, depending upon the Vmax and Km values.[70]

Table 5- Lineweaver-Burk plot the type of inhibition estimation.[104,105]

Enzyme Kinetics (Lineweaver-Burk)	Competitive Inhibitors	Non-Competitive Inhibitors	Mixed type - Inhibitors	Un-competitive inhibitors
Binding	**Active site**	**Allosteric site**	**Allosteric site**	**Allosteric site**
Km	Increase (Affinity decrease)	Same (Affinity decrease)	Increase/decrease (Affinity decrease/increase)	Decrease (Affinity increase)
Vmax	Same	Decrease	Increase/decrease	Decrease

2.6 Statistical analysis

To evaluate the effect of salt tolerance on the growth of S. *aureus* ATCC 6538 and MRSA 16 on 6 hrs and 24 hrs student t- test was applied. Similarly, NaCl and POM combination was evaluated using student t- test at 4 hrs and 24 hrs comparison was evaluated with student- t test. To evaluate the larvae survival on with the given treatments the Graph pad prism version 10.0.2 (232) to prepare the Kaplan Meier graph and the analysis was done by using the one-way ANOVA using SPSS version. 29.0.0.0 (241). The statistical analysis of the IC_{50} value of POMo ($Mo_{17}V_3$) and the kind of inhibition exhibited by the molecule was performed using Microsoft Excel 365 (2021). One-way ANOVA was used to analyse the IC_{50} values, revealing a statistically significant difference in IC_{50} across the concentrations of the $Mo_{17}V_3$. The study employed two-way ANOVA analysis to assess the disparity in ATPase enzyme inhibition under two conditions: the absence and presence of an inhibitor, while periodically increasing the ATP substrate concentrations. There was statistically significant difference, found in the inhibition of ATPase activity between the controls without $Mo_{17}V_3$ and the experiments with $Mo_{17}V_3$.

3.0 Results and Discussion

3.1 Screening of the Antibacterial Activity of the Synthetic Compounds

As mentioned earlier, the metal compounds were hypothesized as potential metallic drugs that can be used alone or in complementation of other organic or inorganic entities.[62,73] Therefore, the synthetic compounds were screened to assess the antibacterial activity against *E. coli* and *S. aureus* by the agar diffusion method as mentioned in 2.1.1. In this study, one molybdenum-based Dawson-like compound, two Anderson-type-molybdenum and tungsten-based, two decavandates with organic-inorganic hybrids, and one metal complex with vanadium compounds were evaluated for the first time for their antibacterial activity. Upon analysis it was observed that in this study, the six metal compounds have not shown any antibacterial activity. As shown in **Figure 12 and Figure 13**, no inhibition zones were observed for *E. coli* and *S. aureus* during the screening of the POMs, respectively. The tested concentrations of each of the POM and metal complex were 100 µM, 200 µM, 400 µM, 600 µM, 800 µM, 1000 µM and the results were as same as the negative control of PBS. The positive control with the antibiotic chloramphenicol (30 µg/mL) showed the inhibition against *E. coli* and *S. aureus* in the agar plates upon incubation. **Figure 12** shows the results from both biological replicate activity with compounds against *E. coli.*

Figure 12*- Agar diffusion agar plates for the antibacterial activity screening of E. coli.*

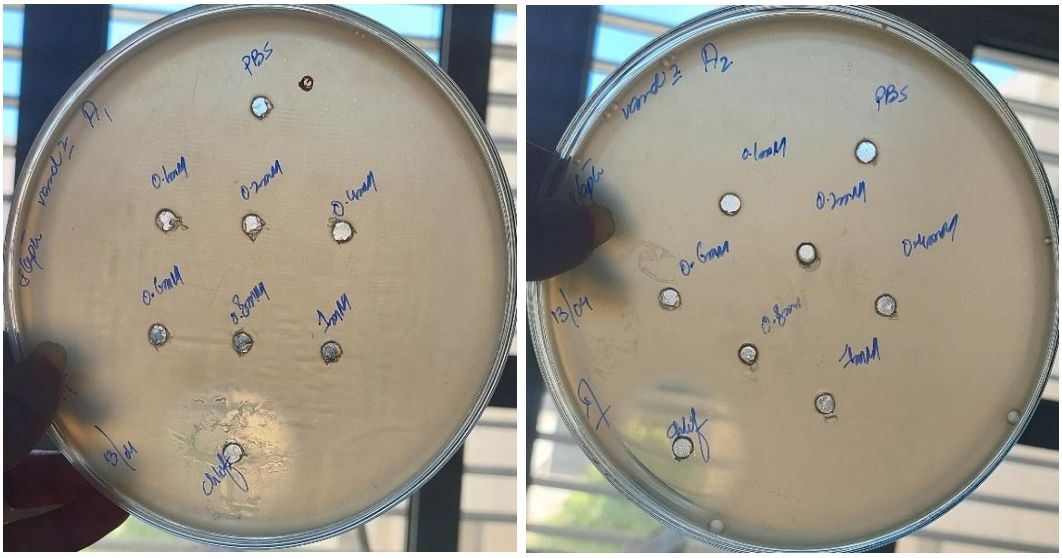

***Figure 13**- Agar diffusion agar plates for the antibacterial activity screening of S. aureus*

In the same manner, **Figure 13** shows the investigated metal complex concentrations from 100 µM, 200 µM, 400 µM, 600 µM, 800 µM, and 1000 µM, and the outcomes were identical to the negative control consisting of PBS. The antibiotic chloramphenicol (30 µg/mL) inhibited the growth of *S. aureus* on the agar plates that served as the positive control.

There are several previous studies with the same POM categories, although structurally different compounds have been done. The POMs exhibit varying levels of activity across different bacterial strains. The enhanced activity was observed by the mixed types of POMs with the substitution of vanadium or molybdenum for the tungsten atoms. Therefore, the oxidation power was highest for the polyoxovanadates (POVs) as compared to polyoxomolybdates (POMos), however, POMos are better in oxidation as compared to polyoxotungstates (POTs).[68] In a similar screening study by Bijelic et al. 2019 [68], the POMs disk diffusion susceptibility method was used to qualitatively assess the antibacterial activity of POMs. The inhibition zone diameters measured during retesting were noted below the baseline values. However, the research reports that not all POMs but three POMs out of the total of thirty nano-polyoxometalates showed good antibacterial action against *S. aureus, B. cereus, E. coli, S. enteritidis*, and *P. aeruginosa*.[68] In another study by Inoue et al. 2005 [106], negative charged POMs, As_4W_{40} and Sb_9W_{21} were studied against *H. pylori* strains as drug-susceptible, metronidazole, and clarithromycin resistant were used for the antibacterial activity of these POMs and the weak activity with MIC value of greater than 256 µg/mL was noted. From these studies it can be noticed that there can be a possibility that either the POMs gave the weak antibacterial activity or no activity at all, which agreed with

the compounds in this study that the POMs and the metal compound have shown no antibacterial activity for both Gram negative, *E. coli* and Gram positive, *S. aureus.*

In a previous study by Marques-Da-Silva et al. 2019 [78], POV showed growth inhibition effectively rather than V_1 itself, which reflected that adding the vanadium atom there could be the possibility of increasing the chances of growth inhibition for *E. coli*. The possible mechanism was suggested that decavanadate (V_{10}) showed the highest GI_{50} as it could induce protein oxidation and vanadyl (V) formation. [78] Furthermore, vanadyl signal could be noticed from 60-90 min in between during incubation so the oxidation-reduction stability of V_{10} and the POVs is not feasible to determine during biological activities. As vanadyl formation was expected to contribute to inhibition there, in this study it can be said that vanadium-based compounds have not been converted into vanadyl, and this can in part explain the absence of inhibitory effect of the compounds in *E. coli* or *S. aureus* growth.[78] Moreover, in another study by Postal et al. 2016[107], the author described the toxic role of vanadium compound decomposition and its effect on *E. coli*. PV_{14} decomposed into $V_{10,}$ and it had a toxic effect on *E. coli* while V_{15} gave V_1 during decomposition, which had no antibacterial activity. The combination of nicotinamide with V_{10} has revealed a comparatively higher toxic effect in the growth of *E. coli* than alone V_{10}.[107] In this work, as vanadium had different anionic architectures that have not been studied earlier for the antibacterial activities, this can be understood that there was no apparent redox reaction occurred reflecting the POMs and metal complex were not probably penetrated into the bacterial cell membranes to display the antibacterial activity.

Gumerova et al. 2018 [72] examined the antibacterial activities of twenty-nine POMs against *M. catarrhalis*. The Preyssler type -POT, P_5W_{30} showed the highest potency, with a MIC of 1 µg/mL. P_2W_{18} and its derivatives may inhibit *M. catarrhalis* with MIC values of 2–8 µg/mL. However, $CoTiW_{11}$ has comparable MIC values to the Dawson-type group against *M. catarrhalis* while it showed resistance against Anderson-type inorganic and organic POTs and POMos. *M. catarrhalis* and *H. pylori* were sensitive to bigger POMs, but this POM is inert against them. The small size and low charge of Anderson-type anions may explain their lack of antibacterial activity.[72] Only POTs (W_{12}^{10-} and W_{22}^{12-}) and octa molybdate Mo_8^{4-}, showed MIC values above 256 µg/mL. Decavanadate had no antibacterial activity, confirming the selective activity of the most common vanadates V_{10} and V_4O_{12} against *S. pneumoniae* with MIC values of 4–32 µg/mL. Tetranuclear vanadium tartrates were one of the few vanadate species that remained stable and hydrolysis-resistant in aqueous solutions over time, like V_{10}, however, POVs failed to kill *M. catarrhalis*. The study found that Dawson-type POMs were more active and selective against *M.*

catarrhalis, while Keggin-type POMs were bacteriostatic.[72] The study found that POM composition, shape, size, and net charge affected performance. In this study medium-sized POTs showed a correlation between activity and net charge.[72] Low molecular weight lipopolysaccharides (LPS) on the surface of *M. catarrhalis* cells contribute to increased hydrophobicity and susceptibility to hydrophobic antimicrobial agents. Possibly due to the interaction between lipid monolayers and super-chaotropic anions, the outer membrane of *M. catarrhalis* strains is more permeable to hydrophilic compounds, such as β-lactam antibiotics.[72]

In a previous study by Marques-Da-Silva et al. 2019 [78] , the effect of vanadate and decavanadate (V_{10}) on the growth of *M. tuberculosis* found that V_{10} had a specific ability to induce antimicrobial activity. It was suggested that mycobacteria or a component excreted by them catalyze the hydrolysis of V_{10}, facilitating the transport of vanadate into the cell. Additionally, *in vivo*, exposure to decavanadate was found to increase the amount of vanadium, particularly in mitochondria.[78] In another study [108], the POTs and POMos were found to be less effective against *S. aureus*, as compared to POV. The proposition was made that POMs have a significant impact on the balance of ions within cells, ultimately resulting in the demise of the organism.[108] Moreover according to literature, Wells-Dawson and Keggin polyoxometalates were found to be the most potent of seventy-six tested POMs in terms of their ability to sensitize methicillin-resistant *S. aureus* strains SR3605 and ATCC-43300 [69,109] Some hetropolytungstates, such as GeW_9, AsW_9 and PVW_9, have shown the antibacterial activity against the cell wall of Gram-negative *E. coli* and Gram-positive *B. subtilis*. The MIC values were in the range of 40-130 μg/mL and the results suggested that the increase of (PhSb) groups in the organic POMs increased the antibacterial activities.[66,110]

On the contrary, a structure-based trend was also noticed in POTs from single to triple Kegging and single to double Dawson-type POTs. An evident decrease in anti-HIV-2 activity was noticed with the increase in the number of Dawson and kegging structures in the compounds. The activity of anti-HIV in the case of double structure Keggin was 3-40 folds less effective for HIV-2(ROD) than for HIV-1 (III_B). For triple structure Keggin, the anti-HIV activity was 80-240 folds less effective against HIV-2(ROD) than HIV-1(III_B).[66] So, it can be observed that the variable characteristics of the POMs have variations in their structure-based activities with regard to antibacterial approaches. According to Barsukova-Stuckart et al. 2012 [110], the hybrid POMs of organoantimony were assessed for antibacterial activity against *E. coli*. The POMs showed antibacterial activity in the range of MIC value of 80- 130 μg/mL.[110] Furthermore, hybrids of organic and inorganic combinations with kegging, cobalt, and gatifloxacin with a higher MIC

value of 2.24 µg/mL were observed against *E. coli*.[78] These studies also reflected the variability in the activity with variation in the structure and type of bacterial strain. A structure-based activity of V_3 complex with *Bacillus stearothermophilus* phosphatase (PhoE) from the dPGM family, was characterized by an X-ray crystallographic technique. It was reported that V_3 forms a network of extensive hydrogen bonding with catalytic residues His10 and Glu83 as a complex of V_3- PhoE and replaces the phosphate.[111,112] There is also the possibility that POMs interfere with the morphological changes of the bacterial cell and lead them to death as in the case of *H. pylori*, the bacillus shape is turned into a cocci or U-shaped form. [69,109] In addition to it, a POMo (V_2Mo_{10}) in the complex of chitosan has changed the shape of the *E. coli* strain and caused disruption of the bacterial cell.[106,113]

In a similar screening study by Gu et al. 2018[114], eight bacterial strains, such as *S. aureus* (YB57), *E. faecalis* (FA2 and FA3), and *E. faecium* (SA2 and SA3) strains were cultured in brain heart infusion (BHI) broth, while *S. aureus* (USA300), *Acinetobacter baumannii* (ABC3), and *S. pneumoniae* (SP) were used to evaluate the antibacterial properties of various polyoxometalates. The results revealed that the hybrid compound H_4W_{12} was only active against the *E. faecalis* FA2 strain, whereas the compound containing molybdenum- Cu(phen)Mo_3 had a broader antibacterial spectrum than those containing tungsten W_{12}, $W_{11}Ti$, CeW_{10}, $LaSiW_{11}$, $CeSiW_{11}$.[114] The study evidenced that POM's antibacterial activity depends more on its component elements than its anionic architectures reflecting that element selection is critical in antibacterial material development. The study indicated that Ce-compounds had comparatively better antimicrobial characteristics, thus authors suggested synthesizing Ce-compounds and studying their antibacterial efficacy and reaction processes.[114] Moreover, other study indicated that the proliferation of bacteria on biomaterial surfaces can be modulated by various parameters, including surface charge and adhesion strength.[115] From the aforementioned studies, it can be noticed that POMs have antibacterial activity.

There could be the possibility that the structural combination of the POMs and metal complex was not in effective conjunction for *E. coli* and *S. aureus*. It can be suggested that the modifications in this structure of the compounds can improve the antibacterial activity. Moreover, it is also possible that these compounds can show an antibacterial effect on other crucial bacterial species however, further screening studies would be required to assess these compounds. There is also an instance of the change of color of the POM while interacting with bacteria. Reduction of the POMos and POTs can be distinguished because of the blue color due to the intervalence transfer of charge as in the case of P_2W_{18} interaction with MRSA can be

observed with the development of the blue color due to the reduction of the POT. For 12 hrs the protoplast remained blue, suggesting that the POT had penetration in the MRSA cell through the cell wall. The hypothesis was that the POT enters the respiratory process as an electron transfer, which has a negative redox potential for the reduction of P_2W_{18}.[80,116] However, in this study none of the metal compounds has shown any reduction based on the change in the color of the media in the presence of *E. coli* and *S. aureus.* There was no visual inhibition zone around any diffusion well reflecting that the compounds were not penetrated into the cell walls of both bacteria.

Hypothetically, during POM and bacterial interaction, the redox reaction occurs and with the ROS production capacity of the POM, there is the probable death of the bacteria, which cannot be stated in this scenario for five POMs and one metal complex in this study.[62,78] There can be the possibility that due to instability of the compounds might be there was hydrolysis of the compounds in the agar media whereas, the metal atoms were delivered to the bacterial cell and there was no inhibition of bacterial growth incubation at 37° C. There could be a possible reason for the bioavailability of the metal compounds to the bacterial cell due to the agar contents of the media. Furthermore, molybdenum, vanadium, and tungsten atoms of the metallic compounds made complexes with the media or with the proteins, peptides, or phosphates in the case of bacterial cell membranes with the possible structural conjunctions or modifications that remained ineffective. However, the exact mechanism that POMs have shown no effect on the bacterial cell membrane is not understood and the structural-activity relationship of POMs interacting with the POMs is required to be further examined.

3.2 Growth of *S. aureus* ATCC 6538 in Saline conditions

As mentioned in the material and method section 2.2, *S. aureus* ATCC 6538 susceptibility was assessed in the presence of a saline environment against NaCl concentrations (1.5%, 3%, 4%,5%, 6%, and 7%, w/v) and the growth kinetics were observed. The **Figure 14** shows the growth of S. *aureus* ATCC 6538 on BHI agar Petri dishes, which were used to perform the growth kinetics assay on the effect of salt on the bacterial growth. **Figure 15** illustrates the behaviour of the growth of *S. aureus,* ATCC 6538 with aforementioned varying concentrations of NaCl from 1.5% to 7% (w/v).

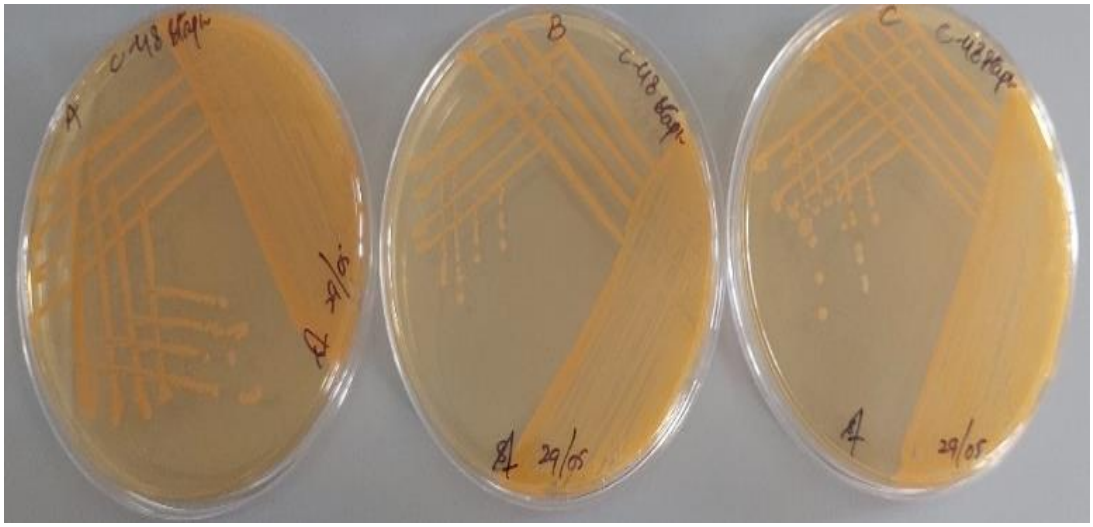

Figure 14- *Culture of S. aureus ATTC-6538 on Brain and heart infusion agar plates.*

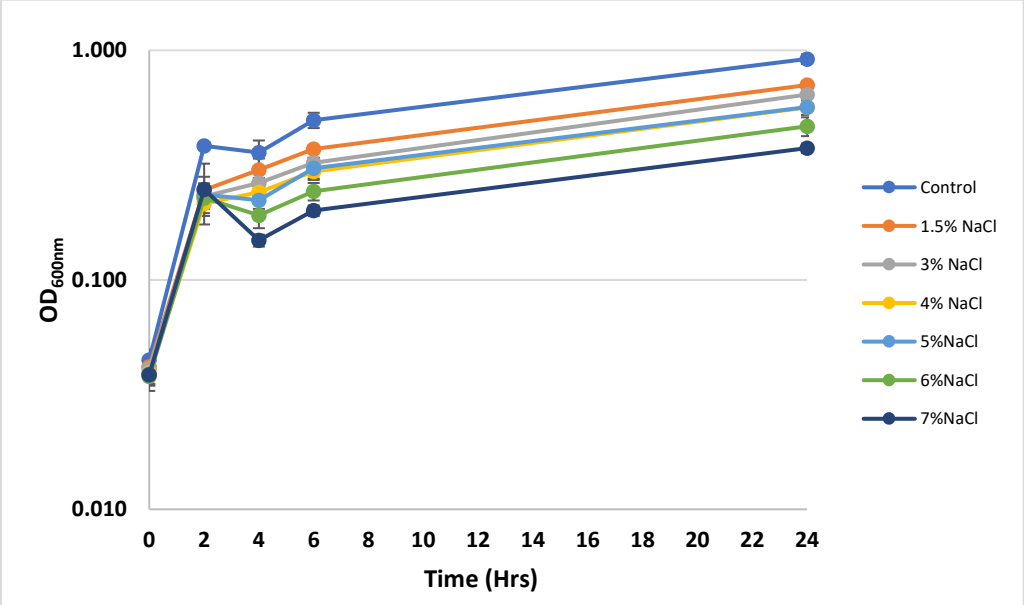

Figure 15- *S. aureus ATCC 6538 growth trends at 37°C in the presence of NaCl concentrations in MH medium*

The growth kinetics of *S. aureus* ATCC 6538, highlight the ability of this bacterial strain to growth in the presence of NaCl, but the higher concentrations (5% to 7%) affect the final biomass (OD_{600nm}) in comparison with the control culture (no NaCl added). Moreover, the concentration of 3% NaCl and subsequently 1.5%, resulting in no impact on bacterial growth and closely resembling the control group devoid of any salt concentration. The capacity of *S. aureus* to tolerate the saline effect seems to be related with mechanisms of generation of osmo-protectants molecules and associated with genetic upregulation or down regulations.

Feng et al. 2022 [117] demonstrated the *S. aureus* ATCC 27217 viability in a solution containing 20% (w/v) NaCl. The morphology of *S. aureus* cells eventually underwent alterations eventually to exposure to a 20% w/v) NaCl solution, resulting in the disruption of the cell membrane and subsequent release of cellular contents. The growth of *S. aureus* was further impeded, and the shape of its cells was compromised due to the elevated salt levels. [117] The study also revealed that *S. aureus* needs more differentially Expressed Genes (DEGs) to adjust to salinity. These pathways largely affected amino acid metabolism, translation, infectious illnesses, purine metabolism, carbohydrate metabolism, and lipid metabolism. High salt levels activate stress response and affect biofilm formation, pathogenicity, transfer system, and osmotic regulation in *S. aureus*. High salinity stress substantially reduces the invasiveness of *S. aureus* by inhibiting its haemolytic activity and coagulase expression.[117] In this study, *S. aureus* has shown no resistance to increasing salt concentration up to 7% (w/v). It also depicted that with increasing concentration the bacterial cell became susceptible and biochemical changes in the saline stress environment the cells were unable to recover.

The salinity can also increase the bioavailability of the antibiotics, which was demonstrated by Chen et al. 2022 [9], that high NaCl salinity might improve bacterial cell permeability and tetracycline bioavailability. Climate change-induced soil salinity may increase antibiotic selection pressure on microorganisms, raising antibiotic resistance risk. The scientists also found that *E. coli* (MC4100/pTGM bioreporter) enhanced membrane permeability at higher NaCl may boost bacterial tetracycline bioavailability. [9] Tetracycline accumulation in *E. coli* was decreased with agar content however, the positive effects of NaCl on cell membrane permeability outweigh its negative effects on water and solute flux, thereby increasing the bioavailability of tetracycline.[9] This study positively demonstrates, the potential of NaCl that can boost the antibiotic effect due to changes in the cell permeability.

A similar investigation by Li et al. 2021 [50] highlighted that LB broth supplemented with 0% NaCl has more viable cells of *E. coli* BL21(DE3) and DH5α at 24 hrs than groups with 1%, 3.5%, and 5% (w/v) NaCl. Hyperosmolarity induced by 5% (w/v). NaCl increases oxidative damage in *E. coli*, whereas the effect of lower concentrations of NaCl on oxidative stress was not statistically significant. The study investigated the effect of various NaCl concentrations on the motility of *E. coli* and found statistically significant dose-dependent inhibition of bacterial movement among the tested concentrations.[50] These results are in accordance with the existing study however, in the case of *S. aureus,* ATCC 6538 has given the growth inhibition in a dose-dependent manner in the presence of salt conditions.

There are physiological and biochemical changes in the abiotic stress conditions as Pinto et al. 2014[118], utilized RNA sequencing to identify C*orynebacterium pseudotuberculosis* differentially expressed genes in response to abiotic stressors. They found that biological processes like cellular adhesion and oxidoreduction are most evident under these conditions.[118] Li et al. 2021 revealed that elevated concentrations of NaCl impeded the growth of *E. coli* BW25113, although lower amounts did not exhibit the same inhibitory effect. Biofilm development, oxidative stress tolerance, and motility, which are connected to environmental survival and within-host pathogenicity, increased with high NaCl concentrations. *E. coli* differentially expressed genes under salt stress were identified and functionally analyzed to determine, which DEGs were significantly enriched in Gene Ontology terms, metabolic pathways, and gene clusters.[50] It can be noticed that variations in the susceptibility to the increasing salt concentration are dependent on the upregulation and downregulation of the genes that can vary from bacterial strain to strain.

Moreover, salinity decreases set expression as RNA-seq showed that the *staphylococcal* enterotoxins gene set was 2.1-fold down-regulated (0% NaCl vs. 20% (w/v) NaCl).[117] Sihto et al. 2015 [119] found that NaCl stress decreased the expression of *staphylococcal* enterotoxin genes in *S. aureus* at the mRNA level. Under extreme salt stress, the enterotoxin gene down-regulates, decreasing its pathogenicity.[119] Masters et al. 2021 [119] showed that *S. aureus* produces many virulence factors and toxins during infection. Thus, *S. aureus* infection pathway downregulation may also reduce pathogenicity.[120] *S. aureus* can tolerate severe salt stress even in the food preservation process. *S. aureus* survives high salinity stress by upregulating aminoacyl-tRNA biosynthesis, betaine biosynthesis, and L-proline content. [117] The high salt damage to the cell structure may liberate proline and other components, lowering L-proline levels that eventually disrupt the cell metabolism. This study provided a scientific foundation for investigating *S. aureus* metabolic alterations in high osmotic environments.[117]

A unique trait of *S. aureus* is its capacity to grow in NaCl concentrations, which is significant since *S. aureus* is the only food-borne pathogen that can develop at water activity levels below 0.9 as it is crucial for microbial growth control.[121] The mechanisms underlying the high NaCl tolerance of *S. aureus* are the osmotic, ionic, and Na^+ ion stresses caused by NaCl. In *S. aureus*, the intracellular concentration of K^+ is unaffected by NaCl stress.[121] Numerous transport systems that are activated or induced by NaCl permit the entry of osmoprotectants into the cell. *S. aureus*, in response to NaCl stress, not only accumulates suitable solutes to maintain turgor pressure but also undergoes substantial gene and protein expression.[121] *S. aureus* may flourish in harsh settings which protect the cell membrane from salt. Many small molecules called compatible

solutes, such as glutamine, proline, and glycine betaine, can intracellularly accumulate in *S. aureus* due to increased biosynthesis or uptake and decreased degradation modes, improving osmotolerance.[117] Salt stress affected transmissible salt resistance genes and their genetically linked antibiotic resistome to propagate ARG. Intracellular oxidative stress increases membrane permeability and ARG conjugations. Free ARGs injected into cells could recombine with host chromosomes for replication. DNA excision, DNA mismatch, endoglucanase, DNA polymerase, and DNA repair protein showed improved ratios. Nevertheless, the antibiotic resistome in saline soils was shaped by mobile genetic elements (MGEs). Antibiotic-resistant genes spread when they coexist with MGEs in prospective hosts and were amplified by intracellular oxidative stress and SOS responses.[8] The oxidative stress and the SOS response accelerated antibiotic efflux/target protection-transposon/integron/plasmid transfer and replication due to salinity. Salt stress increased soil antibiotic resistance gene (ARG), horizontal gene transfer (HGT) and vertical gene transfer (VGT) activity via intracellular organic osmolyte transporters and K^+ absorption proteins. Most bacteria in saline soils balanced their cytoplasm with osmolytes, which may indirectly cause ARG evolution. Salt-mediated gene expression changed activate antibiotic resistance.[8]

The obtained results are consistent with the findings of previous research and from the current results, it is evident that *S. aureus*, ATCC 6538 growth showed suppression under higher salt conditions. According to the growth trends lowest possible salt concentrations as lower (1.5%), medium (3%), and higher (6%) were chosen to proceed to evaluate the synergistic effect of NaCl with P_5W_{30}.

3.3 Growth of MRSA 16in Saline Conditions

The growth of MRSA 16under saline conditions was also evaluated. In **Figure 16** the culture of MRSA 16on BHI agar plates that were used to perform the growth assay to examine the response to NaCl. The growth profile of MRSA 16 is illustrated in **Figure 17**, with varying NaCl concentrations.

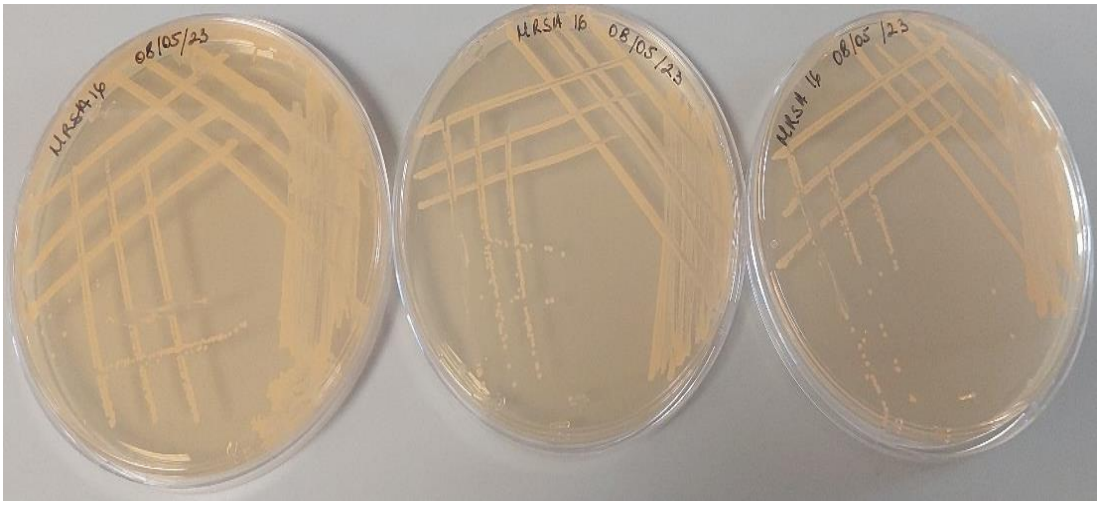

Figure 16*-Culture of S. aureus MRSA 16 on Brain heart and infusion agr plates.*

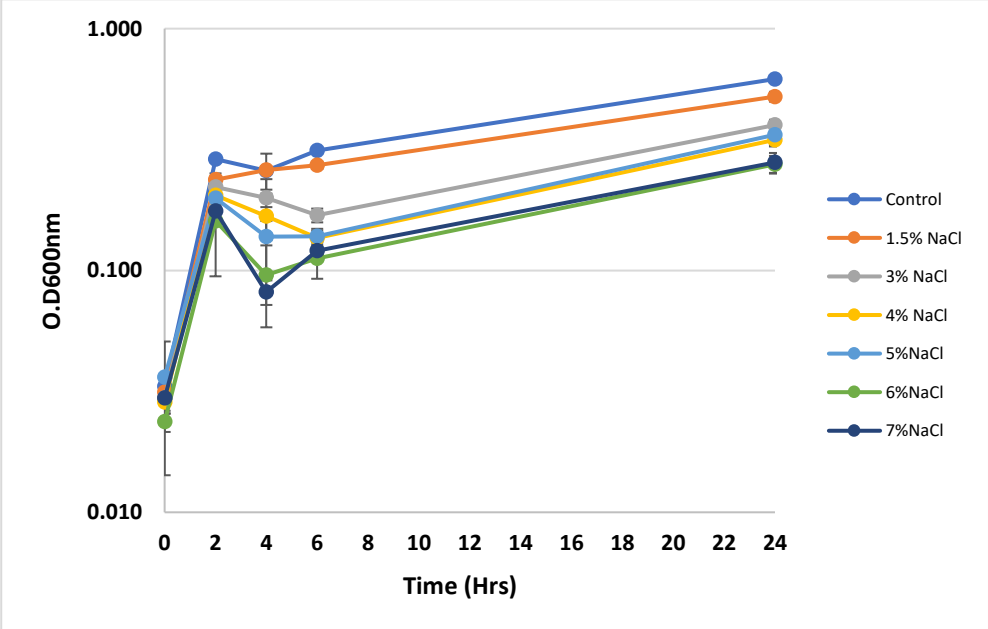

Figure 17- *Methicillin-resistant S.aureus (MRSA 16) growth at 37°C in the presence of different NaCl concentrations MH medium. The data is representative of three biological and 2 technical replicates.*

According to **Figure 17** MRSA 16is able to reach the maximum growth at the different NaCl concentrations tested after 2 hrs and then suffer a slight decrease that was more pronounced at 6 and 7% (w/v) NaCl. After the 6 hrs the MRSA 16 cells start to recover the growth achieving a maximum O.D $_{600nm}$ (biomass) after 24 hrs for all NaCl concentrations tested. At 1.5% (w/v) salt concentration MRSA 16behaved in a similar pattern to the control culture (no NaCl). The lowest biomass (O.D $_{600nm)}$ was observed at 6 and 7% (w/v) NaCl.

Lee et al. 2014[122] investigated the expression of the genes involved in salt tolerance, using quantitative real-time PCR. They found that increasing NaCl concentrations promoted biofilm

formation in *S. aureus* by upregulating *icaA*.[122] Different genes controlled the process at different stages, and no biofilm formation was detected above 5.6% NaCl concentration.[122] Thus, investigating and explaining the impact of NaCl concentration on bacteria should be done according to the strains. [50,123] In the current study, the pattern of susceptibility of *S. aureus,* ATCC 6538 and MRSA 16was very similar. It is recognized that [17] MRSA strains exhibite a higher propensity for salt resistance as compared to the MSSA. SCCmec strains grown in TSB with 2% NaCl tolerated the stress that differed substantially.[17] The *icaADBC* operon activation and polysaccharide intercellular adhesion synthesis depends on the NaCl concentration, resulting in salt tolerance differences between MRSA and MSSA strains.[17]

There are several regulatory proteins and genes involved in the process of biofilm formation which tolerates the salt stress the *S. aureus.* [23] Julia M Ross et al. 2015 [23] examined how NaCl affected stabilization in *S. aureus*, focusing on polysaccharide intercellular adhesin (PIA) synthesis and protein expression at high NaCl levels. Twelve proteins were found to have higher abundance with increased NaCl levels, including *IsaA* and *CspA*, through the network of PIA and surface proteins.[23] The *ica* operon produces PIA, comprising genes implicated in translocation, deacetylation, control, and NaCl-dependent activation.[23] The *Staphylococcal* accessory regulator *sarA* regulates the gene expression, including virulence determinants and the PIA-producing *ica*-operon. Therefore, it can be said that the NaCl may interfere with gene regulatory networks to stabilize bacterial stress tolerance.[23] There could be the possibility that the *ars* operon is involved in the salt tolerance response of *S. aureus*.[121] In order to examine the molecular pathways by which *S. aureus*-ATCC1 2600 adapted to osmotic stress, NaCl-sensitive mutants were produced using a Tn917-lacZ insertion in the *ars* operon.[121] The NaCl-sensitive mutant grew slower and had lower culture turbidity in 1.5 M NaCl.[121] Electron microscopy showed huge, pseudo-multicellular mutant cells under NaCl stress furthermore, exogenous osmoprotectants, such as glycine betaine, choline, L-proline, or proline betaine did not reduce the NaCl sensitivity. The complementation of the *ars* operon into the mutant restored the NaCl tolerance, proving that the arsR mutation is linked with the phenotype.[121]

In the study conducted by Ghanima et al. 2008 [18], *S. aureus* susceptibility was affected by the increasing salt concentrations. In high NaCl concentrations, *S. aureus* was tested for antibiotic and antiseptic sensitivity. The bacterial culture on the presence of NaCl altered the susceptibility to the antibiotics ampicillin and amoxicillin, namely the resistance profile was changed to a sensitivity pattern.[18] It was observed that at higher salinity the antibiotic efficacy was improved, by the increase in the inhibition zone diameter, which correlated directly with the NaCl content

(1%, 3%, 5%,7%, 9%, 11%, w/v).[18] The study also reported that ampicillin and amoxicillin alone failed to treat laboratory rats with infection while the rats healed with antibiotics and NaCl injection. As an additional therapy, NaCl may boost antibiotic efficacy in treating *S. aureus* infections.[18] On normal nutrient agar, all *Staphylococcal* isolates were resistant to all studied antimicrobial agents and were able to grow at 9% (w/v) NaCl.[18]

Cross-resistance evolution may indirectly increase ARG abundance from salt exposure. Plasmid-mediated transfer of osmoregulation genes from a halophilic *Gracilibacillus* sp. to nonhalophilic bacteria let their hosts withstand high salt environments.[8]

As the concentration of salt increases, the permeability of the cell membrane may be enhanced, leading to the disruption of the bacterial cell membrane. This disruption facilitates the penetration of antibiotics, however, there was also evidence suggesting that high levels of salinity could have negative consequences, such as an increase in bacterial resistance.[4] Ganjian et al. 2012 [4] evaluated that *S. aureus* (ATCC 25823) could survive osmotic stress and thrive at various salt concentrations however, antibiotic susceptibility decreases at sub-lethal salt concentrations. Salt stress may facilitate the development of methicillin resistance more than other antibiotics because induces the production of penicillin-binding proteins with reduced affinity to β-lactam antibiotics.[4] Moreover, hyper-resistant *Staphylococcus* strains with higher mutation rates and antibiotic-binding site inactivation can result from spontaneous genomic alterations.[4] Whereas the high salt concentrations in food preservation can make *S. aureus* antibiotic-resistant, change its protein profile, and spread food-borne illnesses. The strains showing methicillin resistance are the most, especially those exposed to 35% salt.[4] The protein profile analysis of those strains showed that salt exposure from 5 to 35% decreased the intensity of some protein bands and increased others. They showed that sub-lethal salt stress can affect *S. aureus* antibiotic resistance and protein profile, potentially facilitating food-borne infections with antibiotic-resistant bacteria.[4]

The results obtained in this study align with the findings of prior research. The data clearly indicate that the growth of MRSA 16was inhibited in conditions of high salinity. The MRSA 16was more affected at 6% and 7% (w/v) salt concentrations in comparison with other concentrations. Three distinct salt concentrations were selected for further evaluation, namely the lowest concentration of 1.5% (w/v), the 3% (w/v), concentration and the 6% (w/v) concentration. These concentrations were selected to examine the potential impact of NaCl to the antibacterial activity of the compound P_5W_{30}, which is described below.

3.4 Antibacterial Activities of Preyssler type-POM P_5W_{30} in the presence of NaCl

Previous results indicated that P_5W_{30} exhibits a strong antibacterial activity against *S. aureus*.[37] The MIC values of the POM against *S. aureus* ATCC 6538 were calculated as 32 µM (0.265 mg/mL) and for MRSA16, 600 µM (4.96 mg/mL).[37] Hence, this study represented the initial assessment of the combination of P_5W_{30} with NaCl. The growth profile of *S. aureus* ATCC 6538 in the presence of different NaCl concentrations and ½ MIC, MIC and 2xMIC value of P_5W_{30} is illustrated in **Figure 18, 19 and 20.**

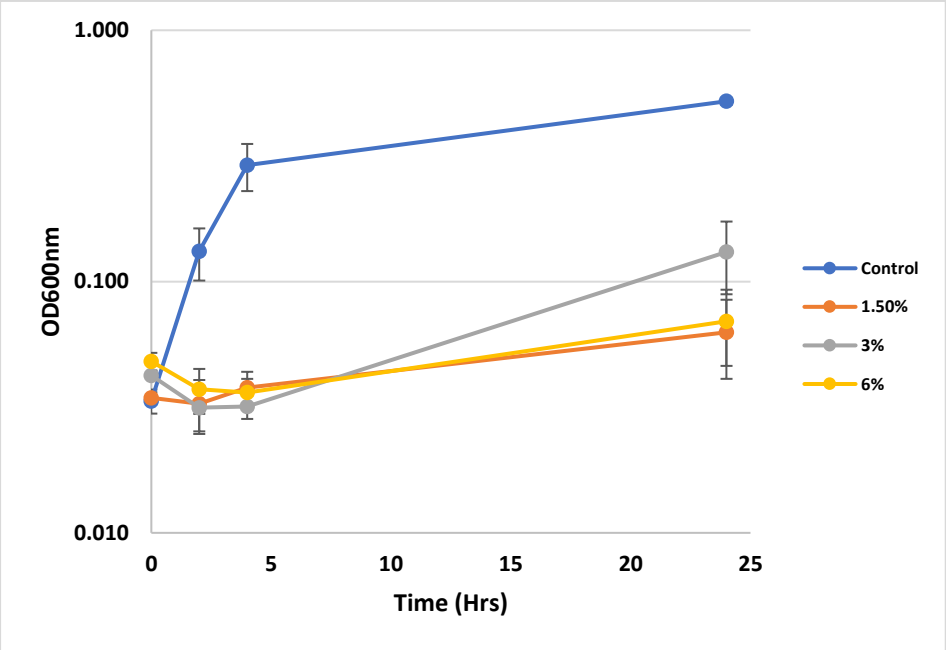

Figure 18- *Growth curve of S. aureus ATCC 6538 in the presence of NaCl concentrations and half of the MIC (16 µM) P_5W_{30}. Data is representative of three biological and two technical replicates.*

In **Figure 18** where it is represented the growth curve of *S. aureus* ATCC 6538 in the presence of ½ MIC of P_5W_{30} and different concentrations of NaCl (1.5%, 3.0% and 6% (w/v)) is possible to observe that the growth decreases along the 24 hrs for the NaCl concentrations 1.5% (w/v) and 6% (w/v) in contrast to the concentration of 3% (w/v) where is observed a recovery of growth after 4 hrs. An evident change was found between the biomass produced (max. OD_{600nm}) at the different concentrations of NaCl and in the presence of 16 µM P_5W_{30} in comparison with the control culture. It is important to notice that at 1.5% and 6% (w/v) the maximum OD_{600nm} was similar (p>0.05).

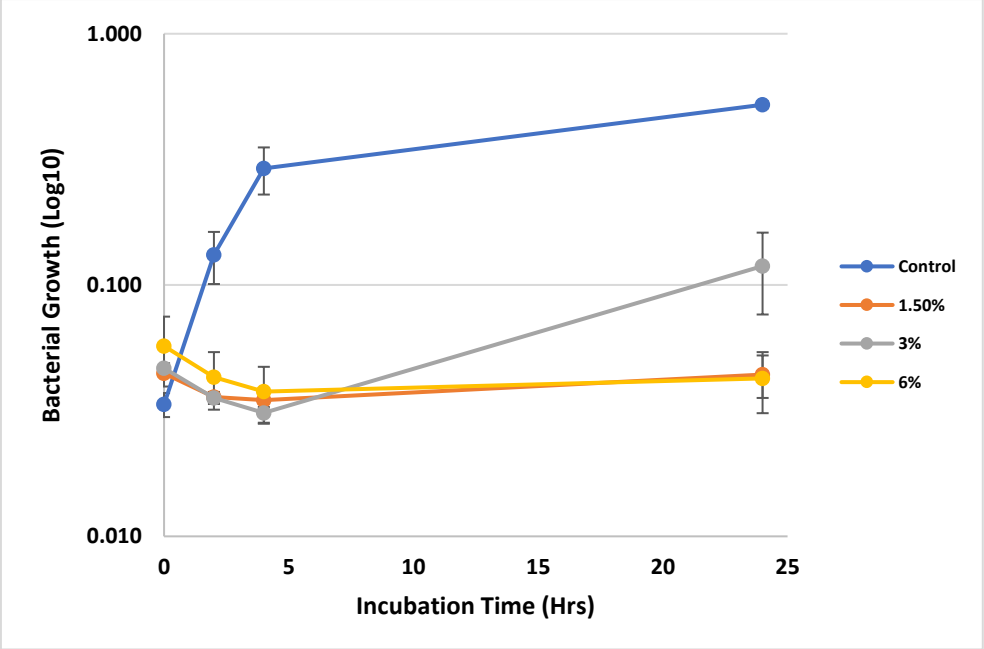

Figure 19- *Growth curve of S. aureus ATCC 6538 in the presence of NaCl concentrations and the the MIC value (32 µM) of P_5W_{30}. Data is representative of three biological and two technical replicates.*

In **Figure 19** where it is represented the growth curve of *S. aureus* ATCC 6538 in the presence of the MIC value (32 µM) of P_5W_{30} and different concentrations of NaCl (1.5%, 3.0% and 6% (w/v)) is possible to observe as in **Figure 18** that the growth decreases along the 24 hrs for the NaCl concentrations 1.5% (w/v) and 6% (w/v) in contrast to the concentration of 3% (w/v) where is observed a recovery of growth after 4 hrs. It was also important to highlight that as in Figure 18 a noticeable variation was found between the biomass produced (max. OD_{600nm}) at the different concentrations of NaCl and in the presence of 32 µM P_5W_{30} in comparison with the control culture. Also, at 1.5% and 6% (w/v) the maximum OD_{600nm} was similar (p>0.05).

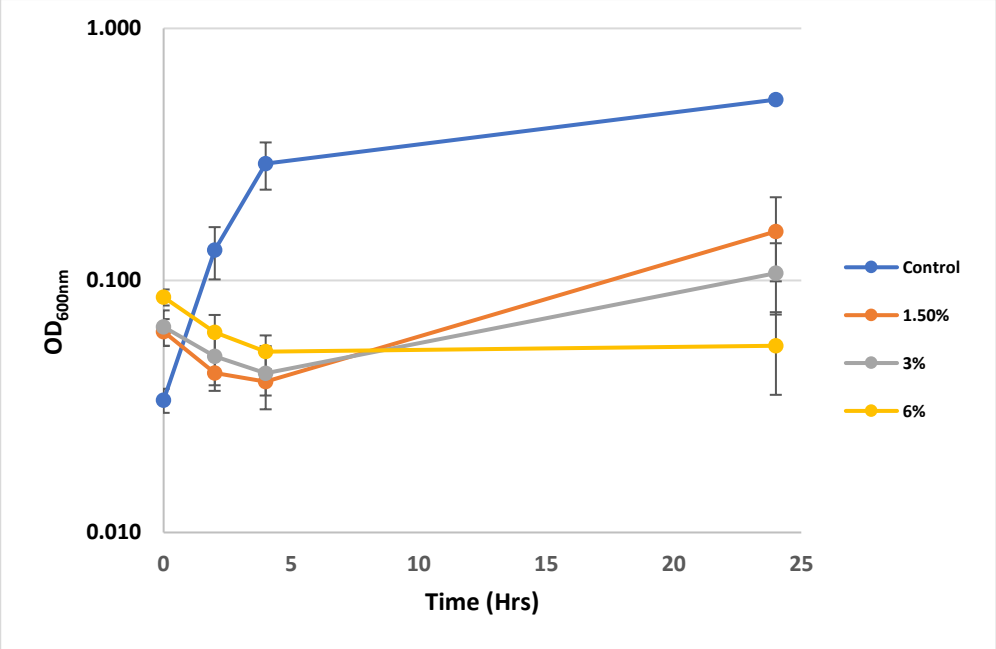

Figure 20- *Growth curve of S. aureus ATCC 6538 in the presence of NaCl concentrations and the the 2x MIC value (64 µM) of P_5W_{30}. Data is representative of three biological and two technical replicates.*

In **Figure 20** it is represented the growth curve of *S. aureus* ATCC 6538 in the presence of 2x MIC of P_5W_{30} and different concentrations of NaCl (1.5%, 3.0% and 6% (w/v)) is illustrated. As observed in **Figure 18** and **19** it is possible to observe that the growth decreases during the first 4 hrs and after this time interval the bacterial cells are able to increase the growth at the concentrations of 1.5% and 3% (w/v) in contrast to the 6% (w/v) concentration at which no recovery of growth is observed. The maximum OD_{600nm} is significantly different ($p<0.05$) for all NaCl concentrations tested in comparison with the control culture. However, is important to highlight that the recovery of the bacterial growth at 1.5% (w/v) is significantly higher ($p<0.05$) in comparison with the 3% (w/v) concentration. For better understanding of the impact of NaCl concentrations at the different MIC values of P_5W_{30} in Table 6 is indicated the percentages of growth inhibition at the different NaCl concentrations and the tested MIC values of P_5W_{30}

Table 6- Percentage Inhibition of the maximum growth of *S. aureus* ATCC 6538 in the combination of P_5W_{30} and salt concentrations.

P_5W_{30}	**1.5% (w/v) NaCl**	**3% (w/v) NaCl**	**6% (w/v) NaCl**
16 µM (½MIC)	88%	75%	87%
32 µM (MIC)	92%	77%	92%
64 µM (2xMIC)	70%	80%	89%

The presence of particular types of antibiotics in saline soils assumes greater significance in terms of eliciting antibiotic resistance reactions to salt.[9] The presence of soil salinity has the potential to diminish the bioavailability of dissolved antibiotics to microorganisms.[9] It was noticed that elevated levels of NaCl in culture media exert osmotic stress on microbial cells, resulting in a decrease in turgor pressure across the cell membrane, the release of intracellular water, and cellular contraction.[53]

Bacillus subtilis can increase the Mg^{2+} influx (hyperpolarization) to resist the antibiotic effects so, it is suitable to look for the ions or nanoparticles in the POMs, which can have strong interactions with bacterial cell membranes by getting adsorbed onto the lipid membrane, causing instability in the membrane and can bypass the cationic influx process of the MDR (multi-drug resistant) bacteria. Similarly, the Preyssler-type of POMs P_5W_{30} has a small size having recognized thermal and hydrolytic stability with a good structural affinity for biomolecules. P_5W_{30} has the possibility to interact with the outer membrane of *B. subtilis* causing the accumulation of the Mg^{2+}, decreasing the cations in the bacterial cell, and increasing the negative charge that ultimately leads the hyperpolarization.[62,1241] In the work by Chen et al. 2021 [62,124], P_5W_{30} was reported in the combination of spectinomycin for *B. subtilis* and methicillin-resistant *S. aureus* while the MIC value was almost 10 times less than the spectinomycin alone. Thus, the synergistic effects of POMs can promote the targeting of the antimicrobials and control the possible multiple drug resistance of the bacteria hence, $P_5W_{30,}$ had the potency to cause the hyperpolarization of bacterial cells and blocks the Mg^{2+} transportation, decreasing the influx of cation, which results in perturbation of ribosomal structure and instability of the bacterial morphological structure.[124] Moreover, photocatalytic inactivation was reported for E. *coli* and *B. subtilis* with polyoxotungstate and molybdate acids as H_3PW_{12}, H_3PMo_{12}, and H_4SiW_{12}. Similarly, in a multilayer film of methyl violet and compound- PV_6Mo_6, a self-assembly was created which showed antibacterial activity against *E. coli*.[66,125]

In another experiment, Fe_3O_4@PDA@POM performance was checked for antibacterial activity against *E. coli* and *C. albicans* which was better than the PDA-doped material itself. This POM has high stability for 12 hrs in solution with a pH in the range of 6-8 including 0.75% NaCl.[62] The bactericidal effect of Fe_3O_4@PDA@POM_can be due to the large surface area for the cationic interaction with the negatively charged bacterial cell wall causing electrostatic damage to the bacterial cell membrane, which leads towards the leaking of intercellular materials out from the cell cytoplasm. There is another possibility of having this electrostatic interference with the cell wall, cytoplasm, and the positively charged protein areas that forces the efflux of Cu^{2+}

ions from the cell and damages the bacterial cell wall or fails the respiratory chain. Furthermore, due to high redox potentials POMs can halt the respiratory pathway of the bacteria by oxidizing the electron carriers while affecting ATP production and causing damage to the bacteria. Moreover, GSH (Glutathione) which is a tripeptide having sulfhydryl groups as an antioxidant and prevents cellular damage to the bacterial cell, is also affected by the POMs as they increase the ROS level with the oxidation of bacterial substances including lipids and proteins.[62]

AgPW@PDA@Nisin, a conjugated complex on the polydopamine has the capability to destroy the *S. aureus* cytoplasmic membrane by changing the permeability and causing cell death with the MIC of 4 μg/mL.[62,126] Furthermore, the increased antibacterial activity (on A549 cell) against *E. coli* was checked for Tyrosine-reduced AuNPs functionalized with phosphomolybdic and phosphoric acid.[61] Moreover, In order to improve carrageenan-based films' efficacy, the article suggests metal compounds, such as Wells-Dawson polyoxometalates Mo_{18}, can enhance antibacterial and food preservation properties. The antibacterial film made from -carrageenan and Wells-Dawson polyoxometalate with a concentration of 8 mg/mL, proved efficient against *E. coli* and *S. aureus*. It was concluded that Polyoxometalates have demonstrated extraordinary antibacterial properties and can be used as substitutes for commercial antibacterial agents.[109]

From the results taken from the OD values, NaCl shortened the latent growth period of *S. aureus*, causing a lag phase that accelerated more than *E. coli*. Both bacteria thrived best at 0% NaCl and decreased above it however, the growth retardation of both bacteria at 37°C was perfectly proportional to NaCl concentration. These bacteria may be inhibited by high NaCl concentrations, reducing food processing and preservation contamination. The specific growth rate of *S. aureus* rose with NaCl but did not double the time. In growth curves, *S. aureus* outperformed *E. coli* at varied NaCl concentrations.[127] Naziba et al. 2023 [39] reported that NaCl affected the morphology of *E. coli* and *S. aureus*, but had a less severe influence on cell damage, especially in the case of *S. aureus*. Low salinity induces an instantaneous influx of small solutes, which reduces physical stress. In contrast, high salinity causes water efflux, which is compensated by an increase in compatible solutes including proline, glutamate, glycine betaine, ectoine, and trehalose.[127]

3.4.2 Growth of MRSA 16in the presence of NaCl and P_5W_{30}

To evaluate the growth kinetics of MRSA 16in the presence of NaCl and P_5W_{30}, the experiments were performed with NaCl at 1.5%, 3%, and 6% (w/v) and with half of the MIC (300 μM) value

of the POM and also with the MIC value (600 µM) of the POM. The growth curves are represented in **Figure 21 and 22**, respectively.

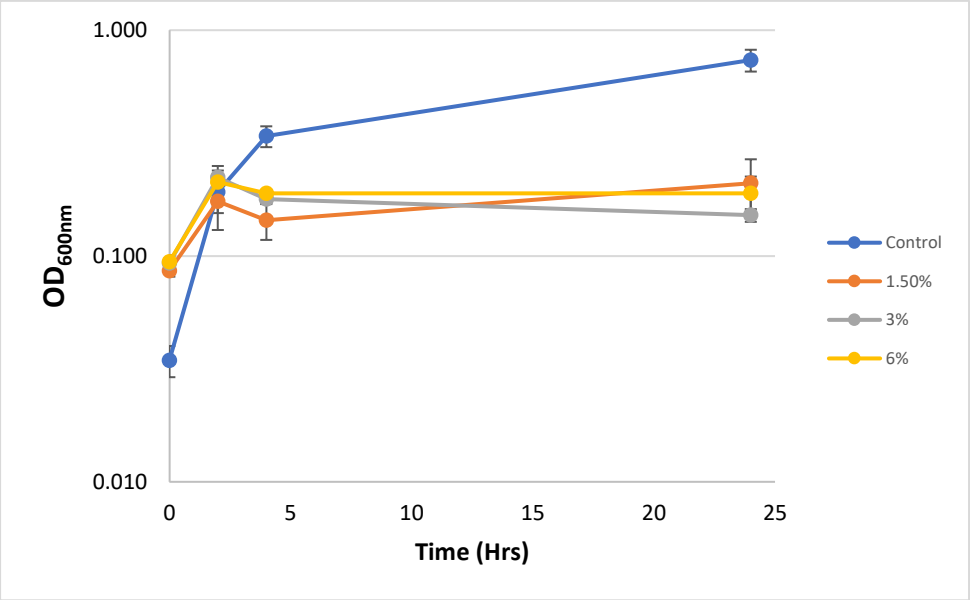

***Figure 21**- Growth curve of MRSA 16 in the presence of the different NaCl concentrations and half of the MIC (300 µM). Data is representative of three biological and two technical replicates.*

In **Figure 21**, is possible to observe that after 2 hrs of incubation MRSA 16 was able to growth and then suffer a decrease at all tested NaCl concentrations in the presence of 300 µM (½ MIC) concentration of P_5W_{30}. After 24 hrs the maximum OD_{600nm} value at all tested NaCl concentrations in the presence of P_5W_{30} (300 µM [½ MIC]) were significantly lower (p<0.05) in comparison with the control culture (no addition of NaCl and P_5W_{30}).

The growth of MRSA 16 in the presence of 1.5%, 3%, and 6% (w/v) of NaCl and P_5W_{30} at the MIC value (600 µM) is represented in **Figure 22**. The growth curve evidences an increase effect of the combination between NaCl and the compound P_5W_{30}, namely at 6% NaCl the growth was drastically reduced, just observing a slight increase in the OD_{600nm} value after 1 hr of growth and then a stabilization with a tendency for reduction over the 24 hrs. The intermediate concentration of 3% (w/v) of NaCl allowed a better survival of MRSA 16 and the lowest concentration of 1.5% (w/v) increased the bacterial survival. The Effect of NaCl for MRSA 16 is more pronounced at ½ MIC for the 1.5% NaCl at the MIC value the inhibition is much lower. As mentioned in Table 7, the remaining inhibition values were not significantly different for NaCl concentrations or the ½ MIC or MIC. These results highlight that P_5W_{30} in combination with NaCl is able to efficiently affect the growth of the MRSA 16 strain.

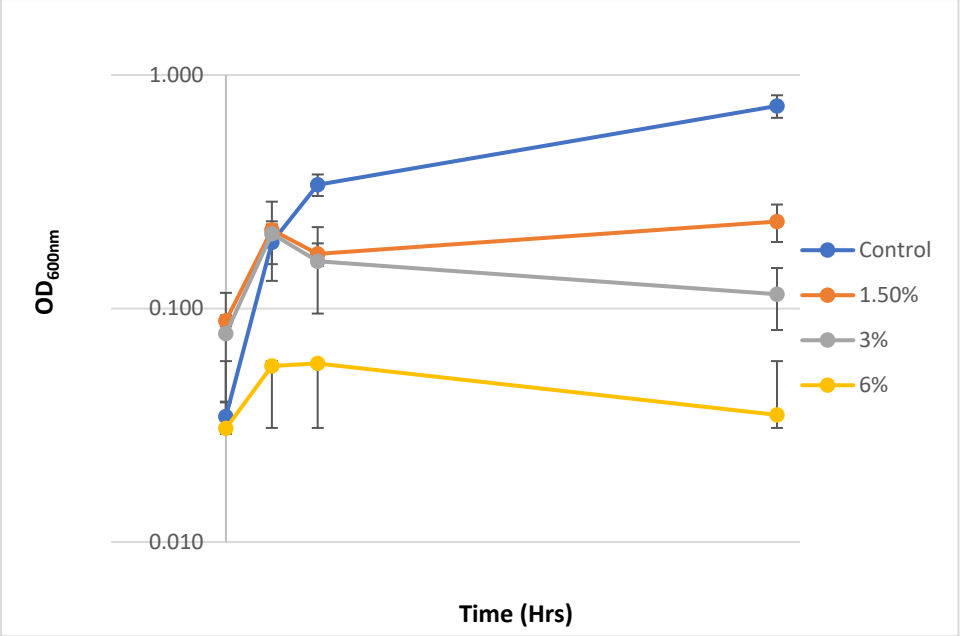

Figure 22- *Growth curve of MRSA 16 in the presence of the different NaCl concentrations and the MIC value (600 µM) of P_5W_{30}. Data is representative of three biological and two technical replicates.*

Table 7- Percentage Inhibition of MRSA 16growth in the combination of P_5W_{30} MIC values and salt concentrations.

P_5W_{30}	**1.5% (w/v) NaCl**	**3% (w/v) NaCl**	**6% (w/v) NaCl**
300 uM (½MIC)	73%	73%	80%
600 uM (MIC)	19%	81%	83%

Faleiro et al. 2022 [37] found the POTs P_2W_{18}, P_2W_{17}, P_2W_{15}, and Preyssler P_5W_{30} structures affect Gram-negative and Gram-positive bacteria, both antibiotic-resistant and susceptible. P_5W_{30} anti-quorum sensing activity was evaluated and its antibiofilm activity against MRSA 16alone and in conjunction with antibiotic cefoxitin. The study also indicates that P_5W_{30} was effective against *S. aureus* ATCC 6538. Macrolide antibiotics are known to impede the translation process and protein synthesis. However, in the case of *S. aureus,* resistance arises due to alterations in the target site and the presence of ATP-binding cassette transporters.[128] The primary mechanisms responsible for chloramphenicol resistance in *S. aureus* include enzymatic inactivation, efflux mechanisms, and the involvement of the 23S rRNA methyl transferase.[128] It is reasonable to hypothesize that P_5W_{30} may exhibit comparable effects to P_2W_{18} in combating MRSA16. The effect of treating MRSA 16 cells with P_5W_{30} at double MIC value or P_5W_{30} in conjunction with cefoxitin was evaluated using transmission electron microscopy. [37] At double of MIC value of, P_5W_{30} caused severe injury to MRSA 16cells, resulting in shape deformation and loss of cell

integrity. It has been reported that the interaction of P_2W_{18} with MRSA cell walls results in alterations to the transcriptome and cell growth rate modulation by P_5W_{30}.[37]

Is known that NADH/ubiquinone/cytochrome-c electron transport system, which has a negative redox potential, reduces P_2W_{18}. P_2W_{18} exposure impairs *mecA* and *pbp* gene transcripts in MRSA strains.[129] The membranes of microbial efflux pumps that transfer protein cause the most cross-resistance exposure to chromium salt for 48 hrs increased the mRNA expression in *S. aureus* bacterial culture. These results suggest that drug-resistance genes n*orA*, *mepA*, and *femX* were upregulated in heavy metals pre-exposed or heavy metals-antibiotics co-exposed *S. aureus*. [39] Wilkinson et al. 2018 [33] reported that oxacillin synergistic was effective against MRSA at a concentration of 5 μM of P_2W_{18}, and the POM improved its efficacy. The POM was likewise nontoxic to mammalian cell cultures in vitro. The study found that effective POM doses reduced *mecA* gene transcription, but higher POM oxacillin doses boosted transcription.[33] Farzana et al. 2018 [38] aimed to examine the antibacterial and antioxidant properties of POMs and their synergistic action with β-lactam antibiotics against MRSA. Different concentrations were used to determine the antimicrobial activity of POMs and the maximum inhibition zones were observed at 20 mg/mL and it was found that POMs had potent antibacterial and antioxidant properties and could be employed synergistically with β-lactam antibiotics.[38] The study implied that POMs may treat drug-resistant bacteria due to their significant antibacterial and antioxidant action. The investigation also emphasized the synergistic action of POMs with β-lactam antibiotics, suggesting their potential in combination therapy.[38]

Balici et al. 2016 [91] assessed several nano compounds for the antibacterial activity against Gram-positive and Gram-negative bacteria. The diameters of bacterial zone inhibition were evaluated for seven nano compounds, such as Cu_3BiW_9, BiW_9, Ni_3BiW_9, Co_3BiW_9, and Mn_3BiW_9 were antimicrobial against *B. cereus* with the highest inhibition areas.[91] Whereas POMs Cu_3BiW_9 and BiW_9 had the strongest antibacterial potential against *S. aureus* and MRSA strains, while POM compounds Cu_3BiW_9, BiW_9, Ni_3BiW_9, Co_3BiW_9, Mn_3BiW_9, and Fe_3BiW_9 had antibacterial activity against *P. aeruginosa* as similar as gentamicin.[91] Polyoxotungstates cross the peptidoglycan layer, penetrate the bacterial membrane, and disintegrate them. Polyoxotungstates block *mecA* gene transcription and mRNA translation on PBP2, enhancing β-lactam drugs' effectiveness against multidrug-resistant organisms, such as MRSA.[91]

3.5 Evaluation of POM Virulence on Larvae Model

The impact of the exposure of *S. aureus* ATCC 6538 to different NaCl concentrations and P_5W_{30} at the MIC value (32µM) on virulence was evaluated using the Great Wax larvae (*Galleria mellonella*). After injection the larvae survival was monitored for 5 days the results are represented in **Figure 23**. The larvae injected with the control culture only survived for 3 days, whereas the bacterial cultures exposed to the different salt concentrations and P_5W_{30} at the MIC value (32µM) were able to survive for 5 days. The best larvae survival along the 5 days was observed for those that were injected just with bacterial cells that were exposed to P_5W_{30} at the MIC value (32µM) with no addition of NaCl. This observation suggests that the exposure to salt induces the virulence determinants of *S. aureus* ATCC 6538 independently of the NaCl concentration. A 100% survival was observed for larvae injected with PBS, as expected.

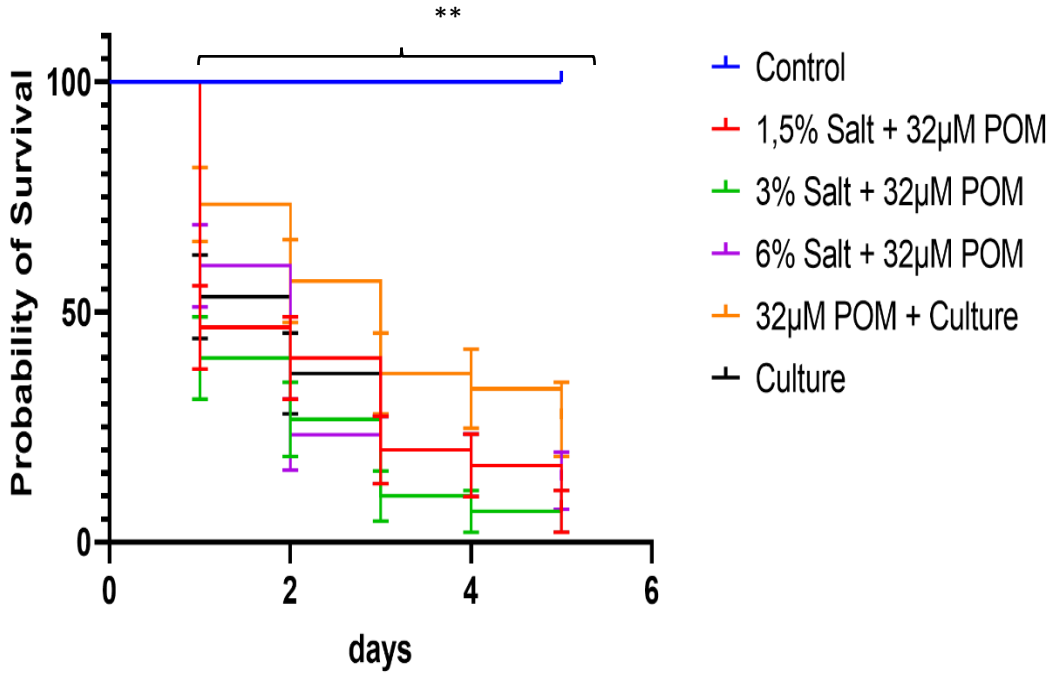

Figure 23- *Kaplan Meier curve for larvae survival after infection with S. aureus ATCC 6538 previously exposed to different NaCl concentrations and P_5W_{30} at the MIC value (32 µM) for 5 days. The Significant difference was found ($p<0.05$) ** among the survival and days of observation with variable treatments.*

The utilization of *G. mellonella* larvae as an infection model has been increasingly prevalent in scientific research. This may be attributed to several factors, including their cost-effectiveness, ease of use, and absence of ethical constraints. [103,130,131] Consequently, these larvae have emerged as a viable substitute for traditional animal models in several experimental contexts. The utilization of *G. mellonella* as a model organism for the study of virulence and novel therapeutic

approaches targeting pathogenic bacteria.[103,132] It emphasizes the potential of *G. mellonella* in monitoring and analyzing host-pathogen interactions. The present model can be employed to examine the effectiveness of alternate therapeutic interventions, such as bacteriophages or adjuvants, in combating drug-resistant bacterial strains.[130,131 129,130.]

In a previous study by Lade et al. 2019[17] and Inés Molina et al. 2020 [133] P_5W_{30} implants contaminated with *S. aureus* reduced larval survival, indicating a bacterial infection that was resistant to antibiotics. The *agr* quorum sensing system detects *S. aureus* proliferation and plays a role in antibiotic resistance. Fibrin and fibronectin-binding protein-coding genes were downregulated. The model was cost-effective and ideal for high-throughput antibacterial screening.[17,133] Similarly, in vivo *G. mellonella* assay was performed to assess the toxicity of the extracts from *Laurus nobilis* which inhibited quorum sensing, virulence factors, and biofilm of foodborne pathogens. The extracts showed antibiotic effects against *S. aureus* multidrug-resistant strains. The extracts inhibited the biofilm for most bacteria tested, with a reduction of up to 40% for Gram-negative bacteria and 76% for Gram-positive bacteria.[133] Moreover, in a previous study by Nale et al. 2016 [90], *G. mellonella* larvae were utilized as a model organism to examine bacteriophage treatment of *Clostridium difficile* infection (CDI). Larvae can replace larger animals for bacterial colonization and antibiotic pharmacokinetics research. This model helped researchers design phage-based CDI treatments by revealing phages' efficacy.[90] Furthermore, Schrama et al. 2013 [103] demonstrated *G. mellonella* infection model demonstrated the capability to distinguish virulence potential among various strains of *L. monocytogenes*. Down-regulation of virulence genes was identified in adapted *L. monocytogenes* cells, suggesting that the influence of adaptation on gene expression varies depending on the strain.[103] The application of the *G. mellonella* model demonstrated its utility in examining the influence of food-related variables, including low pH and sodium, on the virulence of *L. monocytogenes*.

Based on existing literature, it is crucial to propose that the utilization of POM and salt combinations may serve as a fundamental model for designing effective treatments and developing medications, as well as addressing the challenges posed by superbugs bacteria. The findings of this study are crucial to assert that the POM exhibits significant potential for antibacterial activity. Consequently, it holds potential for addressing the issue of antibiotic-resistant bacteria. It is worth noting that the salt percentages in the human body and commercial food products differ, and the susceptibility of *S. aureus* strains varies in different environments due to their varying halotolerant capacities. This variability was observed by comparing the halotolerance capacity of the control strain (ATCC 6538) with that of MRSA 16. This study

proposes a methodology to investigate the effects of varying salt concentrations exceeding 6% on the evaluation of POM in combination with different concentrations. Specifically, half of the MIC of POM (16 μM) and twice the MIC (64 μM) should be selected for evaluation based on observations from the halotolerance section of the assay. In this section, it was observed that treatment with POM at concentrations of 1.5% and 6% of the MIC effectively inhibited more than 50% of growth in *S. aureus*, ATCC 6538. However, the behaviour of the treatment in an in vivo model was found to differ from these observations. The combinations of NaCl in conjunction with POM at its MIC value demonstrated significant virulence in larvae. This information also highlights the potential variability in the outcomes of human intestinal models or skin cell lines when exposed to combinations of salt and POM. Additional research is necessary to assess the congruity of the findings obtained from larvae in relation to intestinal models and skin cell lines, with regard to their efficacy in combating bacterial infections and addressing the escalating issue of antibiotic resistance induced by multidrug-resistant strains of *S. aureus*.

3.6 ATPase Assay

As mentioned earlier, it was also imperative to evaluate the Ca^{2+}-ATPase activity of the $Mo_{17}V_3$ for the first time. As there is not much information available on the POMos for the IC_{50} and type of inhibition in the literature (Table 8). However, the determination of alternative drug targeting sites is of considerable significance, as the utilization of alternative drugs such as metal compounds, has the potential to contribute to the development of antibiotic resistance.

3.6.1 Inhibition Effect of POMo on SERCA-ATPase activity

As mentioned in section 3.5.1, the experiments were performed to evaluate the ATPase activity of the POMo, $Mo_{17}V_3$. This is the first time that the effect of the compound on the Ca^{2+}-ATPase enzyme inhibition activity on SERCA has been reported. The effect was observed for the increasing POMo concentrations of 0.5 to 5 μM and the inhibition capacity was calculated as the percentage of Ca^{2+} -ATPase enzyme activity that was inhibited by 50%, which is known as IC_{50}. The Ca^{2+}-ATPase assays were performed and was visualised in the enzyme kinetics graphs for POMo within the range of 0.5 -5 μM. As the enzyme kinetics graphs are shown in **Figure 24** (control without compounds) and **Figure 25**, (with compound), the IC_{50} in term of percentage ATPase activity was calculated from the height of absorbance scale (mm) over the base of time scale 100 sec and Michalis Menten enzyme kinetics plot was drawn for POMo increasing concentration and ATPase activity. **Figure 26** depicts a Michalis Menten plot, and the polynomial equation was determined to calculate the IC_{50} of the $Mo_{17}V_3$ in SR- Ca^{2+}-ATPase as

1.84 µM which was very close to the estimated IC_{50} 2 µM concentration of the POMo. So, it could be stated that 1.84 µM was the concentration of the compounds resulted 50% inhibition of ATPase activity as IC_{50}.

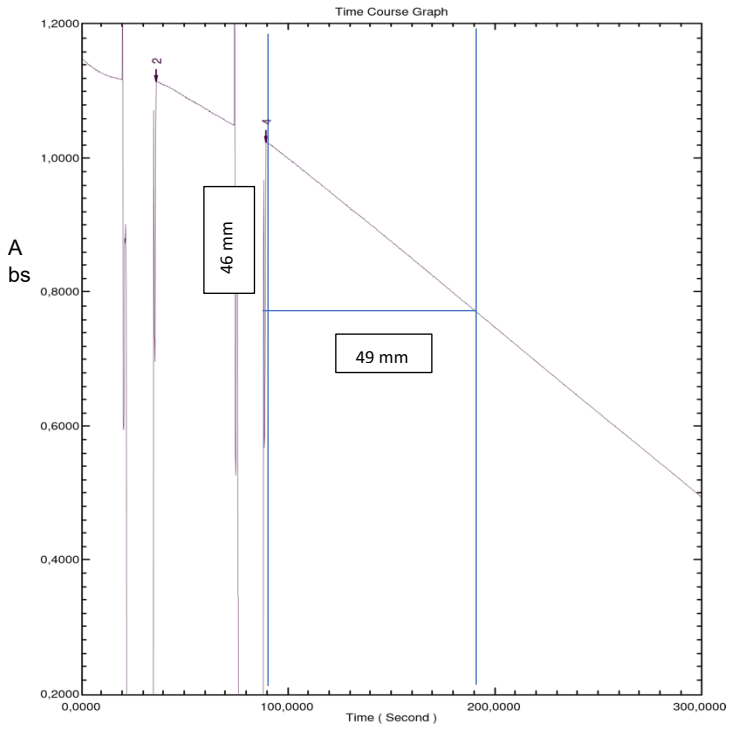

Figure 24- *Control Reaction without any addition of the compound ($Mo_{17}V_3$)- The blue lines are self-drawn to estimate the slope of the ATPase- activity.*

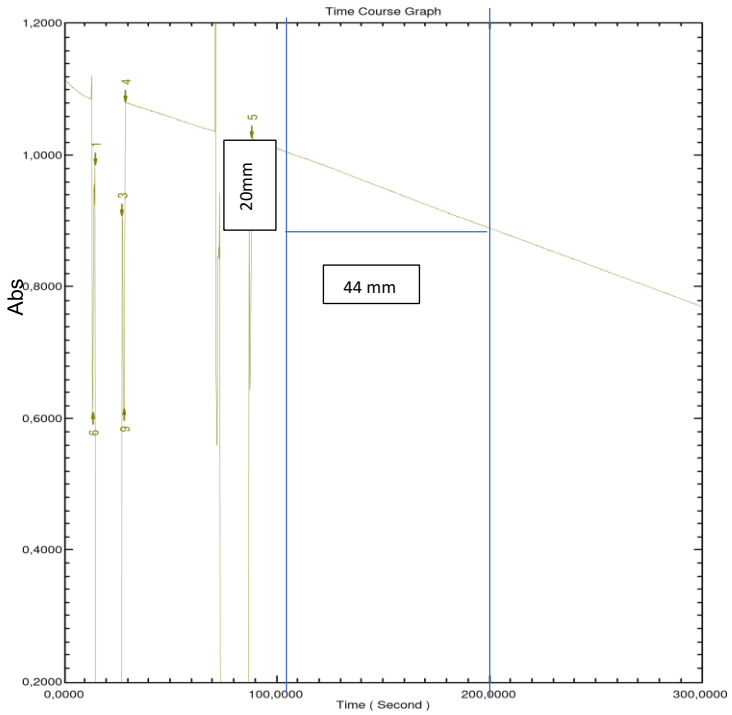

Figure 25*- Reaction in the presence of 2 µM of the compound ($Mo_{17}V_3$)- The blue lines are self-drawn to estimate the slope of the ATPase- activity.*

According to the results the POMo concentration of 2 µM was observed close to 50% reduction of the activity of the ATPase enzyme. Moreover, based on the calculative method using the Michalis Menten equation **Figure 26**, the value was found 1.84 µM. As the calculated IC_{50} value was very close the 2 µM concentration of the POMo consequently, this the compounds concentration of 2 µM was used to determine the type of inhibition exhibited by the inhibitor ($Mo_{17}V_3$).

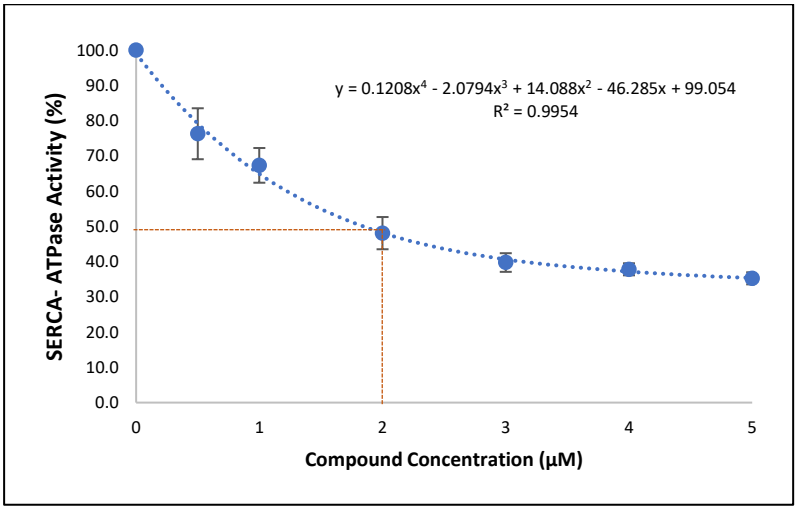

Figure 26- *SERCA- ATPase inhibition activity by the POMo ($Mo_{17}V_3$). The brown lines are self-drawn to indicate the 50% of the ATPase activity inhibition.*

POMs studies to estimate the IC_{50} have been increased in past two decades specially, vanadium compounds as polyoxovandates (POVs), have been the subject of extensive research over an extended period. However, there is currently a growing interest in exploring the medicinal applications and implications of these compounds.[71,77] In Table 8, the POMs and the subgroups including the metal compounds and oxides have been mentioned which have been studied in last two decades. It is evident that there is no information available for the ATPase activity of the molybdenum-based POMs therefore, the compound $Mo_{17}V_3$ is a very unique compound in combination of vanadium atoms as in past vanadium-based POMs have been studied as an efficient ATPase inhibitor.

In a study by Fonseca et al. 2020 [55], ATPase inhibition was reported for decavanadate V_{10}, which had an IC_{50} value of 15 µM, and monomeric vanadate V_1, with a value of 80 µM. In addition to it, the IC_{50} value of MnV_{11} was noticed at 31 µM while with the increased numbers of vanadium atoms in the POV as MnV_{13}, the value was higher at 58 µM. In general, it can be noticed that

IC_{50} value was lower with V_{10} (15 μM) but was higher when the number of vanadium atoms were less than ten vanadium (V_1= 80 μM) and greater than ten vanadium atoms (MnV_{11} = 31 μM and MnV_{13} = 58 μM). It can be the probable reason of the importance of decavanadates as potential metallic drug in biomedical applications as the minimum values of IC_{50} was for decavanadate V_{10} with lowest IC_{50} value of 15 μM. However, the POMo, $Mo_{17}V_3$ has been very 8 times more efficient (IC_{50}=1.84 μM) in comparison to the even though the vanadium atoms in combination are less but the combination with molybdenum made the IC_{50} potential higher than the mentioned POVs.[55] In another research by Fraqueza et al. 2019 [96], the compound PV_{14} was studied for in-vitro Ca^{2+} - ATPase in terms of IC_{50} and the value of IC_{50} was reported as 5 μM which was found higher than the $Mo_{17}V_3$, reflecting that the POMo under the study is almost 3 times efficient as compared to PV_{14}.

On the other side many polyoxotungstates (POTs) were also reported by Aureliano et al. 2022[57] for SERCA inhibition with higher efficiency than $Mo_{17}V_3$. The POTs such as P_5W_{30}, P_2W_{15}, P_2W_{17}, P_2W_{18}, $P_2W_{15}V_3$, P_2W_{12} with the IC_{50} values of 0.37 μM, 0.55 μM, 0.72 μM, 0.60 μM, 0.95 μM, 11.0 μM respectively.[57] All POTs, except P_2W_{12} (11.0 μM), have shown the lower value of IC_{50} as compared to $Mo_{17}V_3$ (1.84 μM) indicating that these POTs had better ATPase inhibiting efficiency for SERCA (except P_2W_{12}) on an average, 2-5 times higher affinity for the ATPase enzyme. Here it is also noticeable that the highest efficiency can be observed in the compounds having highest atoms of tungsten (P_5W_{30} = 0.37 μM). However, in comparison of P_2W_{12}, the POMo- $Mo_{17}V_3$, had 6 times stronger ATPase inhibitory capacity. From the Table 8, it can also be noticed that the lowest inhibitory values in the cited literature are form the group of POTs. It also stressed the need to evaluate the IC_{50} from the molybdenum-based compounds so the comprehensive view of using the efficient POMs would be suggested for the metallic drug developments.

In further studies on POTs lower IC_{50} values were noted for Se_2W_{29} as 0.3 μM. Se_2W_{29} has shown as IC_{50} value very similar to P_5W_{30} (0.3 μM) with the difference of only one tungsten atom less in comparison therefore highly efficient in ATPase inhibition as compared to $Mo_{17}V_3$ (IC_{50} =1.84 μM).[70] Whereas, some other POTs including decaniobate compound such as TeW_6, Nb_{10}, AsW_{19}, AsW_9, SiW_9, P_2W_{12}, and $CoW_{11}Ti$ were reported with IC_{50} values of 200 μM, 35 μM, 28 μM, 20 μM, 16 μM, 11 μM, and 4 μM, respectively.[55,57,70,78] Furthermore, isopolyanion-W_{22} was found with the IC_{50} value of 68 μM.[57,70,78] In the mentioned literature studies, the IC_{50} values were noticed higher depicting them as inefficient inhibitors.[55] Moreover, the highest IC_{50} values for TeW_6 as 200 μM was 109 times less efficient than $Mo_{17}V_3$in ATPase activity in SERCA.[70]

The only compound such as decaniobdate (35 µM) in this study was 19 times less efficient in IC_{50} than $Mo_{17}V_3$.

According to literature, as shown in **Table 8**, there are some studies to evaluate the IC_{50} against the ATPase activity in PMCA to evaluate the effect of the same compounds in different ATPase enzymes in different vesicles. The same POTs (P_5W_{30}, P_2W_{15}, P_2W_{17}, P_2W_{18}, $P_2W_{15}V_3$, and P2W12) were also studied in PMCA, and their inhibition was even more potent than that of SERCA activity. It indicated the possibly of interactions and conformational changes, that the same metal compounds can exhibit differently with P-type ATPases with the varying affinities and inhibition capacities.[57] For example in this study done by Aureliano et al. 2022[57], the lowest IC_{50} in SERCA was for P_5W_{30} (0.37 µM) and P_2W_{18} (0.55 µM) P_5W_{30} however, in PMCA lowest inhibitory activity was noticed for P_2W_{17} (0.10 µM) in PMCA which was higher in IC_{50} value (0.72 µM) than P_2W_{18}, P_2W_{15} and P_2W_{18}.[57] In accordance with these variability in different type of ATPases, it can also be predicted that as $Mo_{17}V_3$ would also either show higher or even lower IC_{50} in PMCA. However, the further studies would require evaluating the behaviour of POMos in PMCA ATPases.

Table 8-IC_{50} and type of inhibition of the compounds in SERCA and PMCA from literature:

Component	Compounds	IC_{50} µM (SERCA)	Type inhibition (SERCA)	IC_{50} µM (PMCA)	Type Inhibition (PMCA)	Ref.
Tungsten	Se_2W_{29}	0.3	---	---	---	[70]
	P_5W_{30}	0.37	Mixed Type	0.18	Mixed Type	[57]
	P_2W_{15}	0.55	Mixed Type	---	---	[57]
	P_2W_{18}	0.6	Mixed Type	0.3	Mixed Type	[57,70]
	P_2W_{17}	0.72	Mixed Type	0.1	Non-Competitive	[57]
	$P_2W_{15}V_3$	1	Non-Competitive	0.23	Non-Competitive	[57]
	$CoW_{11}Ti$	4	---	---	---	[70]
	P_2W_{12}	11	---	0.25	Non-Competitive	[57,70]
	SiW_9	16	---	---	---	[70]
	AsW_9	20	---	---	---	[70]
	As_2W_{19}	28	---	---	---	[70]
	W_{22}	68	---	---	---	[70]
	TeW_6	200	Mixed Type	---	---	[70]
	W_1	400	---	---	---	[98]
	HWO_4^{2-}	400	---	---	---	[97]
Niobium	Nb_{10}	35	Non-Competitive	---	---	[97]
	PV_{14}	5	Mixed Type	---	---	[96]

Vanadium	V_{10}	15	Non-Competitive	---	---	[78,97]
	PDC- V(V)	25	---	---	---	[134]
	MnV_{13}	31	Mixed Type	---	---	[78]
	MnV_{11}	58	Mixed Type	---	---	[78]
	V_1	80	---	---	---	[96,134]
	BMOV	40	---	---	---	[134]
	HAIDA- V(IV)	325	---	---	---	
Molybdenum	MoO_4^{2-}	4.5mM	---	---	---	[97]
Gold	C_3H_9PAuCl	0.8	Non-Competitive	2.8	Mixed Type	[54,55]
	$C_{18}H_{15}PAuCl$	0.9	Mixed Type	0.9	Non-Competitive	
	$C_6H_4NAuCl_2O_2$	4.5	Non-Competitive	4.9	Non-Competitive	
	$C_{27}H_{36}AuClN_2$	16.3	Mixed Type	21	Mixed Type	

Other than SERCA and PMCA, ATPase studies with the POMs, the POTs like As_2W_{19}, SiW_9, P_2W_{12}, and W_{22} have shown no activity on Na^+/K^+ ATPase enzyme after 30 min with a concentration of 10 µM. As mentioned previously, Se2W29 was reported with the highest inhibition with in $Ca2^+$-ATPase enzyme activity however, it remained the weakest in the inhibition for Na^+/K^+ ATPase with only 14% inhibition.[54,55,70] Another POT, TeW_6 with IC_{50} value 200 µM has shown a low Na^+/K^+ ATPase inhibition of 10% which can be possible because of the large size of the POT which prevents the compound interference with the Na^+/K^+ ATPase in ex-vivo study of the epithelial cells. [70] Moreover, the ortho-tungstate compound (HWO_4^{2-}) exhibited an IC_{50} value of 1.5mM for NA^+/K^+- ATPase, which is highly low in comparison of the IC_{50} of 400 µM in SERCA.[96] On the other side, Gumerova et al. 2018[70] also evaluated the compound PV_{14} ex- vivo fish muscle the effective time (ET_{50}) to reach a maximum 50% of the effect of the POM. In contrast, Some POMs have reported high inhibition for the Na^+/K^+ ATPase pumps such as PV_{14} had given 50% inhibition for the concentrations below 1 µM. [70] Furthermore, ex-vivo experiments reported IC_{50} values of 1.4 µM for the inhibition of Na^+/K^+ ATPase which is lower concentration as compared to 5 µM in SERCA. The POT, P_5W_{18} has shown remarkable inhibition for both Na^+/K^+ ATPase and Ca^{2+} - ATPase pumps. For SERCA the IC_{50} value noted was 0.6 µM and for Na^+/K^+ ATPase the inhibition was 99%.[70] These studies showed that the POMs could show different activities in different ATPase pumps and not all POMs have similarities in their interaction with the membranes which can be dependent in their structural and chemical properties and interaction with the membrane proteins.[70]

A presumptive correlation was noticed between IC_{50} of POTs, charge density, and size. [81,116] POTs effect was evaluated on epithelial chloride secretion, triggered by the Na^+/K^+-ATPase basolateral activity with the utilization of a killifish model for epithelial skin basal membrane.[75] To understand the POTs correlation for size, charge density with IC_{50} for SERCA inhibition, some studies were analysed. [70] With for the POTs there was no correlation noticed however, with the high-affinity POTs having an IC_{50} value lower than 16 μM, the correlation between the IC_{50} value and the charge density was noted as per division of the numbers of Tungsten atoms and the volume of anions in POTs. [70] In the case of P_2W_{18} and Se_2W_{29} which were with lower charge densities, SERCA inhibition was more efficient reflecting that there is possible shape complementation between the inhibitor and the inhibition site of the enzyme. [70] On the other hand, in the ex-vivo study for Na^+/K^+ ATPase, no evidence of the charge density and ET_{50} value was found how a probability of length between the distant POT anions was noticed.[70]

Other than POMs, the inorganic gold compounds were also studied to assess the effect on SR-CA^{2+} ATPase activity, Compounds C_3H_9PAuCl and $C_{18}H_{15}PAuCl$ showed the values of IC_{50} as 0.8 μM and 0.9 μM, respectively, which were almost 2 times more efficient than $Mo_{17}V_3$ in SERCA. In the same study, two more gold compounds $C_6H_4NAuCl_2O_2$ and $C_{27}H_{36}AuClN_2$ were reported with IC_{50} values higher than $Mo_{17}V_3$ in the range of 4.5 μM and 16.3 μM, respectively.[55] On the contrary, the same gold compound C_3H_9PAuCl which was observed lowest with IC_{50} value (0.8 μM) in SERCA showed 3 times less efficient IC_{50} of 2.8 μM in PMCA whereas, it was noticeable that $C_{18}H_{15}PAuCl$ had given the same inhibition value in SERCA and PMCA as (0.9 μM).Moreover, the gold compound, $C_6H_4NAuCl_2O_2$ was reported with IC_{50} Values of 4.9 in PMCA which is almost 3 times less effective than $Mo_{17}V_3$ in SERCA and $C_{27}H_{36}AuClN_2$ with $IC_{50\ of}$ 21.0 μM, which remained 11 times less efficient than $Mo_{17}V_3$ in case of SERC. Nevertheless, it is imperative to consider the cytotoxic effect of the gold compounds $C_6H_4NAuCl_2O_2$ and C_3H_9PAuCl, as they exhibited significantly low IC_{50} values. However, it is noteworthy that these compounds showed pronounced toxicity after 24 hrs of incubation with the cell line. [54] These studies showed that some gold compounds are more efficient inhibitor than POMo in SERCA while the behaviours was changed in PMCA with less efficiency as compared to POMo ($Mo_{17}V_3$). The gold compounds trend of variable activity in P-type, ATPases of SERCA and PMCA remained in agreement with previously stated POMs studied from the literature as mentioned in Table 8, but the cytotoxic studies are required for further evaluate the POMs with lower IC_{50} concentrations.

Finally, there is a comparison of some inhibitory drugs providing an inhibition higher or lower than the IC_{50} value of the $Mo_{17}V_3$ compound. The drugs with lower IC_{50} than the studies compound was thapsigargin from the range of 0.001-0.029 μM, and cyclopiazonic acid in the range of 0.1-0.2 μM however, the drugs which showed higher IC_{50} than the $Mo_{17}V_3$ were reported with IC_{50} range of 66-72 μM for macrocyclic lactones, chlorpromazine with 62.5 μM, curcuminoids with 7-17 μM, omeprazole with 30.50 μM and celecoxib with IC_{50} value of 35 μM. The aforementioned medicines exhibit weaker inhibitory capacities compared to the $Mo_{17}V_3$ molecule, despite their utilization in biomedical contexts for the treatment of various disorders.[54–57] Molybdenum-based nanocluster POMs have been recognized as significant entities in the field of medication delivery.[85]

This study presents novel findings indicating that $Mo_{17}V_3$ exhibits the capability to selectively interact with the Ca^{2+} ATPase pump located in the sarcoplasmic reticulum calcium ATPase (SERCA). In the reflection of mentioned studies from the literature it can be evidently noticed that the IC_{50} value of 1.84 μM is very effective in comparison of several investigations regarding many POMs, inorganic compounds, and organic drugs. It was also noticed that the same compound can provide different IC_{50} values for P-type ATPase pumps in the SERCA and PMCA along with the Na^+/K^+ pumps in ex-vivo studies. However, further investigation is required to assess the potential of utilizing SERCA as a metallodrug or in conjunction with other pharmaceutical agents, given its impact on neurological dysfunctions. Given the high sensitivity of neurons to medicines, it is imperative to evaluate the toxic effects on both neurons and astrocytes, which are healthy cells in the context of neurological therapy.[54]

3.6.2 Incubation of the POMo

The compound stability is an important factor for antibacterial activity potentials in the area of biomedical or commercial applications. The stability of the POMs is evaluated by nuclear magnetic resonance (NMR) spectroscopy which is a prolong phenomenon and it is time consuming. Therefore, in this the POMo $Mo_{17}V_3$ was incubated for consecutive 2 hrs at room temperature 22° C, in the experimental medium of physiological pH to estimate any change in its inhibition capacity meanwhile. During this time duration of the incubation, it was observed that the compound inhibition trend approached the trend line of the control experiment. This indicated that the compound was not stable in the medium (HEPES) during incubation at ambient temperature and it gave as same results are control without the compound.

According to the literature, there have been reports indicating that the POMs exhibit instability in the context of incubation investigations. POMs exhibit the potential to undergo decomposition when exposed to a suitable media and in the presence of bacterial metabolic activity. In certain instances, the POMs have exhibited alterations in the medium, which serves as an indication of decomposition. This observation suggests that POMs are not the sole contributors to the potential impact on biological interferences. To effectively utilize POMs in biological applications, it is crucial to comprehend their speciation and stability in the presence of biomolecules.[65] Moreover, one of the factors contributing to the instability of POMs is the occurrence of photo-corrosion on the surface of the substrate. Additionally, the loss of POM's structural integrity and detachment from the surface are also significant factors.[67]

There can be the evident possibility that the POMs go under speciation as it was reported that molybdenum oxide has the characteristics to degrade into MoO_4^{2-} in the serum during incubation whereas, in the pure aqueous solution at 4.0 pH, V_{10} was stable for weeks.[82,112] At acidic pH (2-6), it is highly stable oxido-vanadate and V_{10} had protonation states within the 2-6 pH range. The half-life of decavanadate was reduced to 12 hrs at 25°C and at 13 hrs at 37°C in buffered media as metal compounds could undergo speciation depending on the buffer in use itself hence, stability remained important.[80,112] In previous studies, the reduction of V_{10} to oxovanadium on the actin muscle protein was after 90 min of incubation with the observation that reduction of decavanadate at the actin ATP binding site is required for the vanadate reduction. However, in the presence of biomolecules such as G-actin, the half-life increases 5.5 folds.[96]

On the contrary, there are also evidences for the stable compounds during incubation that after 30 min of incubation of the POTs, the inhibition remains the same in the presence and absence of the compound and it remained stable with the same results.[57] Similarly, the gold compound was also stable for 30 min in the medium with or without protein the reaction was the same.[54] Moreover, Falerio et al. 2022 [37] evaluated the stability of the POTs, P_2W_{17} and P_2W_{15} in the MHB medium using ^{31}P and ^{183}W NMR spectroscopy. After the incubation the predominantly observed POT was P_2W_{17}, with a prevalence of 100% as compared to 97% for P_2W_{15}. It was also important to mention that the solutions of P_2W_{18} and P_5W_{30} exhibited a blue color upon dissolution in MHB, which suggests a reduction in W ions.[37] In addition to it, several POVs are usually colorful; therefore, the colour might change during speciation. It can also vary as per incubation time with the bacterial organisms, and MIC assay can be unsuitable to detect the speciation of the compound.[59] It is reported that addition of *M. smegmatis* or *M. tuberculosis* in

the solution of V_{10} with a pH in the range of 5-7 triggered the decomposition of the V_{10} and caused instability of the POV in the presence of bacteria.[80,112]

Given the observed instability of the POMo ($Mo_{17}V_3$) following a 60 min incubation in the medium, it would be prudent to investigate the process of compound speciation and the various binding modalities of the compound and enzyme complex in relation to conformational changes in ATPase. It is important to acknowledge that the compound's stability directly impacts its effectiveness therefore, the assessment of a compound's stability and its potential decomposition into other species is crucial in the investigation of its biological applications such as in case of this study with the antibacterial and ATPase activities. Additionally, it is worth considering that the observed interactions may not solely be attributed to the compound itself, but rather to the decomposed species resulting from it. During the incubation period, factors such as temperature and reaction duration with the medium can influence the inhibitory capacity of the compound**.** As mentioned, 2.1 section of the screening assay for the antibacterial activity with $Mo_{17}V_3$ and the rest of the listed compounds in Table.1, it can be predicted that the compounds were not stable to give any antibacterial activity, or the compounds were decomposed in the media to other species with or without any interactions with the cell membrane proteins. However, further studies would be required to evaluate the mechanism of the POMs and the metal compound to find out the exact reason of giving no antibacterial activity.

3.6.3 Type of Inhibition of the POMo

As mentioned in 2.5.3, the type of information outlined in the materials and methods section was determined by generating a Lineweaver-Burk plot of Ca^{2+}-ATPase activity, using the experimental scheme presented in the Table 4. The concentration of POMo was consistently maintained at a level of 2 μM throughout all experimental procedures, whereas the concentration of ATPase was varied as 0.1 mM, 0.25 mM, 0.5 mM, 1.0 mM, 2.50 mM. The determination of Vmax and Km values involved the analysis of experimental graphs obtained from two sets of experiments: one conducted under without inhibitor ($Mo_{17}V_3$) and the other conducted in the presence of the inhibitor. These experiments were performed by varying the concentration of ATPase (substrate) and measuring the corresponding results. The measurement of the activity was conducted in nanomoles of ATP per minute, with reference to the ADP production with extinction coefficient of NADH as ε340 = 6220 M-1cm-1. The Lineweaver-Burk plot was employed to estimate the Vmax and Km (Michaelis constant) values through the regression equation, by utilizing the reciprocal of the determined substrate and inhibitor activity as mentioned in Table 8.

The Lineweaver-Burk plot was constructed based on the reciprocal of ATP and inhibitor activity measurements, and the regression equation was employed to determine the Vmax and Km values. In the absence of the inhibitor ($Mo_{17}V_3$), the Km was determined to be 0.662 mM, while the Vmax was measured to be 66.23 nM ATP/min. However, when the inhibitor was present, Km increased to 0.126 mM the Vmax decreased to 32.26 nM ATP/min. The **Figure 27** was drawn as Lineweaver-Burk plot with the blue line as control experiments in the absence of the inhibitor, whereas the orange line reflected the ATPase activity in the presence of the inhibitor.

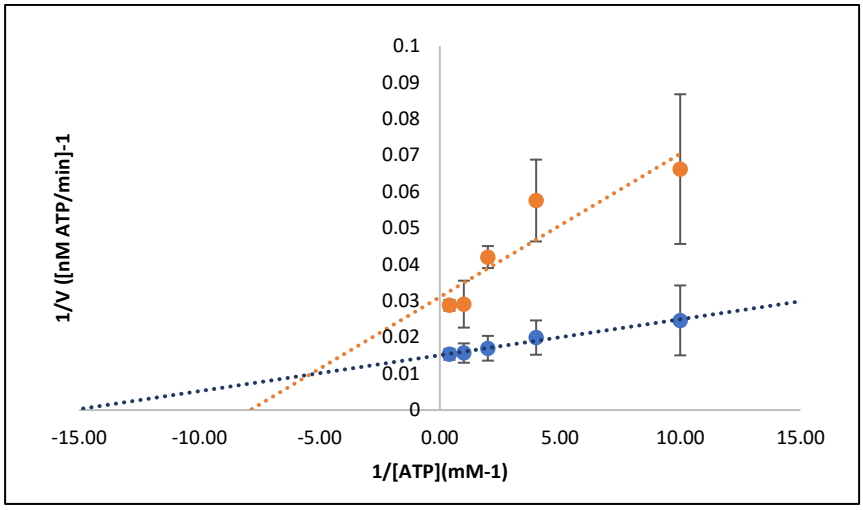

***Figure 27**- Lineweaver-Burk graph to estimate the type of inhibition. The blue line represents the control and orange line represents the experiment with POMo.*

Based on the results it was apparent that the there was a drop in the Vmax value and an increase in the Km value, indicating a mixed type of inhibition, suggesting that the inhibitor binds to the enzyme rather than the enzyme-substrate complex.[54,70] In comparison to the control group without the inhibitor, the Vmax has dropped by 49%. Additionally, the presence of $Mo_{17}V_3$ has led to a significant rise of 190% in the Km value. The binding of the inhibitor ($Mo_{17}V_3$) is shown to occur specifically with the enzyme, rather than with the enzyme-substrate complex, as evidenced by the lack of drop in the Km value.

The utilization of enzyme inhibition has proven to be a successful approach in manipulating enzymatic activity and interfering with pathways associated with diseases. Inhibitors engage in competitive interactions with the substrate for occupancy of the enzyme's active site. Inhibitors exhibit the ability to bind to a distinct location on the enzyme, hence inducing modifications in its structure or activity. Inhibitors have the ability to bind to the complex formed by the enzyme and substrate, hence impeding the synthesis of the desired product. The active site of the target enzyme is utilized in order to build inhibitors that are compatible with its three-dimensional

structure. The design of inhibitors with similar qualities is dependent on the understanding of the enzyme's known ligands or substrate.[135]

With respect to Table 8 with the literature, the POTs, P_5W_{30}, P_2W_{15}, and P_2W_{17} also exhibited a mixed kind of inhibition, as evidenced by a drop in the value of Vmax and an increase in Km when compared to the control. The POTs have shown a comparable form of mixed inhibition, similar to that observed in $Mo_{17}V_3$. The experimental results clearly indicate a decrease in the Vmax values when comparing them to the Vmax of the control samples lacking a compound protein conformational impact. Additionally, the Km value exhibited an increase, suggesting the occurrence of a typical mixed type of inhibition.[57] Similarly, Se_2W_{29} and TeW_6 had a mixed type of inhibition for Ca^{2+} ATPase activity as the $Mo_{17}V_3$ has, suggesting that there is the possibility of having the same mode of protein interaction however the IC_{50} values were significantly different with a lower value of Se_2W_{29} (IC_{50}= 0.3 μM) than our studied POMo and TeW_6 with very high value (IC_{50}= 200 μM).[70] Among the POTs, P_2W_{18}, P_2W_{12}, and TeW_6 also exhibited a mixed type of inhibitory effects, as reported in previous work.[55,57,70] Furthermore, the POVs, MnV_{11} , MnV_{13} and PV_{14} were also reported for mixed inhibitory effects.[96] From these studies it can be observed that type of inhibition is independent of IC_{50} values of the compounds these IC_{50} are higher are lower. The mentioned POMs bound to the ATPase enzyme regardless of substrate binding to the enzyme.

On the other hand, the compounds $P_2W_{15}V_3$ demonstrated non-competitive inhibition of SERCA enzyme activity, resulting in a reduction in the Vmax. However, it had no impact on the Km value. This observation may be attributed to the V_3 component of the molecule interacting to the enzyme in a distinct manner.[57] Consistent with findings from a separate investigation, it has been demonstrated that V_{10}, exhibited a non-competitive inhibitory pattern with Ca^{2+} ATPase activity which is comparable to Nb_{10}. [56,70,78,96] POMo ($Mo_{17}V_3$) is classified as a Wells-Dawson-type compound, featuring a V_3 moiety within its molecular structure. However, it exhibits a mixed type of inhibition behaviour, in contrast to the V_3 non-competitive inhibition behaviour shown in the Wells-Dawson anion - $P_2W_{15}V_3$. It also reflected the V_3 moieties with different metal compounds can also have the variability in type of inhibition.

There are also evidences of organic compounds type inhibition in SERCA, such as the gold compounds, $C_6H_4NAuCl_2O_2$ and C_3H_9PAuCl exhibited a non-competitive inhibition pattern, as evidenced by their Km values being comparable to those of the control group, but the Vmax values dropped.[55] Gold Compounds $C_{27}H_{36}AuClN_2$ and $C_{18}H_{15}PAuCl$, exhibited mixed-type

inhibition, as evidenced by a decrease in Vmax and an increase in Km. This suggests that these compounds interacted with the SR Ca^{2+}-ATPase, regardless of whether the substrate was bound to the enzyme or not. Additionally, this provides insight into the existence of distinct protein binding sites for substrate and inhibitor binding, with the allosteric site serving as the binding site for the inhibitor.[55] Whereas in PMCA, gold compounds, specifically $C_6H_4NAuCl_2O_2$ and $C_{18}H_{15}PAuCl$, were found to decrease the Vmax. However, these compounds did not have any impact on the Km value, indicating that they exhibit non-competitive inhibition towards the ATPase enzyme.[54] The compound C_3H_9PAuCl and $C_{18}H_{15}PAuCl$ showed change in the type of inhibition in SERCA and PMCA however, $C_6H_4NAuCl_2O_2$ and $C_{27}H_{36}AuClN_2$ were reported with the same type of inhibition in both P-type ATPases. From these investigations, it can be stated that the same inorganic gold compounds can have the same of different behaviour in type of inhibition in cell membranes. However, the potential cause for similarities or differences in the amino acid charge density, amino acid residues on the binding sites, and the potential presence of distinct binding sites on the ATPase enzyme of PMCA and SERCA may be attributed to the varying inhibition effects resulting from the binding of gold compounds to these enzymes. Nevertheless, the precise nature of the conformational changes occurring in the membrane structure remained uncertain.[54] In a similar way, it is imperative to study the conformational changes and protein interactions of molybdenum- based POMs as well to understand their applicability in the development of the new drugs. However, the studies from the past are used to have an estimate of POMs interaction with the biomolecules.

3.7 Interaction of the Compounds with Proteins

The interaction between proteins and POMs is of significant importance due to the binding affinity between proteins and metal compounds present in the cellular environment and blood flow because his interaction enhances the delivery and activity of metal-based drugs.[63,77] Protein molecules have the potential to undergo unfolding when interacting with POM. The crucial determinant for the contact between protein and POMs is the negative charge of the POMs.[74,77] This interaction occurs by non-covalent means, specifically targeting the positively charged regions of the peptides. Consequently, this interaction facilitates the unfolding process of the protein molecules.[74,77] In a study by Sciortino and the group, it was noticed that Nb_{10} prevented V_{10} from binding to Ca^{2+} ATPase, reflecting both compounds act on the same target protein system however, Nb_{10} was stable at the β-site of the protein domain and V_{10} at the catalytic nucleotide α-site therefore, their potential was biologically synergetic on the G-actin.[77] Furthermore, in a prior investigation, ^{31}P NMR spectroscopy was employed to evaluate the

interaction between tungstophosphoric acid (WPA) and NA^+/K^+-ATPase at the molecular level in the solid state. Strong non-covalent interactions were observed between WPA and protein, primarily by hydrogen bonding of protein by O_1 and O_2 of the POM. Notably, O_2 accounted for 70% of the protein interaction.[74] PV_{14} exhibited much greater inhibition of NA^+/K^+-ATPase compared to V_{10} (three times stronger) and V_1. However, it is not possible to definitively attribute this impact only to PV_{14}, as it is plausible that the observed inhibition could be attributed to the reduction of vanadate in other species such as vanadyl.[96]

In previous studies, in addition to Ca^{2+} ATPase, the connection between POM and actin and myosin has also been observed. However, the precise mechanism behind this contact remains unclear.[96] It is hypothesized that the mechanism may include either electrostatic interference of hydrogen bonds or direct interaction with cysteine of actin and ATPase enzymes. However, the precise mechanisms by which various types of POMs form bonds with proteins in order to recognize specific target sites and their relative affinities with the structural conformation of ATPases have not been fully elucidated.[96] This information is crucial for the development of drugs that can effectively target and inhibit specific enzymes for therapeutic purposes.[96] Nevertheless, this study provides evidence that the POMo ($Mo_{17}V_3$) has a noteworthy potential as a candidate inhibitor and could potentially be suggested as a metallic medication. However, the instability of the instability noticed during the incubation of the POMo required further investigation is necessary to explore its interaction with the protein domains of ATPases either alone or in synergism with other compounds.

3.7.1 Structural Modifications in POMo

It has been evidenced that the effectiveness of hybrid molecules containing transition metals in five centrally coordinated geometries was lower when compared to hybrid molecules with six transition metal-coordinated geometries.[68] The activity of the POM ligands, when bound to two ligands as a single entity, was found to be higher in comparison to the monodentate combination. Hence, it has been proposed that specific structural modifications may facilitate the delocalization of electrons, thereby enhancing the hybrid interaction.[68]

3.7.2 Synergism of POMos

In a similar concept, the POMo, $MnMo_6$ in combination with organic Eudesmic acid (EU), was evaluated as a tubulin inhibitor on HUVEC normal cells, demonstrating reduced cellular toxicity. The administration of POMo, both independently and in conjunction with EU_2POMo, demonstrated inhibitory effects on breast cancer cell lines.[68,88] The experimental results indicate

that EU_2POMo exhibited a higher level of safety compared to HUVEC, as well as demonstrating superior cellular uptake and apoptosis in comparison to POMo. EU facilitated the entry of POMo into cellular structures and triggers the process of apoptosis.[68,88] Similarly, chitosan, a type of polymeric network with cationic properties, has been found to improve the stability and loading capacity of anionic drug delivery systems. The utilization of chitosan-$MnMo_6$ resulted in a notable enhancement in cell accumulation, reaching a value of 98.9%.[79] In contrast, the utilization of free $MnMo_6$ yielded a cell accumulation rate of 58%. The cell line, MDAMB-231 treatment involving the administration of $MnMo_6$ at its IC_{50} level resulted in the inhibition of cell migration, a critical characteristic observed in malignant tumors.[79] The utilization of chitosan-encapsulated POM, nanocomposites has been found to enhance both as cell penetration and antibacterial activity.[61,68] According to these investigations, it can be suggested that the POMo ($Mo_{17}V_3$) in the combination with other nanocomposites can improve in structure with better stability and even improved IC_{50} to be applied in culture lines further to be proposed in biomedical applications.

3.7.3 Biomedical Trials with Molybdenum POMs

Molybdenum base POM effectivity was examined for the treatment of diabetes affecting α-glucosidase as Mo_9V_3 showed the IC_{50} value for glucosidase enzyme as 9.6 mM which was found better than the antidiabetic inhibitor acarbose with an IC_{50} value of 38.2 mM and also showed the mixed type of inhibition. Moreover, high-potency POMs affecting the α- glucosidase were noticed as P_2Mo_{18} and PMo_{12} with IC_{50} values of 0.17 mM and 6.1 mM.[112] A synergistic effect of [Mo_{154}] @VLPs was reported as bioinorganic hybrid molybdenum POM with virus-like particles (VLPs) with the protein of human papillomavirus capsid. It showed that the hybrid was less toxic on HEK293 (human embryonic kidney cell line) with a dose of 50 μM and 10 μM and cell viability of 90% and 82%, respectively.[61]

Similarly, in the study from elsewhere, the subunit vaccine was prepared using co-assembly of nanoparticle poly- 4-vinyl pyridine (P4VP) with ultra-small, molybdenum POM ($Mo_{72}Fe_{30}$), the extracted whole soluble protein from *M. bovis* was used to prepare a virus like supra particle under acidic conditions to check the response on the immune response.[84] In the 6th week, the co-assembled subunit vaccine raised the Ig-G antibodies to titer 67.9% as compared to the first week in mice, and the T-cell immune response was higher than the BCG vaccine. However, the immune response of $Mo_{72}Fe_{30}$ and extracted bacterial protein independently were lower, suggesting the co-assembly can increase immunity. It has not affected the liver, kidneys, and pancreas with any negative effects.[84] It can be suggested that although the POMo ($Mo_{17}V_3$) has

an efficient IC_{50} value than this POM available in combination with other NPs there is the possibility of its application to evaluate the immunomodulatory responses which require further computational analysis to design the stable metal compounds and clinical experiments.[84,85]

3.7.3.1 Prospectives of Computational Analysis

Computational studies using molecular docking and molecular dynamics to develop novel drugs show the intricacy of POMs.[73] Molecular modeling can rationalize biological processes and reveal the structure of protein-POM interactions to design stable metallodrugs.[77] Quantitative multidimensional regression models can predict the protein affinity using charge density, size, and shape.[63] Atomistic simulations showed the variability of POM hydrogen bonding and water interactions with moderately charged chaotropic and highly charged kosmotropic POMs, which resulted in higher dissolving energies and less affinity with protein. The lower the charge density of the anion, the weaker the hydration and the better the propensity to assemble with biomolecules or organic moieties.[63] Moreover, hydrolysis of phosphoester bonds by artificial phosphoesterases molybdate anions was studied computationally.[63,71] The literature has reported the existence of covalent interactions between POMs and biomolecules. However, due to experimental constraints, it is still challenging to determine the specific binding modalities, types of interactions, and the influence of media composition on these interactions.[63,80] The efficacy of the computational approach for the in-situ formation of the molybdenum binuclear $[[Mo_2O_8H_4]^0$ species from $[Mo_7O_{24}]^6$ was also evaluated in the case of the catalyst $[W_7O_{24}]^6$. The hydrolysis of tungstate exhibits higher activation barriers compared to the hydrolysis of molybdenum, leading to the formation of fewer thermodynamically stable molecules.[63] In accordance with this evidence, it can be suggested that by applying the computational approaches modifications of the POMo ($Mo_{17}V_3$) stable compound can be achieved to design the metallic drugs to combat the emerging problem of antibiotic resistance.

3.8 POM´s Antibacterial Activity and ATPase Relation

This study aimed to identify potential solutions for the escalating global problem of antibiotic resistance. The potential of metal compounds to address this issue is attributed to their unique physio-chemical and biological properties. Consequently, studies were conducted to assess the antibacterial activity of five POMs, one metal complex, and the halotolerance of *S. aureus* species in the presence of P_5W_{30}. Furthermore, an assessment was conducted on the ATPase activity of POMo ($Mo_{17}V_3$). The antibacterial activity of the screened POMs and compound against *E. coli* and *S. aureus* was found to be negligible. However, it is noteworthy that the

compound $Mo_{17}V_3$, which also lacked antibacterial activity, exhibited a significant IC_{50} value in inhibiting ATPase activity in SERCA membranes.

There is similar evidence in which the POVs (V_{10}, MnV_{11}, and MnV_{13}) have shown the reserve relation with the growth of *E. coli* and Ca^{2+} ATPase inhibition which reflected that the inhibition of ATPase enzyme activity cannot be related to inhibition of the bacterial growth.[78] The bacterial inhibition for the growth was observed more with V_{10} rather than V_1 and this similarity was also noticed in derivatives of V_{10} e.g., V_9Mo and V_9Pt.[112,136] The antibacterial activity of the POMs can also be related to the total net charge and the MIC values show that Dawson-type- POMs have shown the highest inhibitory activities against the *M. catarrhalis* however, presslyer-type has shown the bacteriostatic effect with the same bacteria. Presslyer-type anion has shown a MIC value of 1ug/mL against *M.catarrhalis* but on the other side, it has shown no effect on *E. coli* with a MIC value of more than 256 ug/mL.[77] These investigations reveal that while the POMs may not exhibit any impact on bacterial growth, they may exhibit distinct behaviour in terms of SERCA for ATPase inhibition which is in agreement with our study.

4 Conclusion

The study emphasizes the critical importance of addressing antibiotic resistance, a prominent global health concern, through innovative approaches. The research focused on the evaluation of metal-based compounds, for their antibacterial activity against *E. coli* and *S. aureus*. While some POMs and metal complexes demonstrated antibacterial potential against specific bacterial strains, the ones studied for the first time to assess the antibacterial activity in this context did not exhibit such activity against *E. coli* and *S. aureus*. This underscores the complexity of developing effective antibacterial agents, highlighting that the efficacy of metal compounds varies based on their composition, structure, and the targeted bacterial strains.[65,66,69,111] Understanding the intricate interactions between POMs and bacterial cell membranes remains a priority, necessitating further investigation. The study provides quantitative insights into the relationship between varying salt concentrations and the growth kinetics of *S. aureus* strains, particularly *S. aureus* ATCC 6538 and the resistant strain, MRSA 16. It highlights that susceptibility to salt concentrations increases with higher salt levels, revealing the significance of salt stress in bacterial research and practical applications. Additionally, the research underscores the importance of considering strain-specific variations in bacterial responses to salt stress, with potential implications for fields like food safety and healthcare treatments.[19,69,117] Moreover, the study offers a quantitative understanding of the osmo-tolerance of *S. aureus* strains in the presence of different salt concentrations. It sheds light on how salt influences bacterial growth, gene regulations, and antibiotic resistance.[30,31,119] The research suggests that salt stress can potentially impact bacterial susceptibility to antibiotics, emphasizing the need to consider strain-specific variations in responses. The study also highlights a discrepancy in the observed behaviour of synergistic effects of P_5W_{30} and salt, treatments in an in vivo model using larvae. Specifically, the combination of 1.5% salt with POM at its MIC resulted in significant virulence in the larvae, contrary to halotolerance treatment results. This discrepancy suggests potential variability in the outcomes when transitioning from the larval model to more complex human intestinal models or skin cell lines. Such variations could have implications for the efficacy of these treatments in combating bacterial infections and addressing the critical issue of antibiotic resistance caused by multidrug-resistant strains of *S. aureus.*

In this study, the first-time examination of POMo-$Mo_{17}V_3$, was done in SERCA for Ca^{2+}-ATPase activity. In comparison of several POMs an efficient IC_{50} value on SERCA vesicles was found as 1.84 µM which reflected an evident potential of $Mo_{17}V_3$ to be further investigates as proposed metallic drug to substitute the antibiotic as a contributing factor in case emerging antibiotic

resistance. Furthermore, the stability of $Mo_{17}V_3$ was estimated in the medium at room temperature 22° C for 2 hrs in order to estimate the degradability of the POM in the medium however, the compound was not found stable upon analysis after an hour. There might be a reason for speciation during the incubation however the colour of the compound was not changed as in the case of some POVs.[59] Considering the apparent absence of stability exhibited by our compound after being incubated in the medium for a duration of 60 min, it would be advisable to undertake an investigation into the phenomenon of compound speciation. Moreover, using the POMo in synergism with the antibiotic of other nanoparticles can provide stable results for application in the biomedical and industrial sectors.[62,67,68] Finally, the type of inhibition of the POMo as an inhibitor was evaluated and a mixed type of inhibition was found depicting inhibitor has a binding affinity for the enzyme rather than the enzyme-substrate complex.[54,70] The study contributes valuable quantitative data regarding the potential of POMs and the effects of varying salt concentrations on bacterial behaviour. These findings are essential for the development of novel antibacterial agents and the management of antibiotic resistance. The variability observed in the study underscores the importance of tailored approaches and further exploration of metal compounds as potential antibacterial agents and ATPase protein targeting sites.

4.1 Limitations of POMs

POMs possess clinical usefulness, yet their charge and structure may lead to toxicity when present at concentrations higher than IC_{50} in milli moles.[61,64,79,88] The presence of negative charges and dispersion of POM clusters might give rise to non-specific interactions between biomolecules and POM. Furthermore, the POMs have the potential to display both kinetic and thermodynamic instability. The degradation of the subject is influenced by various factors, including the concentrations of the solution, the presence of external organic and inorganic substances, and the physiological pH. Their excretion rate is limited, leading to the accumulation of toxins.[61,64,66,80]

4.2 Future perspectives

As the biological mechanism of POMs on biomolecules has not yet been elucidated and insufficient biological research has been conducted on the POM.[69,70] This study proposes the need for additional research to elucidate the mechanism of action of the most potent POMs. It also recommends exploring and assessing their efficacy against various bacterial species and clinical isolates, evaluating their cytotoxicity and potential adverse effects, investigating the development of resistance, optimizing the composition of POMs, and exploring their potential as therapeutic agents for the infections.[72,85] The utilization of molecular approaches is

recommended for confirming the diagnosis of microbial diseases and detecting strains that are resistant to the drugs, despite the existing constraints in terms of cost and feasibility at a smaller scale.[25] The lack of an adaptive immune system and the inability to examine chronic infections limit the model. Future research can compare it to clinically relevant infection models and use various materials.[17,133] The research underscores the need for additional studies to validate the findings obtained from the larval model in the context of more complex human systems. These investigations are essential to bridge the gap between model organisms and human applications, ultimately contributing to our understanding of effective strategies against antibiotic-resistant bacteria. The potential of these proposed variations in treatment concentrations should be further explored to refine and optimize antibacterial therapies. Moreover, the further study is required to estimate the virulence of salt and P_5W_{30} in larvae for MRSA 16which was not continued due to unavailability of larvae.

It would be worthwhile to explore the many ways in which the compound and enzyme complex bond, particularly in connection to the conformational changes observed in ATPase. In order to optimize the utilization of POMs in biological contexts, it is imperative to possess a comprehensive understanding of their speciation and stability when interacting with biomolecules.[65] In immunopharmacology and oncology, POM-based therapeutic medications alone or in combination with other chemotherapeutic drugs can play an important role.[76] Since the inhibition of POMs in the plasma membrane is inadequately understood, it is necessary to investigate the effect of POMs of the on the SERCA and PMCA ATPase pumps.[57,70] Co-assembly of antigen-NPs with morphological applications results in an enhanced immune response. [84] Understanding the mechanism of action of metal-substituted POMs, which are novel synthetic enzymes, requires meticulous characterization and justification. [63,80] As per the evidence from the previous studies, other than the exception of V_{10} and Nb_{10}, there is not much information available on and binding sites of the ATPase enzyme with the POMs.[57] However, there is not study available in literature to understand the mechanism of POMos and the confirmational changes with Ca^{2+} - ATPase of SERCA. Due to the fact that acute and sub-chronic toxicity cannot be estimated in vitro, they must be addressed prior to clinical research on POM. Since very little is known about the physiological effects of POM, additional toxicity data will be required for systematic hazard assessment as trials and studies progress.[75] To discover new-generation antibiotics, in-vivo toxicity studies with protracted POM dosing and monitoring are required [66]

5 References

(1) Zhang, Y.; Pi, Y.; Hua, Y.; Xie, J.; Wang, C.; Guo, K.; Zhao, Z.; Yong, Y. Bacteria Responsive Polyoxometalates Nanocluster Strategy to Regulate Biofilm Microenvironments for Enhanced Synergetic Antibiofilm Activity and Wound Healing. *Theranostics* **2020**, *10* (22), 10031–10045. https://doi.org/10.7150/thno.49008.

(2) Shree, P.; Singh, C. K.; Sodhi, K. K.; Surya, J. N.; Singh, D. K. Biofilms: Understanding the Structure and Contribution towards Bacterial Resistance in Antibiotics. *Medicine in Microecology*. Elsevier B.V. June 1, 2023. https://doi.org/10.1016/j.medmic.2023.100084.

(3) Olanbiwoninu, A. A.; Popoola, B. M. Biofilms and Their Impact on the Food Industry. *Saudi Journal of Biological Sciences*. Elsevier B.V. February 1, 2023. https://doi.org/10.1016/j.sjbs.2022.103523.

(4) Ganjian, H.; Nikokar, I.; Tieshayar, A.; Mostafaei, A.; Amirmozafari, N.; Kiani, S. Effects of Salt Stress on the Antimicrobial Drug Resistance and Protein Profile of Staphylococcus Aureus. *Jundishapur J Microbiol* **2012**, *5* (1), 328–331. https://doi.org/10.5812/kowsar.20083645.2375.

(5) Munita, J. M.; Arias, C. A. Mechanisms of Antibiotic Resistance. *Microbiol Spectr* **2016**, *4* (2). https://doi.org/10.1128/microbiolspec.VMBF-0016-2015.

(6) Dhanda, G.; Acharya, Y.; Haldar, J. Antibiotic Adjuvants: A Versatile Approach to Combat Antibiotic Resistance. *ACS Omega*. American Chemical Society March 28, **2023**, pp 10757–10783. https://doi.org/10.1021/acsomega.3c00312.

(7) Ribeiro, S. M.; Felício, M. R.; Vilas Boas, E.; Gonçalves, S.; Costa, F. F.; Samy, R. P.; Santos, N. C.; Franco, O. L. *New Frontiers for Anti-Biofilm Drug Development*; **2016**.

(8) Xu, Y.; You, G.; Yin, J.; Zhang, M.; Peng, D.; Xu, J.; Yang, S.; Hou, J. Salt Tolerance Evolution Facilitates Antibiotic Resistome in Soil

Microbiota: Evidences from Dissemination Evaluation, Hosts Identification and Co-Occurrence Exploration. *Environmental Pollution* **2023**, *317*. https://doi.org/10.1016/j.envpol.2022.120830.

(9) Chen, Z.; Yin, L.; Zhang, W.; Peng, A.; Sallach, J. B.; Luo, Y.; Li, H. NaCl Salinity Enhances Tetracycline Bioavailability to Escherichia Coli on Agar Surfaces. *Chemosphere* **2022**, *302*. https://doi.org/10.1016/j.chemosphere.2022.134921.

(10) Salam, M. A.; Al-Amin, M. Y.; Salam, M. T.; Pawar, J. S.; Akhter, N.; Rabaan, A. A.; Alqumber, M. A. A. Antimicrobial Resistance: A Growing Serious Threat for Global Public Health. *Healthcare (Switzerland)*. Multidisciplinary Digital Publishing Institute (MDPI) July 1, **2023.** https://doi.org/10.3390/healthcare11131946.

(11) Silva, V.; Caniça, M.; Capelo, J. L.; Igrejas, G.; Poeta, P. Diversity and Genetic Lineages of Environmental Staphylococci: A Surface Water Overview. *FEMS Microbiology Ecology*. Oxford University Press November 1**, 2020**. https://doi.org/10.1093/femsec/fiaa191.

(12) Vaezi, S. S.; Poorazizi, E.; Tahmourespour, A.; Aminsharei, F. *Biofilm Formation Of Staphylococcus Aureus In Presence Of Sodium Chloride, Ethanol And Ph Different Levels And Application Of Artificial Neural Networks To Describe The Combined Effect Of Them*; 2021; Vol. 10. http://intjmi.comhttp://intjmi.com.

(13) Zhang, Y.; Pi, Y.; Hua, Y.; Xie, J.; Wang, C.; Guo, K.; Zhao, Z.; Yong, Y. Bacteria Responsive Polyoxometalates Nanocluster Strategy to Regulate Biofilm Microenvironments for Enhanced Synergetic Antibiofilm Activity and Wound Healing. *Theranostics* **2020**, *10* (22), 10031–10045. https://doi.org/10.7150/thno.49008.

(14) Jim O'Neill. *Tackling Drug-Resistant Infections Globally: Final Report and Recommendations. The Review on Antimicrobial Resistance.*; **2016**. https://amr-review.org/ (accessed 2023-10-13).

(15) Gómez-Sequeda, N.; Ruiz, J.; Ortiz, C.; Urquiza, M.; Torres, R. Potent and Specific Antibacterial Activity against Escherichia Coli

O157:H7 and Methicillin Resistant Staphylococcus Aureus (MRSA) of G17 and G19 Peptides Encapsulated into Poly-Lactic-Co-Glycolic Acid (PLGA) Nanoparticles. *Antibiotics* **2020**, *9* (7), 384. https://doi.org/10.3390/antibiotics9070384.

(16) Senobar Tahaei, S. A.; Stájer, A.; Barrak, I.; Ostorházi, E.; Szabó, D.; Gajdács, M. Correlation Between Biofilm-Formation and the Antibiotic Resistant Phenotype in Staphylococcus Aureus Isolates: A Laboratory-Based Study in Hungary and a Review of the Literature. *Infect Drug Resist* **2021**, *Volume 14*, 1155–1168. https://doi.org/10.2147/IDR.S303992.

(17) Lade, H.; Park, J. H.; Chung, S. H.; Kim, I. H.; Kim, J. M.; Joo, H. S.; Kim, J. S. Biofilm Formation by Staphylococcus Aureus Clinical Isolates Is Differentially Affected by Glucose and Sodium Chloride Supplemented Culture Media. *J Clin Med* **2019**, *8* (11). https://doi.org/10.3390/jcm8111853.

(18) Ghanima, K. K.; Al-Mathkhury, H. J. F.; Ahmed, D. A. *Effect of Salinity on Antibiotic Resistance in Staphylococcus Aureus.*; **2008**; Vol. 21. https://www.iasj.net/iasj/download/fd13fd9c85b87874 (accessed 2023-09-23).

(19) Reginald Bennett, M. S. *Bad Bug Book Handbook of Foodborne Pathogenic Microorganisms and Natural Toxins*; **2012**. https://www.fda.gov/food/foodborne-pathogens/bad-bug-book-second-edition (accessed 2023-10-12).

(20) Stewart, C. M.; Cole, M. B.; Legan, J. D.; Slade, L.; Vandeven, M. H.; Schaffner, D. W. Staphylococcus Aureus Growth Boundaries: Moving towards Mechanistic Predictive Models Based on Solute-Specific Effects. *Appl Environ Microbiol* **2002**, *68* (4), 1864–1871. https://doi.org/10.1128/AEM.68.4.1864-1871.2002.

(21) Montville, T. J. *Food Microbiology: An Introduction*, Third edition.; Matthews, K. R., Kniel, K. E., Eds.; ASM Press: Washington, DC, **2012**.

(22) M. Abu-Ghazaleh, B. Effect of Sodium Chloride on Subsequent Survival of Staphylococcus Aureus in Various Preservatives. *Food Nutr Sci* **2016**, *07* (11), 955–963. https://doi.org/10.4236/fns.2016.711094.

(23) Julia M Ross, N. I.; Marten, M. R. Proteome Analyses of Staphylococcus Aureus Biofilm at Elevated Levels of NaCl. *Clinical Microbiology: Open Access* **2015**, *04* (05). https://doi.org/10.4172/2327-5073.1000219.

(24) Yehia, H. M.; Alkhuriji, A. F.; Savvaidis, I.; Al-Masoud, A. H. Bactericidal Effect of Nisin and Reuterin on Methicillin-Resistant Staphylococcus Aureu(MRSA) and S. Aureus ATCC 25937. *Food Science and Technology (Brazil)* **2022**, *42*. https://doi.org/10.1590/fst.105321.

(25) Gurung, R. R.; Maharjan, P.; Chhetri, G. G. Antibiotic Resistance Pattern of Staphylococcus Aureus with Reference to MRSA Isolates from Pediatric Patients. *Future Sci OA* **2020**, *6* (4). https://doi.org/10.2144/fsoa-2019-0122.

(26) Foster, T. J. Potential for Vaccination against Infections Caused by Staphylococcus Aureus. *Vaccine* **1991**, *9* (4), 221–227. https://doi.org/10.1016/0264-410X(91)90103-D.

(27) Shettigar, K.; Murali, T. S. Virulence Factors and Clonal Diversity of Staphylococcus Aureus in Colonization and Wound Infection with Emphasis on Diabetic Foot Infection. **2020**. https://doi.org/10.1007/s10096-020-03984-8/Published.

(28) Rozgonyi, F.; Kocsis, E.; Kristóf, K.; Nagy, K. Is MRSA More Virulent than MSSA? *Clinical Microbiology and Infection*. Blackwell Publishing Ltd 2007, pp 843–845. https://doi.org/10.1111/j.1469-0691.2007.01780.x.

(29) Le, K. Y.; Otto, M. Quorum-Sensing Regulation in Staphylococci—an Overview. *Front Microbiol* **2015**, *6*. https://doi.org/10.3389/fmicb.2015.01174.

(30) Alibayov, B.; Baba-Moussa, L.; Sina, H.; Zdeňková, K.; Demnerová, K. Staphylococcus Aureus Mobile Genetic Elements. *Mol Biol Rep* **2014**, *41* (8), 5005–5018. https://doi.org/10.1007/s11033-014-3367-3.

(31) Adame-Gómez, R.; Castro-Alarcón, N.; Vences-Velázquez, A.; Toribio-Jiménez, J.; Pérez-Valdespino, A.; Leyva-Vázquez, M. A.; Ramírez-Peralta, A. Genetic Diversity and Virulence Factors of S. Aureus Isolated from Food, Humans, and Animals. *Int J Microbiol* **2020**, *2020*. https://doi.org/10.1155/2020/1048097.

(32) Miller, B. W.; Torres, J. P.; Tun, J. O.; Flores, M. S.; Forteza, I.; Rosenberg, G.; Haygood, M. G.; Schmidt, E. W.; Concepcion, G. P. Synergistic Anti-Methicillin-Resistant Staphylococcus Aureus (MRSA) Activity and Absolute Stereochemistry of 7,8-Dideoxygriseorhodin C. *Journal of Antibiotics* **2020**, *73* (5), 290–298. https://doi.org/10.1038/s41429-019-0275-8.

(33) Wilkinson, K.; Wilkinson, T.; Adamson, C.; Herzog, T.; Covey, T.; Lloyd, B.; Nicholaou, M. *Polyoxometalate Induces Susceptibility of Methicillin-Resistant Staphylococcus Aureus to Oxacillin*; 2018. https://doi.org/https://doi.org/10.29074/ascls.118.000760.

(34) Nguena-Dongue, B. N.; Tchamgoue, J.; Tchangoue, Y. A. N.; Lunga, P. K.; Toghueo, K. R. M.; Zeuko'o, M. E.; Melogmo, Y. K. D.; Tchouankeu, J. C.; Kouam, S. F.; Fekam, B. F. Potentiation Effect of Mallotojaponin B on Chloramphenicol and Mode of Action of Combinations against Methicillin-Resistant Staphylococcus Aureus. *PLoS One* **2023**, *18* (3 March). https://doi.org/10.1371/journal.pone.0282008.

(35) Enderle, A. G.; Franco-Castillo, I.; Atrián-Blasco, E.; Martín-Rapún, R.; Lizarraga, L.; Culzoni, M. J.; Bollini, M.; De La Fuente, J. M.; Silva, F.; Streb, C.; Mitchell, S. G. Hybrid Antimicrobial Films Containing a Polyoxometalate-Ionic Liquid. *ACS Appl Polym Mater* **2022**, *4* (6), 4144–4153. https://doi.org/10.1021/acsapm.2c00110.

(36) Mastoor, S.; Nazim, F.; Rizwan-ul-Hasan, S.; Ahmed, K.; Khan, S.; Ali, S. N.; Abidi, S. H. Analysis of the Antimicrobial and Anti-Biofilm Activity of Natural Compounds and Their Analogues against Staphylococcus Aureus Isolates. *Molecules* **2022**, *27* (20). https://doi.org/10.3390/molecules27206874.

(37) Faleiro, L.; Marques, A.; Martins, J.; Jordão, L.; Nogueira, I.; Gumerova, N. I.; Rompel, A.; Aureliano, M. The Preyssler-Type Polyoxotungstate Exhibits Anti-Quorum Sensing, Antibiofilm, and Antiviral Activities. *Biology (Basel)* **2022**, *11* (7). https://doi.org/10.3390/biology11070994.

(38) Farzana R; Iqra P; Hunaiza T. *Antioxidant and Antimicrobial Effects of Polyoxometalates*; 2018. http://www.alliedacademies.org/microbiology-current-research/.

(39) Naziba, T. I.; Samsad, F. M.; Yasmin, R.; Amin, M. B.; Rahman, T.; Dockrell, D. H.; Mohasin, M. Chromium/Cadmium Plays a Pivotal Role to Emerge Amoxicillin Resistant Staphylococcus Aureus. **2023**. https://doi.org/10.1101/2023.02.28.530213.

(40) Neopane, P.; Nepal, H. P.; Shrestha, R.; Uehara, O.; Abiko, Y. In Vitro Biofilm Formation by Staphylococcus Aureus</Em> Isolated from Wounds of Hospital-Admitted Patients and Their Association with Antimicrobial Resistance. *Int J Gen Med* **2018**, *Volume 11*, 25–32. https://doi.org/10.2147/IJGM.S153268.

(41) Dash, P.; Rana, K.; Turuk, J.; Palo, S. K.; Pati, S. Antimicrobial Resistance and Biofilm Formation of Staphylococcus Aureus Isolates from Febrile Cases: Findings from a Rural Cohort of Odisha, India. *Pol J Microbiol* **2023**, *72* (2), 209–214. https://doi.org/10.33073/pjm-2023-005.

(42) Tahaei, S. A. S.; Stájer, A.; Barrak, I.; Ostorházi, E.; Szabó, D.; Gajdács, M. Correlation between Biofilm-Formation and the Antibiotic Resistant Phenotype in Staphylococcus Aureus Isolates: A Laboratory-Based Study in Hungary and a Review of the Literature.

Infect Drug Resist **2021**, *14*, 1155–1168. https://doi.org/10.2147/IDR.S303992.

(43) Qian, W.; Li, X.; Yang, M.; Liu, C.; Kong, Y.; Li, Y.; Wang, T.; Zhang, Q. Relationship Between Antibiotic Resistance, Biofilm Formation, and Biofilm-Specific Resistance in Escherichia Coli Isolates from Ningbo, China. *Infect Drug Resist* **2022**, *15*, 2865–2878. https://doi.org/10.2147/IDR.S363652.

(44) Kichana, E.; Opare-Boafoa, M. S.; Obeng Bekoe, E. M. Prevalence of Multidrug-Resistant Escherichia Coli in Household Drinking Water in Rural Ghana. *Journal of Water Sanitation and Hygiene for Development* **2022**, *12* (12), 862–868. https://doi.org/10.2166/washdev.2022.082.

(45) Mirghani, R.; Saba, T.; Khaliq, H.; Mitchell, J.; Do, L.; Chambi, L.; Diaz, K.; Kennedy, T.; Alkassab, K.; Huynh, T.; Elmi, M.; Martinez, J.; Sawan, S.; Rijal, G. Biofilms: Formation, Drug Resistance and Alternatives to Conventional Approaches. *AIMS Microbiology*. AIMS Press **2022**, pp 240–278. https://doi.org/10.3934/microbiol.2022019.

(46) Abalkhail, A.; AlYami, A. S.; Alrashedi, S. F.; Almushayqih, K. M.; Alslamah, T.; Alsalamah, Y. A.; Elbehiry, A. The Prevalence of Multidrug-Resistant Escherichia Coli Producing ESBL among Male and Female Patients with Urinary Tract Infections in Riyadh Region, Saudi Arabia. *Healthcare (Switzerland)* **2022**, *10* (9). https://doi.org/10.3390/healthcare10091778.

(47) Jain, P.; Bepari, A. K.; Sen, P. K.; Rafe, T.; Imtiaz, R.; Hossain, M.; Reza, H. M. High Prevalence of Multiple Antibiotic Resistance in Clinical E. Coli Isolates from Bangladesh and Prediction of Molecular Resistance Determinants Using WGS of an XDR Isolate. *Sci Rep* **2021**, *11* (1). https://doi.org/10.1038/s41598-021-02251-w.

(48) Kaur, N. Prevalence and Antibiotic Susceptibility Pattern of Methicillin Resistant Staphylococcus Aureus in Tertiary Care

Hospitals. *Br Biotechnol J* **2014**, *4* (3), 228–235. https://doi.org/10.9734/BBJ/2014/4245.

(49) Lin, T. Z.; Jayasvasti, I.; Tiraphat, S.; Pengpid, S.; Jayasvasti, M.; Borriharn, P. The Predictors Influencing the Rational Use of Antibiotics Among Public Sector: A Community-Based Survey in Thailand. *Drug Healthc Patient Saf* **2022**, *Volume 14*, 27–36. https://doi.org/10.2147/DHPS.S339808.

(50) Li, F.; Xiong, X. S.; Yang, Y. Y.; Wang, J. J.; Wang, M. M.; Tang, J. W.; Liu, Q. H.; Wang, L.; Gu, B. Effects of NaCl Concentrations on Growth Patterns, Phenotypes Associated With Virulence, and Energy Metabolism in Escherichia Coli BW25113. *Front Microbiol* **2021**, *12*. https://doi.org/10.3389/fmicb.2021.705326.

(51) Olar, R.; Badea, M.; Chifiriuc, M. C. Metal Complexes—A Promising Approach to Target Biofilm Associated Infections. *Molecules*. MDPI February 1, **2022**. https://doi.org/10.3390/molecules27030758.

(52) Bâlici, Ștefana; Rusu, D.; Páll, E.; Filip, M.; Chirilă, F.; Nicula, G. Z.; Lauravică, M.; Ungur, R.; Matei, H. V.; Fiț, N. I. In Vitro Antibacterial Susceptibility of Different Pathogens to Thirty Nano-Polyoxometalates. *Pharmaceuticals* **2022**, *15* (1). https://doi.org/10.3390/ph15010033.

(53) Bayani, M. M.; Patricia, M.; Azanza, V. *Inhibition of Staphylococcus Aureus by Garlic and NaCl in Broth Systems*.

(54) Berrocal, M.; Cordoba-Granados, J. J.; Carabineiro, S. A. C.; Gutierrez-Merino, C.; Aureliano, M.; Mata, A. M. Gold Compounds Inhibit the Ca2+-Atpase Activity of Brain Pmca and Human Neuroblastoma Sh-Sy5y Cells and Decrease Cell Viability. *Metals (Basel)* **2021**, *11* (12). https://doi.org/10.3390/met11121934.

(55) Fonseca, C.; Fraqueza, G.; Carabineiro, S. A. C.; Aureliano, M. The Ca2+-Atpase Inhibition Potential of Gold(I, Iii) Compounds.

Inorganics (Basel) **2020**, *8* (9), 1–11. https://doi.org/10.3390/inorganics8090049.

(56) Gil, F.; Custódia, F.; Emir, A.-S.; Annette, R.; Manuel, A.; Aureliano, M. Extended Abstract of Vienna Polyphenols 2017 Polyoxometalates as Inhibitors of P-Type ATPases and the Role of Polyphenols. **2017**, *5*. https://doi.org/10.18143/AISANH_v5i2_7.

(57) Aureliano, M.; Fraqueza, G.; Berrocal, M.; Cordoba-Granados, J. J.; Gumerova, N. I.; Rompel, A.; Gutierrez-Merino, C.; Mata, A. M. Inhibition of SERCA and PMCA Ca2+-ATPase Activities by Polyoxotungstates. *J Inorg Biochem* **2022**, *236*. https://doi.org/10.1016/j.jinorgbio.2022.111952.

(58) Gardner, A.; Stauff, S.; Petley-Ragan, L.; Wismer, P.; Ayu, D.; Ungu, K. *Labster Virtual Lab Experiments Genetics of Human Diseases*.

(59) Marques-da-Silva, D.; Mal, S. S.; Aureliano, M.; Lagoa, R. The Growth Curve Method to Rapidly Derive the Antibacterial Potential of Polyoxovanadates; MDPI AG, 2022; p 2. https://doi.org/10.3390/bitap-12790.

(60) Veríssimo, M. I. S.; Evtuguin, D. V.; Gomes, M. T. S. R. Polyoxometalate Functionalized Sensors: A Review. *Frontiers in Chemistry*. Frontiers Media S.A. March 8, 2022. https://doi.org/10.3389/fchem.2022.840657.

(61) Wang, X.; Wei, S.; Zhao, C.; Li, X.; Jin, J.; Shi, X.; Su, Z.; Li, J.; Wang, J. Promising Application of Polyoxometalates in the Treatment of Cancer, Infectious Diseases and Alzheimer's Disease. *Journal of Biological Inorganic Chemistry*. Springer Science and Business Media Deutschland GmbH August 1, 2022, pp 405–419. https://doi.org/10.1007/s00775-022-01942-7.

(62) Chang, D.; Li, Y.; Chen, Y.; Wang, X.; Zang, D.; Liu, T. Polyoxometalate-Based Nanocomposites for Antitumor and Antibacterial Applications. *Nanoscale Advances*. Royal Society of

Chemistry August 17, **2022**, pp 3689–3706. https://doi.org/10.1039/d2na00391k.

(63) Gil, A.; Carbó, J. J. Computational Modelling of the Interactions Between Polyoxometalates and Biological Systems. *Frontiers in Chemistry*. Frontiers Media S.A. April 14, 2022. https://doi.org/10.3389/fchem.2022.876630.

(64) Taghiyar, H.; Yadollahi, B.; Kajani, A. A. Controlled Drug Delivery and Cell Adhesion for Bone Tissue Regeneration by Keplerate Polyoxometalate (Mo132)/Metronidazole/PMMA Scaffolds. *Sci Rep* **2022**, *12* (1). https://doi.org/10.1038/s41598-022-18622-w.

(65) Aureliano, M. The Future Is Bright for Polyoxometalates. *BioChem* **2022**, *2* (1), 8–26. https://doi.org/10.3390/biochem2010002.

(66) Čolović, M. B.; Lacković, M.; Lalatović, J.; Mougharbel, A. S.; Kortz, U.; Krstić, D. Z. Polyoxometalates in Biomedicine: Update and Overview. *Curr Med Chem* **2019**, *27* (3), 362–379. https://doi.org/10.2174/0929867326666190827153532.

(67) Cherevan, A. S.; Nandan, S. P.; Roger, I.; Liu, R.; Streb, C.; Eder, D. Polyoxometalates on Functional Substrates: Concepts, Synergies, and Future Perspectives. *Advanced Science*. John Wiley and Sons Inc. April 1, **2020**. https://doi.org/10.1002/advs.201903511.

(68) Bijelic, A.; Aureliano, M.; Rompel, A. Im Kampf Gegen Krebs: Polyoxometallate Als Nächste Generation Metallhaltiger Medikamente. *Angewandte Chemie* **2019**, *131* (10), 3008–3029. https://doi.org/10.1002/ange.201803868.

(69) Bijelic, A.; Aureliano, M.; Rompel, A. The Antibacterial Activity of Polyoxometalates: Structures, Antibiotic Effects and Future Perspectives. *Chemical Communications* **2018**, *54* (10), 1153–1169. https://doi.org/10.1039/c7cc07549a.

(70) Gumerova, N.; Krivosudský, L.; Fraqueza, G.; Breibeck, J.; Al-Sayed, E.; Tanuhadi, E.; Bijelic, A.; Fuentes, J.; Aureliano, M.;

Rompel, A. The P-Type ATPase Inhibiting Potential of Polyoxotungstates. *Metallomics* **2018**, *10* (2), 287–295. https://doi.org/10.1039/c7mt00279c.

(71) Aureliano, M.; Mitchell, S. G.; Yin, P. Editorial: Emerging Polyoxometalates with Biological, Biomedical, and Health Applications. *Frontiers in Chemistry*. Frontiers Media S.A. August 9, 2022. https://doi.org/10.3389/fchem.2022.977317.

(72) Gumerova, N. I.; Al-Sayed, E.; Krivosudský, L.; Ĉipĉić-Paljetak, H.; Verbanac, D.; Rompel, A. Antibacterial Activity of Polyoxometalates against Moraxella Catarrhalis. *Front Chem* **2018**, *6* (AUG). https://doi.org/10.3389/fchem.2018.00336.

(73) Shahabadi, N.; Mahdavi, M.; Zendehcheshm, S. Can Polyoxometalates (POMs) Prevent of Coronavirus 2019-NCoV Cell Entry? Interaction of POMs with TMPRSS2 and Spike Receptor Domain Complexed with ACE2 (ACE2-RBD): Virtual Screening Approaches. *Inform Med Unlocked* **2022**, *29*. https://doi.org/10.1016/j.imu.2022.100902.

(74) Bošnjaković-Pavlović, N.; Bajuk-Bogdanović, D.; Zakrzewska, J.; Yan, Z.; Holclajtner-Antunović, I.; Gillet, J.-M. Reactivity of 12-Tungstophosphoric Acid and Its Inhibitor Potency toward Na + /K + -ATPase: A Combined 31 P NMR Study, Ab Initio Calculations and Crystallographic Analysis. *Hal Open Science* **2017**. https://doi.org/10.1016/j.jinorgbio.2017.08.014ï.

(75) Qu, X.; Xu, K.; Zhao, C.; Song, X.; Li, J.; Li, L.; Nie, W.; Bao, H.; Wang, J.; Niu, F.; Li, J. Genotoxicity and Acute and Subchronic Toxicity Studies of a Bioactive Polyoxometalate in Wistar Rats. *BMC Pharmacol Toxicol* **2017**, *18* (1). https://doi.org/10.1186/s40360-017-0133-x.

(76) Zhang, B.; Qiu, J.; Wu, C.; Li, Y.; Liu, Z. Anti-Tumor and Immunomodulatory Activity of Iron Hepta-Tungsten Phosphate

Oxygen Clusters Complex. *Int Immunopharmacol* **2015**, *29* (2), 293–301. https://doi.org/10.1016/j.intimp.2015.11.003.

(77) Sciortino, G.; Aureliano, M.; Garribba, E. Rationalizing the Decavanadate(V) and Oxidovanadium(IV) Binding to G-Actin and the Competition with Decaniobate(V) and ATP. *Inorg Chem* **2021**, *60* (1), 334–344. https://doi.org/10.1021/acs.inorgchem.0c02971.

(78) Marques-Da-Silva, D.; Fraqueza, G.; Lagoa, R.; Vannathan, A. A.; Mal, S. S.; Aureliano, M. Polyoxovanadate Inhibition of: Escherichia Coli Growth Shows a Reverse Correlation with Ca2+-ATPase Inhibition. *New Journal of Chemistry* **2019**, *43* (45), 17577–17587. https://doi.org/10.1039/c9nj01208g.

(79) Mahvash, S.; Azimian Zavareh, V.; Taymouri, S.; Ramezani-Aliakbari, M.; Dousti, F.; Mirian, M.; Rostami, M. Hybrid Nanocomposite of Imidazolium Based Chitosan and Anderson-Type Manganese Polyoxomolybdate for Boosting Drug Delivery Against Breast Cancer. **2021**. https://doi.org/10.21203/rs.3.rs-729081/v1.

(80) Gumerova, N. I.; Rompel, A. Interweaving Disciplines to Advance Chemistry: Applying Polyoxometalates in Biology. *Inorganic Chemistry*. American Chemical Society May 3, **2021**, pp 6109–6114. https://doi.org/10.1021/acs.inorgchem.1c00125.

(81) Gumerova, N. I.; Rompel, A. Polyoxometalates in Solution: Speciation under Spotlight. *Chem Soc Rev* **2020**, *49* (21), 7568–7601. https://doi.org/10.1039/D0CS00392A.

(82) She, S.; Bian, S.; Huo, R.; Chen, K.; Huang, Z.; Zhang, J.; Hao, J.; Wei, Y. Degradable Organically-Derivatized Polyoxometalate with Enhanced Activity against Glioblastoma Cell Line. *Sci Rep* **2016**, *6*. https://doi.org/10.1038/srep33529.

(83) Wang, J.; Tao, Z.; Tian, T.; Qiu, J.; Qian, H.; Zha, Z.; Miao, Z.; Ma, Y.; Wang, H. Polyoxometalate Nanoclusters: A Potential Preventative and Therapeutic Drug for Inflammatory Bowel Disease.

Chemical Engineering Journal **2021**, *416*. https://doi.org/10.1016/j.cej.2021.129137.

(84) Li, X.; He, X.; He, D.; Liu, Y.; Chen, K.; Yin, P. A Polymeric Co-Assembly of Subunit Vaccine with Polyoxometalates Induces Enhanced Immune Responses. *Nano Res* **2022**, *15* (5), 4175–4180. https://doi.org/10.1007/s12274-021-4004-9.

(85) Ostroushko, A. A.; Gagarin, I. D.; Danilova, I. G.; Gette, I. F. The Use of Nanocluster Polyoxometalates in the Bioactive Substance Delivery Systems. *Nanosystems: Physics, Chemistry, Mathematics* **2019**, *10* (3), 318–349. https://doi.org/10.17586/2220-8054-2019-10-3-318-349.

(86) Croce, M.; Conti, S.; Maake, C.; Patzke, G. R. Nanocomposites of Polyoxometalates and Chitosan-Based Polymers as Tuneable Anticancer Agents. *Eur J Inorg Chem* **2019**, *2019* (3–4), 348–356. https://doi.org/10.1002/ejic.201800268.

(87) Treviño, S.; González-Vergara, E. Metformin-Decavanadate Treatment Ameliorates Hyperglycemia and Redox Balance of the Liver and Muscle in a Rat Model of Alloxan-Induced Diabetes. *New Journal of Chemistry* **2019**, *43* (45), 17850–17862. https://doi.org/10.1039/C9NJ02460C.

(88) Ramezani-Aliakbari, M.; Soltanabadi, A.; Sadeghi-aliabadi, H.; Varshosaz, J.; Yadollahi, B.; Hassanzadeh, F.; Rostami, M. Eudesmic Acid-Polyoxomolybdate Organo-Conjugate as Novel Anticancer Agent. *J Mol Struct* **2021**, *1240*. https://doi.org/10.1016/j.molstruc.2021.130612.

(89) Zhao, S.; Li, Y.; Liu, Q.; Li, S.; Cheng, Y.; Cheng, C.; Sun, Z.; Du, Y.; Butch, C. J.; Wei, H. An Orally Administered CeO2@Montmorillonite Nanozyme Targets Inflammation for Inflammatory Bowel Disease Therapy. *Adv Funct Mater* **2020**, *30* (45), 2004692. https://doi.org/10.1002/adfm.202004692.

(90) Nale, J. Y.; Chutia, M.; Carr, P.; Hickenbotham, P. T.; Clokie, M. R. J. “Get in Early”; Biofilm and Wax Moth (Galleria Mellonella) Models Reveal New Insights into the Therapeutic Potential of Clostridium Difficile Bacteriophages. *Front Microbiol* **2016**, *7* (AUG). https://doi.org/10.3389/fmicb.2016.01383.

(91) Balici, S.; Niculae, M.; Pall, E.; Rusu, M.; Rusu, D.; Matei, H. *Antibiotic-Like Behaviour of Polyoxometalates In Vitro Comparative Study: Seven Polyoxotungstates-Nine Antibiotics against Gram-Positive and Gram-Negative Bacteria*; **2016;** Vol. 67. http://www.revistadechimie.ro485.

(92) Miras, H. N.; Stone, D.; Long, D.-L.; McInnes, E. J. L.; Kögerler, P.; Cronin, L. Exploring the Structure and Properties of Transition Metal Templated(VO4)2} Dawson-Like Capsules. *Inorg Chem* **2011**, *50* (17), 8384–8391. https://doi.org/10.1021/ic200943s.

(93) Thakre, D.; Ali, S. R.; Mehta, S.; Alam, N.; Ibrahim, M.; Sarma, D.; Mondal, A.; De, M.; Banerjee, A. Polyoxovanadates with Ethylidene-Pyridine Functionalized Bisphosphonate Ligands: Synthesis, Structure, Spectroscopic Characterization, Magnetic, and Antibacterial Studies. *Cryst Growth Des* **2021**, *21* (8), 4285–4298. https://doi.org/10.1021/acs.cgd.0c01692.

(94) Barats-Damatov, D.; Shimon, L. J. W.; Feldman, Y.; Bendikov, T.; Neumann, R. Solid-State Crystal-to-Crystal Phase Transitions and Reversible Structure-Temperature Behavior of Phosphovanadomolybdic Acid, H5PV2Mo10O40. *Inorg Chem* **2015**, *54* (2), 628–634. https://doi.org/10.1021/ic502541b.

(95) Somasundaram, J. D.; Ebrahimi, A.; Nandan, S. P.; Cherevan, A.; Eder, D.; Šupolíková, M.; Nováková, E.; Gyepes, R.; Krivosudský, L. Functionalization of Decavanadate Anion by Coordination to Cobalt(II): Binding to Proteins, Cytotoxicity, and Water Oxidation Catalysis. *J Inorg Biochem* **2023**, *239*, 112067. https://doi.org/10.1016/j.jinorgbio.2022.112067.

(96) Fraqueza, G.; Fuentes, J.; Krivosudský, L.; Dutta, S.; Mal, S. S.; Roller, A.; Giester, G.; Rompel, A.; Aureliano, M. Inhibition of Na + /K + - and Ca 2+ -ATPase Activities by Phosphotetradecavanadate. *J Inorg Biochem* **2019**, *197*. https://doi.org/10.1016/j.jinorgbio.2019.110700.

(97) Fraqueza, G.; Ohlin, C. A.; Casey, W. H.; Aureliano, M. Sarcoplasmic Reticulum Calcium ATPase Interactions with Decaniobate, Decavanadate, Vanadate, Tungstate and Molybdate. *J Inorg Biochem* **2012**, *107* (1), 82–89. https://doi.org/10.1016/j.jinorgbio.2011.10.010.

(98) Fraqueza, G.; Batista de Carvalho, L. A. E.; Marques, M. P. M.; Maia, L.; Ohlin, C. A.; Casey, W. H.; Aureliano, M. Decavanadate, Decaniobate, Tungstate and Molybdate Interactions with Sarcoplasmic Reticulum Ca2+-ATPase: Quercetin Prevents Cysteine Oxidation by Vanadate but Does Not Reverse ATPase Inhibition. *Dalton Transactions* **2012**, *41* (41), 12749. https://doi.org/10.1039/c2dt31688a.

(99) Smith', D. P.; Pope, M. T. *Heteropoly 12-Metallophosphates Heteropoly 12-Metallophosphates Containing Tungsten and Vanadium. Preparation, Voltammetry, and Properties of Mono-, Di-, Tetra-and Hexavanado Complexes' y 2*; **1973**; Vol. 12.

(100) El-Guendouz, S.; Aazza, S.; Lyoussi, B.; Bankova, V.; Popova, M.; Neto, L.; Faleiro, M. L.; Miguel, M. da G. Moroccan Propolis: A Natural Antioxidant, Antibacterial, and Antibiofilm against Staphylococcus Aureus with No Induction of Resistance after Continuous Exposure. *Evidence-Based Complementary and Alternative Medicine* **2018**, *2018*, 1–19. https://doi.org/10.1155/2018/9759240.

(101) Apolónio, J.; Faleiro, M. L.; Miguel, M. G.; Neto, L. No Induction of Antimicrobial Resistance in Staphylococcus Aureus and Listeria Monocytogenes during Continuous Exposure to Eugenol and Citral.

FEMS Microbiol Lett **2014**, *354* (2), 92–101. https://doi.org/10.1111/1574-6968.12440.

(102) da Silva, C. I.; Aazza, S.; Faleiro, M. L.; Miguel, M. da G.; Neto, L. The Antibacterial, Anti-Biofilm, Anti-Inflammatory and Virulence Inhibition Properties of Portuguese Honeys. *J Apic Res* **2016**, *55* (4), 292–304. https://doi.org/10.1080/00218839.2016.1243294.

(103) Schrama, D.; Helliwell, N.; Neto, L.; Faleiro, M. L. Adaptation of Listeria Monocytogenes in a Simulated Cheese Medium: Effects on Virulence Using the Galleria Mellonella Infection Model. *Lett Appl Microbiol* **2013**, *56* (6), 421–427. https://doi.org/10.1111/lam.12064.

(104) Walsh, R. Comparing Enzyme Activity Modifier Equations through the Development of Global Data Fitting Templates in Excel. *PeerJ* **2018**, *6*, e6082. https://doi.org/10.7717/peerj.6082.

(105) Surya N; Vinod N; Kisan K; Ram S. *New Horizons in Natural Compound Research*; Elsevier, **2023**. https://doi.org/10.1016/C2022-0-00460-8.

(106) Inoue, M.; Segawa, K.; Matsunaga, S.; Matsumoto, N.; Oda, M.; Yamase, T. Antibacterial Activity of Highly Negative Charged Polyoxotungstates, K27[KAs4W40O140] and K18[KSb9W21O86], and Keggin-Structural Polyoxotungstates against Helicobacter Pylori. *J Inorg Biochem* **2005**, *99* (5), 1023–1031. https://doi.org/10.1016/j.jinorgbio.2005.01.010.

(107) Postal, K.; Maluf, D. F.; Valdameri, G.; Rüdiger, A. L.; Hughes, D. L.; de Sá, E. L.; Ribeiro, R. R.; de Souza, E. M.; Soares, J. F.; Nunes, G. G. Chemoprotective Activity of Mixed Valence Polyoxovanadates against Diethylsulphate in E. Coli Cultures: Insights from Solution Speciation Studies. *RSC Adv* **2016**, *6* (115), 114955–114968. https://doi.org/10.1039/C6RA15826A.

(108) Fukada, N.; Yamase, T.; Tajima, Y. Inhibitory Effect of Polyoxotungstates on the Production of Penicillin-Binding Proteins and .BETA.-Lactamase against Methicillin-Resistant Staphylococcus

Aureus. *Biol Pharm Bull* **1999**, *22* (5), 463–470. https://doi.org/10.1248/bpb.22.463.

(109) Zhou, F.; Wang, D.; Zhang, J.; Li, J.; Lai, D.; Lin, S.; Hu, J. Preparation and Characterization of Biodegradable κ-Carrageenan Based Anti-Bacterial Film Functionalized with Wells-Dawson Polyoxometalate. *Foods* **2022**, *11* (4). https://doi.org/10.3390/foods11040586.

(110) Barsukova-Stuckart, M.; Piedra-Garza, L. F.; Gautam, B.; Alfaro-Espinoza, G.; Izarova, N. V.; Banerjee, A.; Bassil, B. S.; Ullrich, M. S.; Breunig, H. J.; Silvestru, C.; Kortz, U. Synthesis and Biological Activity of Organoantimony(III)-Containing Heteropolytungstates. *Inorg Chem* **2012**, *51* (21), 12015–12022. https://doi.org/10.1021/ic301892s.

(111) Rigden, D. J.; Littlejohn, J. E.; Henderson, K.; Jedrzejas, M. J. Structures of Phosphate and Trivanadate Complexes of Bacillus Stearothermophilus Phosphatase PhoE: Structural and Functional Analysis in the Cofactor-Dependent Phosphoglycerate Mutase Superfamily. *J Mol Biol* **2003**, *325* (3), 411–420. https://doi.org/10.1016/S0022-2836(02)01229-9.

(112) Aureliano, M.; Gumerova, N. I.; Sciortino, G.; Garribba, E.; McLauchlan, C. C.; Rompel, A.; Crans, D. C. Polyoxidovanadates' Interactions with Proteins: An Overview. *Coordination Chemistry Reviews*. Elsevier B.V. March 1, **2022**. https://doi.org/10.1016/j.ccr.2021.214344.

(113) Fiorani, G.; Saoncella, O.; Kaner, P.; Altinkaya, S. A.; Figoli, A.; Bonchio, M.; Carraro, M. Chitosan-Polyoxometalate Nanocomposites: Synthesis, Characterization and Application as Antimicrobial Agents. *J Clust Sci* **2014**, *25* (3), 839–854. https://doi.org/10.1007/s10876-013-0685-x.

(114) Gu, J.; Zhang, L.; Yuan, X.; Chen, Y. G.; Gao, X.; Li, D. Synthesis and Antibacterial Activity of Polyoxometalates with Different

Structures. *Bioinorg Chem Appl* **2018**, *2018*. https://doi.org/10.1155/2018/9342326.

(115) Gottenbos, B. Antimicrobial Effects of Positively Charged Surfaces on Adhering Gram-Positive and Gram-Negative Bacteria. *Journal of Antimicrobial Chemotherapy* **2001**, *48* (1), 7–13. https://doi.org/10.1093/jac/48.1.7.

(116) Gumerova, N. I.; Rompel, A. Synthesis, Structures and Applications of Electron-Rich Polyoxometalates. *Nat Rev Chem* **2018**, *2* (2), 0112. https://doi.org/10.1038/s41570-018-0112.

(117) Feng, Y.; Ming, T.; Zhou, J.; Lu, C.; Wang, R.; Su, X. The Response and Survival Mechanisms of Staphylococcus Aureus under High Salinity Stress in Salted Foods. *Foods* **2022**, *11* (10). https://doi.org/10.3390/foods11101503.

(118) Pinto, A. C.; de Sá, P. H. C. G.; Ramos, R. T. J.; Barbosa, S.; Barbosa, H. P. M.; Ribeiro, A. C.; Silva, W. M.; Rocha, F. S.; Santana, M. P.; de Paula Castro, T. L.; Miyoshi, A.; Schneider, M. P. C.; Silva, A.; Azevedo, V. Differential Transcriptional Profile of Corynebacterium Pseudotuberculosis in Response to Abiotic Stresses. *BMC Genomics* **2014**, *15* (1), 14. https://doi.org/10.1186/1471-2164-15-14.

(119) Sihto, H.-M.; Tasara, T.; Stephan, R.; Johler, S. Temporal Expression of the Staphylococcal Enterotoxin D Gene under NaCl Stress Conditions. *FEMS Microbiol Lett* **2015**, *362* (6). https://doi.org/10.1093/femsle/fnv024.

(120) Le Masters, T.; Johnson, S.; Jeraldo, P. R.; Greenwood-Quaintance, K. E.; Cunningham, S. A.; Abdel, M. P.; Chia, N.; Patel, R. Comparative Transcriptomic Analysis of Staphylococcus Aureus Associated with Periprosthetic Joint Infection under in Vivo and in Vitro Conditions. *The Journal of Molecular Diagnostics* **2021**, *23* (8), 986–999. https://doi.org/10.1016/j.jmoldx.2021.05.011.

(121) Scybert, S.; Pechous, R.; Sitthisak, S.; Nadakavukaren, M. J.; Wilkinson, B. J.; Jayaswal, R. K. NaCl-Sensitive Mutant of

Staphylococcus Aureus Has a Tn917-LacZ Insertion in Its Ars Operon. *FEMS Microbiol Lett* **2003**, *222* (2), 171–176. https://doi.org/10.1016/S0378-1097(03)00312-4.

(122) Lee, S.; Choi, K.-H.; Yoon, Y. Effect of NaCl on Biofilm Formation of the Isolate from Staphylococcus Aureus Outbreak Linked to Ham. *Korean J Food Sci Anim Resour* **2014**, *34* (2), 257–261. https://doi.org/10.5851/kosfa.2014.34.2.257.

(123) Lim, Y.; Jana, M.; Luong, T. T.; Lee, C. Y. Control of Glucose- and NaCl-Induced Biofilm Formation by Rbf in Staphylococcus Aureus. *J Bacteriol* **2004**, *186* (3), 722–729. https://doi.org/10.1128/JB.186.3.722-729.2004.

(124) Chen, K.; Yu, Q.; Liu, Y.; Yin, P. Bacterial Hyperpolarization Modulated by Polyoxometalates for Solutions of Antibiotic Resistance. *J Inorg Biochem* **2021**, *220*, 111463. https://doi.org/10.1016/j.jinorgbio.2021.111463.

(125) Yu, X.; Chen, C.; Peng, J.; Shi, Z.; Shen, Y.; Mei, J.; Ren, Z. Antibacterial-Active Multilayer Films Composed of Polyoxometalate and Methyl Violet: Fabrication, Characterization and Properties. *Thin Solid Films* **2014**, *571*, 69–74. https://doi.org/10.1016/j.tsf.2014.09.029.

(126) Zhang, C.; Zhao, M.; Zou, H.; Zhang, X.; Sheng, R.; Zhang, Y.; Zhang, B.; Li, C.; Qi, Y. An Enhanced Antibacterial Nanoflowers AgPW@PDA@Nisin Constructed from Polyoxometalate and Nisin. *J Inorg Biochem* **2020**, *212*, 111212. https://doi.org/10.1016/j.jinorgbio.2020.111212.

(127) Omotoyinbo, O. V; Omotoyinbo, B. I. Effect of Varying NaCl Concentrations on the Growth Curve of Escherichia Coli and Staphylococcus Aureus. *Cell Biology* **2016**, *4* (5), 31–34. https://doi.org/10.11648/j.cb.20160405.11.

(128) Ojo, K. K.; Striplin, M. J.; Ulep, C. C.; Close, N. S.; Zittle, J.; Luis, H.; Bernardo, M.; Leitao, J.; Roberts, M. C. Staphylococcus Efflux

Msr(A) Gene Characterized in Streptococcus, Enterococcus, Corynebacterium, and Pseudomonas Isolates. *Antimicrob Agents Chemother* **2006**, *50* (3), 1089–1091. https://doi.org/10.1128/AAC.50.3.1089-1091.2006.

(129) Inoue, M.; Suzuki, T.; Fujita, Y.; Oda, M.; Matsumoto, N.; Yamase, T. Enhancement of Antibacterial Activity of β-Lactam Antibiotics by [P2W18O62]6−, [SiMo12O40]4−, and [PTi2W10O40]7− against Methicillin-Resistant and Vancomycin-Resistant Staphylococcus Aureus. *J Inorg Biochem* **2006**, *100* (7), 1225–1233. https://doi.org/10.1016/j.jinorgbio.2006.02.004.

(130) Ménard, G.; Rouillon, A.; Cattoir, V.; Donnio, P. Y. Galleria Mellonella as a Suitable Model of Bacterial Infection: Past, Present and Future. *Frontiers in Cellular and Infection Microbiology*. Frontiers Media S.A. December 22, 2021. https://doi.org/10.3389/fcimb.2021.782733.

(131) Admella, J.; Torrents, E. Investigating Bacterial Infections in Galleria Mellonella Larvae: Insights into Pathogen Dissemination and Behavior. *J Invertebr Pathol* **2023**, *200*. https://doi.org/10.1016/j.jip.2023.107975.

(132) Mannala, G. K.; Rupp, M.; Alagboso, F.; Kerschbaum, M.; Pfeifer, C.; Sommer, U.; Kampschulte, M.; Domann, E.; Alt, V. Galleria Mellonella as an Alternative in Vivo Model to Study Bacterial Biofilms on Stainless Steel and Titanium Implants. *ALTEX* **2021**, *38* (2), 245–252. https://doi.org/10.14573/altex.2003211.

(133) Inés Molina, R. D.; Campos-Silva, R.; Díaz, M. A.; Macedo, A. J.; Blázquez, M. A.; Alberto, M. R.; Arena, M. E. Laurel Extracts Inhibit Quorum Sensing, Virulence Factors and Biofilm of Foodborne Pathogens. *LWT* **2020**, *134*. https://doi.org/10.1016/j.lwt.2020.109899.

(134) Aureliano, M.; Henao, F.; Tiago, T.; Duarte, R. O.; Moura, J. J. G.; Baruah, B.; Crans, D. C. Sarcoplasmic Reticulum Calcium ATPase Is

Inhibited by Organic Vanadium Coordination Compounds: Pyridine-2,6-Dicarboxylatodioxovanadium(V), BMOV, and an Amavadine Analogue. *Inorg Chem* **2008**, *47* (13), 5677–5684. https://doi.org/10.1021/ic702405d.

(135) Singh, S. *Molecular Enzymology and Drug Targets © Enzyme Inhibitors: Strategies and Challenges in Drug Design*; 2023.

(136) Kostenkova, K.; Arhouma, Z.; Postal, K.; Rajan, A.; Kortz, U.; Nunes, G. G.; Crick, D. C.; Crans, D. C. PtIV- or MoVI-Substituted Decavanadates Inhibit the Growth of Mycobacterium Smegmatis. *J Inorg Biochem* **2021**, *217*, 111356. https://doi.org/10.1016/j.jinorgbio.2021.111356.

(137) Foster, T. (1996). *Staphylococcus*. Medical Microbiology - NCBI Bookshelf. Retrieved October 17, 2023, from https://www.ncbi.nlm.nih.gov/books/NBK8448/

(138) Joan L.Slonczewski, J. L. **(2016)**. *Staphylococcus aureus*. Microbewiki. Retrieved October 17, 2023, from https://microbewiki.kenyon.edu/index.php?title=Staphylococcus_aureus&oldid=121014